Available online at www.sciencedirect.com

Applied Catalysis A: General 253 (2003) 545–602

www.elsevier.com/locate/apcata

Erratum

Perspectives in catalytic applications of mesostructured materials[☆]

D. Trong On, D. Desplantier-Giscard[1], C. Danumah, S. Kaliaguine*

Département de Génie Chimique, Université Laval, Ste-Foy, Qué., Canada G1K 7P4

Abstract

This review paper deals with proven and potential applications of mesoporous molecular sieves in catalysis. In addition to introduction and conclusion, the text is divided into two parts, respectively, dedicated to the design of solid catalysts and catalyst supports and to some relevant examples of catalytic processes.

Keywords: Mesoporous molecular sieves; Micelle templated silica; Mesostructured materials; Nanocatalysts; Mesoporous catalyst supports

1. Introduction

Designing an heterogeneous catalyst involves both the proper control of the surface chemistry and a rigorous control of the surface geometry at the micro-, meso- and macroscales. This is because high surface areas or high active phase dispersions as well as fast mass transfer of the reactants and products to and from the catalytic sites are required from any active catalyst.

It is, therefore, clear that the new materials designated as mesoporous molecular sieves (MMSs) have introduced a new degree of freedom in the conception of catalysts. Indeed, MMSs are very high surface area materials (up to $1600\,m^2\,g^{-1}$ for mesostructured silica) having monodispersed pore diameters in the range 2–50 nm and a stereoregular arrangement of these channels which mimics the liquid crystals formed by the surfactants used in their preparation [1–3]. It is not the purpose of the present text to discuss the synthesis mechanism of MMSs as this is already broadly covered in numerous reviews [4–21].

In discussing catalytic applications, reference will, however, be made to three kinds of relevant materials obtained following different synthetic procedures. The first one is the so-called M41S family of silica and aluminosilicates introduced by the Mobil group [1,4,22–33] which includes hexagonal MCM-41, cubic MCM-48 and lamellar MCM-50 phases. The preparation of M41S materials involves ionic surfactants, exemplified by cetyltrimethyl ammonium bromide (CTAB), as structure directing agents. It may be conducted in basic conditions in which case it follows an ionic assembly mechanism schematically represented as S^+I^-. This mechanism was extended by Stucky and co-workers to a whole series of other electrostatic assembly mechanisms, including a reversed S^-I^+ and counter-ion mediated $S^+X^-I^+$ and $S^-M^+I^-$ pathways [34–39].

The second one was introduced by the group of Pinnavaia who produced MMSs using two neutral routes based on hydrogen bonding and self assembly of non-ionic primary amines such as hexadecyl amine or polyethylene oxide (EO) surfactants and neutral oligomeric silica precursors S^0I^0 [40–48]. The hexagonal mesoporous silica (HMS and MSU) produced by

---

[☆] doi of original article 10.1016/S0926-860X(01)00842-0.

* Corresponding author.

E-mail address: kaliagui@gch.ulaval.ca (S. Kaliaguine).

[1] Present address: Silicycle Inc., 1200 Ave., St. Jean Baptiste, Suite 114, Qué., Canada G2E 5E8.

0926-860X/$ – see front matter © 2003 Elsevier Science B.V. All rights reserved.
doi:10.1016/S0926-860X(03)00195-9

this technique are less ordered, showing a wormhole like pore structure, than MMS's produced with ionic surfactants. They have, however, a monodispersed pore diameter, thicker pore walls, a higher degree of condensation, and therefore, a higher thermal stability. In addition, the mesopores of HMS being shorter allow a faster diffusion of reactants.

Finally, Stucky and co-workers introduced a new synthesis route involving amphiphilic di- and tri-block copolymers as organic structure directing agents [49–52]. These materials, exemplified by hexagonal (p6 mm) SBA-15, have long range order, large monodispersed mesopores (up to 50 nm) and thicker walls (typically between 3 and 9 nm) which make them more thermally and hydrothermally stable than previous materials. One of the advantages of the thicker walls is the ability to form stable crystal nuclei of the constitutive oxide within the walls. Stable mesostructured nanocrystalline ZrO_2 and TiO_2 were, for example, prepared in this manner. Because the EO and polypropylene oxide (PO) block copolymers used have very weak interactions with the inorganic surface, the surfactant separation from the composite, either by calcination or solvent extraction, is easier than in the case of ionic surfactants. It is, for example, possible to desorb large block copolymers from SBA-15 at temperature on the order of 140 °C whereas the desorption of cationic surfactants would occur around 360 °C. The decomposition temperature of $PEO_{20}PPO_{70}PEO_{20}$ (Pluronic 123) is 270 °C which must be compared with that of cationic surfactants around 360 °C. Thus, the calcination temperature of SBA-15 can be much lower than in MCM-41.

In what follows, we intend to discuss the new perspectives opened by the possibility to apply MMS in the preparation of industrial catalysts. Because, the literature on this topic has enjoyed an explosive growth over the last few years an exhaustive treatment of the subject within reasonable page limits is not any more possible. For this reason, it was decided to divide the presentation into two parts. In the first one, we will deal with the use of MMS in preparing materials of interest either as catalysts or as catalyst supports, not necessarily referring to particular catalytic applications. In the second part, a series of catalytic processes in which MMS have entered in the preparation of the catalysts will be reviewed. The selection of processes reflects our personal interests or our perception of the potential significance of MMS in the particular field covered. In addition, it was decided to avoid dealing with partial oxidation processes as a very broad coverage of this topic will be published shortly by Jacobs [53] following his invited lecture at the Second International Symposium on Mesoporous Molecular Sieves.

2. MMS in the design of catalytic materials

Any chemical composition based classification of mesostructured materials must begin with mesostructured silica's which have been most studied due to their easier synthesis and more stable structures. A very large variety of materials has been prepared using all the possibilities of inclusion chemistry to introduce catalytically active species in mesoporous silica guest materials [54]. These include co-condensation of active species during the MMS synthesis or post-synthesis methods such as ion-exchange, impregnation, adsorption, grafting of reactive metal complexes (alkoxides, carbonyls, chlorides, metallocenes ...) deposition of clusters or layers of metal oxides or of metal clusters, grafting of silanes, etc. Obviously in all these syntheses, the mesostructured pore lattice yields a clear advantage by providing enough space for the insertion of bulky active complexes.

In addition, the literature provides numerous examples of non-silica mesostructured materials [15,19,52]. Among these, oxides such as alumina, TiO_2, ZrO_2, Ta_2O_5, Nb_2O_5, aluminophosphates, Zr oxyphosphate, and many others have been prepared. These may be of interest as catalysts or catalyst supports. Metals such as Pt and alloys such as Pt–Ru have been produced by the S^0I^0 neutral templating route using concentrated EO surfactants [55–57]. Mesostructured carbons may be produced by calcining an organic material in the mesopores of a silica MMS and dissolving the silica backbone in hot NaOH or HF [58–65]. Some of these mesostructured carbons are stable at temperatures as high as 1600 °C. Some have microporous walls which makes them attractive supports for metals such as Pd. Finally, a whole family of periodic mesoporous hybrid organic–inorganic materials similar in nature to silicon rubbers have been proposed [66–75]. They are prepared from bridged silsesquioxane species $(RO)_3Si–R'–Si(OR)_3$ and have, therefore, the R′ group inserted in their walls. These materials may find applications as catalyst materials for not too high temperature reactions.

It is also of potential interest for catalytic applications that ordered mesoporous materials, and in particular SBA-15 type silica may be prepared in a variety of morphologies and textures [76–96]. Spheres, hollowspheres, fibers, giroids, toroids, discoids have been produced. SBA-15 may be shaped into micron size spheres, toroids or giroids and into fiber-like materials with length of several hundreds of micrometers and diameters in the 10 μm range [90]. It is especially important that such large particles can be made by direct synthesis as classical industrial catalysts shaping operations such as extrusion may damage the thin walls of mesostructured materials. Some work was performed to establish the mechanical resistance of composite hexagonal surfactant templated silica's which were, however, found to retain their mesoscopic order up to the surprisingly high pressure of 12 GPa [97,98]. These effects could also be monitored by the fluorescence of a rigidochromic complexe of Re: $ClRe(I)(CO)_3$(bathophenanthrolinedisulfonic acid, disodium salt) grafted inside the pore lattice [99]. The effect of composition on particle stacking, pore volume and specific surface area was also discussed ([100] and references therein) and a quantitative study relating elastic deformation of the channels to the applied strain and also the elasticity limit to wall thickness was reported [101]. It was concluded that MMS are the strongest among low density materials and that this stability is strongly dependent on pore size and wall thickness.

2.1. Supported metals

2.1.1. Platinum

Junges et al. [102] have proposed a new approach to the preparation of MMS supported metals by introducing platinum compounds in the synthesis gel of MCM-41. They compared the neutral complex $[Pt(NH_3)_2Cl_2]$ with a cationic form $[Pt(NH_3)_4]^{2+}(NO_3{}^-)_2$ and an anionic one $[PtCl_6]^{2-}(K^+)_2$. The neutral compound was found more appropriate, yielding 80% incorporation in the final solid and a better Pt dispersion (4 nm Pt crystallites) in the calcined and reduced material. The incorporation of up to 5 wt.% Pt did not prevent the formation of a highly ordered MCM-41 hexagonal phase with any of the three precursors. This result is important as it shows that the nature of the Pt compound can be selected so that in the synthesis gel, the Pt precursor is entrapped in molecular dispersion in the hydrophobic part of the composite. This may, therefore, be an original manner to take advantage of the surfactant as a dispersing agent. The same work showed, however, that a better Pt dispersion yielding a higher activity in CO oxidation for Pt/MCM-41 was obtained with the more classical post-synthesis incipient wetness impregnation by an aqueous solution of $Pt(NH_3)_4(NO_3)_2$.

Other preparation methods include incipient wetness impregnation with H_2PtCl_6 [103–105] or ion-exchange of Al-MCM-41 with $Pt(NH_3)_4(NO_3)_2$ [106]. In [107], Yao et al. introduced a new technique designated as vacuum evaporation impregnation (VEI). The silica MCM-41 was suspended in an aqueous solution of $Pt(NH_3)_4(NO_3)_2$ at pH 5, heated at 70 °C and vacuum evaporated. A very high (1.03) Pt dispersion a 1.3 wt.% loading was measured from CO chemisorption assuming a Pt/Co ratio of 1. The solids prepared by this technique were compared with materials prepared by more usual ones. Solids ions exchanged with $Pt(NH_3)^{4+}$ at pH 9 gave high loading (12.3 wt.%) but the MCM-41 collapsed partially, and at pH 5, the mesopore structure was maintained but the loading was very low (0.29%). Two materials were also prepared by equilibrium adsorption. In this case, when the precursor was H_2PtCl_6 at pH 1 essentially not deposition was observed and when $Pt(acac)_2$ was adsorbed from a dichloromethane solution the loading was 0.39% and the dispersion 0.26. Thus, the VEI technique appears as far superior.

One of the issues of significance for industrial supported Pt catalysts is their deactivation by sulfur and nitrogen compounds. It had been known for some times that the sulfur and nitrogen resistance of a noble metal can be enhanced by utilizing strongly acidic supports such as zeolites [108]. The explanation for this effect involves the interaction of a noble metal cluster with the hydrogen atom from the acidic site, yielding a delocalized positive charge which protects the metal nanoparticle from sulfidation [109]. It was indeed shown in [105] that a Pt/Al-MCM-41 having a Si/Al ratio of 16 is essentially as sulfur resistant as a Pt/USY catalyst in the hydrogenation of naphthalene in the presence of 200 ppm S. Interestingly, Pt supported on a pure silica MCM-41 showed a significant S tolerance in the same conditions.

MCM-41 supported Pt was already shown to yield superior catalysts for hydrogenation of aromatics in diesel [105] and kerosene fuels [110], hydrocracking of 1,3,5-tri-isopropylbenzene [103], isopropylation of naphthalene [103], hydrogenation of phenanthrene [103] and naphthalene [111]. Pt supported on FSM-16 was found very active in the secondary hydrogenation of the products of propylene oligomerization, yielding branched alkanes in the C_5–C_8 range [112].

The production of non-supported mesostructured Pt and Pt alloys templated by EO surfactants was already discussed above [55–57]. Another approach to the preparation of mesoscale structured nanoporous platinum sponges was recently proposed by Ryoo et al. SBA-15 [113], MCM-48 [114] or MCM-41 [115,116] pore lattice was replicated by filling with Pt wires obtained by repeated deposition with $Pt(NH_3)_4(NO_3)_2$ followed by HF dissolution of the silica wall.

2.1.2. Palladium

The introduction of a metal complex in the MMS gel synthesis was also applied by Junges et al. to the preparation of Pd-MCM-41 catalysts using $Pd(NH_3)_2Cl_2$ and $Pd(acac)_2$ as the precursor [117]. As in the case of Pt, the solids prepared by this technique were compared with materials prepared by incipient wetness impregnation of MCM-41 with $Pd(NH_3)_4(NO_3)_2$ or $Pd(NH_3)_4Cl_2$ solutions or by ion-exchange with $Pd(NH_3)_4(NO_3)_2$ [118]. It was also found that the ion-exchange method yielded a higher Pd dispersion and a higher activity in CO oxidation than the in situ addition technique. A high activity in the liquid phase hydrogenation of the olefinic bond in crotonaldehyde was also observed with the ion-exchanged solids.

Mehnert and Ying [119] and Ying [120] have demonstrated that Pd deposited on MCM-41 by chemical vapor grafting yield excellent C–C coupling catalysts.

In [121,122], an MCM-41 material was ammonium exchanged, extruded with an alumina binder, impregnated by incipient wetness with $Pd(NH_3)_4Cl_2$ and calcined at 288 °C. The resulting catalyst was found to be more active in benzene hydrogenation than Pd/USY, Pd/ZSM-5 or Pd/SiO_2 of similar Pd contents.

As mentioned above, mesostructured carbons have been prepared by Ryoo and co-workers [58,59,62–64] and by Hyeon and co-workers [60,61]. In a recent paper, it was demonstrated that MCM-48 is a better template for this type of material as the carbons prepared from MCM-41 collapse upon template dissolution. The CMK-1 prepared with MCM-48 as the template has uniform mesopores and a population of micropores which was found suitable for retention of Pd microparticles [58,123].

2.1.3. Ruthenium

Parvulescu and co-workers prepared Ru-MCM-41 and Ru-MCM-48 catalysts for the diastereoselective hydrogenation of a prostaglandin F2α intermediate [124–128]. In a first series of works, they prepared high Ru loading catalysts (3, 5 and 10 wt.% Ru) from $Ru(acac)_3$, $RuCl_3$ and $Ru(NH_3)_6Cl_3$. In all cases, reduction in H_2 at 400 °C did not yield full reduction of the metal. For example, even at 5 wt.% loading the degree of reduction determined from the oxygen balance in a TPO experiment was in the range of 87–91% [126]. In another series of two Ru-MCM-41 catalysts prepared by adsorption of ruthenocene from a diethyl ether solution with 0.13 and 0.67 wt.% Ru, the degree of reduction after calcination at 550 °C followed by reduction in H_2 at 350 °C was found to be only 16.6 and 39.5%, respectively [128]. This is associated with the ability of the silica surface to oxidize ruthenium.

In a recent work by Hartman and co-workers, Ru was supported on MCM-41, MCM-48 and SBA-15 from a variety of presursors including aqueous $RuCl_3$, $Ru(NH_3)_6Cl_3$ and $Ru_3(CO)_{12}$. After dehydration at 300 °C, the samples were reduced in dry hydrogen at 400 °C and evacuated [129,130]. $RuCl_3$ yielded the largest crystals (>4 nm) while with the other two precursors small clusters (1–2 nm) located in the channels were obtained. A detailed study of the thermal decomposition of grafted $Ru(NH_3)_6{}^{3+}$ complex by TG/MS, UV–VIS and ESR spectroscopy was conducted. The redox behavior was found to be significantly different from the one in X and Y zeolites and strongly dependent on the presence of water.

As part of a systematic investigation of bimetallic nanoparticles formed by the thermolysis of large bimetallic carbonyl clusters, Thomas and co-workers found that the $[Ru_6C(CO)_{16}Cu_2Cl_2]_2{}^{2-}$ anion is of special interest. They demonstrated that upon thermolysis of this anion at the surface of a MCM-41 support, the metal cluster is neither segregated nor aggregated [131–133]. They explained this behavior by a strong interaction of the carbonylate anion with surface silanols, by the anionic character of the clusters which keeps them apart during deposition and by the formation of Cu–O bonds which anchor the particle to the silica surface. A detailed study by temperature resolved FT-IR, X-ray absorption near edge structure (XANES) and X-ray absorption fine structure (EXAFS) as well as STEM-EDX indicated that the particle diameter was almost monodispersed with an average value at ≃1.6 nm corresponding to Cu_4Ru_{12} bimetallic particles located inside the MCM-41 channels. These materials were found active in a variety of hydrogenations of unsaturated compounds including hex-1-ene, diphenylacetylene, phenylacetylene, *trans*-stilbene, *cis*-cyclooctene and D-limonene.

2.1.4. Copper

A recent paper describes the preparation of monodispersed diameter copper particles in mesoporous alumina [134]. The precusor for this material is a binary $CuO–Al_2O_3$ mesophase produced by an original synthesis technique involving a solution of Al Keggin polycations (Al_{13}), copper nitrate and a mixture of sodium palmitate and CTAB [135]. Reducing this mesophase in H_2 at 350 °C yielded a population of copper particles with 1–2 nm size which upon calcination in N_2 then air at 500 °C yielded sintered CuO particles of about 35–40 nm, and a population of non-sintered subnanometric particles. Further reduction leads to both large monodispersed particles and Cu^0 particles of less than 1 nm. The reduced catalysts are very selectively converting cinnamaldehyde into cinnamylalcohol. This paper allows to foresee that, whenever the synthesis of multi-element mesophases will progress, a variety of interesting new mesostructured oxide supported metal catalysts will emerge.

2.2. Supported metal oxides

The deposition of an oxide over another high surface area oxide involves phenomena comparable to wetting, with some of the host–guest complexes yielding monolayers even after calcination and some others producing clustered nanoparticles of the guest [136]. Thus, the study of the formation and structure of 'MO_x' overlayers on silica is relevant for a rational preparation of MMS supported metal oxides. There are several reasons to prepare such catalysts. First the high surface area and high OH surface concentration of MMS allow for large supported oxide surface area. Their large pores also permit access to bulkier reagents. In principle, the same results may be reached by preparing a mesoporous guest oxide but the supported system is often more thermally and hydrothermally stable.

2.2.1. Titanium dioxide

MMS supported titanium oxides were prepared either as oxidation catalysts with peroxides as the oxidizing agent or as photocatalysts. The post-synthesis procedures involve the grafting of a titanium precursor such as titanocene dichloride [137–140], $TiCl_4$ [141], $Ti(OEt)_4$ [142], Ti-isopropoxide [143,144], tetrakis(dimethyl amido) titanium [144] and titanyl acetylacetonate [145] followed by calcination. Alternatively, titanium was deposited in MCM-41 from a sol obtained by controlled hydrolysis of titanium isopropoxide in the presence of ethanol and nitric acid [146]. In this work, it was shown that TiO_x loaded Al-MCM-41 was active in the photocatalytic degradation of aqueous acetophenone and more so than TiO_x/Si-MCM-41. Doping with Fe, Mn or V instead of Al suppressed completely the photocatalytic activity. In [141], $TiCl_4$ was reacted with as synthesized MCM-41 and FSM-16 and both hydrolysis of $TiCl_4$ and surfactant removal were performed at calcination. Well dispersed, isolated titania nanoclusters were produced with 30–70 Ti atoms per cluster, and remained attached to the walls via Si–O–Ti bonds. High surface area was maintained and the thermal stability of the framework was increased. The catalysts were found active in α-terpineol oxidation by H_2O_2 and photodegradation of Rhodamine CG by air-saturated aqueous solution.

Ti(IV) grafted on MCM-41 and MCM-48 were found active in peroxidative bromination of phenol red both in aqueous solution and in organic solvents [138]. This report is the first of a functional biomimic of haloperoxidase enzymes that performs well under comparable reaction conditions.

Ti was grafted on SBA-15 in [143] with Si/Ti varying from 80 to 5. The specific surface area and BJH pore diameter are slightly decreased compared to the parent SBA-15 support. The fraction of tetrahedral Ti measured by XPS changes from 83 to 25%. At $Si/Ti = 5$, the average number of Ti atom per unit surface area is $2.4\,Ti\,nm^{-2}$ compared to the value of $5.5\,Ti\,nm^{-2}$ for the 0 1 0 plane of anatase. Thus, the TiO_2 film cannot be a complete monolayer.

2.2.2. *Vanadium oxide*

VO_x centers were produced at the surface of silica MCM-48 by gas phase deposition or liquid phase impregnation of vanadyl acetylacetonate [147–149] and on Ti substituted MCM-41 impregnated with vanadyl sulfate [150,151].

In the first case, the interaction of the $VO(acac)_2$ complex with the surface involves a combination of ligand-exchange and hydrogen bond interaction of the pseudo π system of the (acac) ring and surface silanols. A maximum of 60% of the surface was covered with $VO(acac)_2$ species, which was limited by the availability of surface silanols. After calcination, vanadium is present as pseudotetrahedral VO_x species linked together with an average of 5.6 V in the surface ensembles at the concentration of $1.7\,mmol\,V\,g^{-1}$ or 8.7 wt.% V. Even at this high loading, the MCM-48 surface is only 20% covered with VO_x species.

In addition, the grafting of VO_x structures on the MCM-48 surface was also achieved using dimethyldichlorosilane (DMDCS) as a coupling agent [152–154]. Pure silica MCM-48 was first silylated using appropriate amounts of DMDCS, then hydrolyzed in water to create $Si–O–Si(CH_3)_2OH$ surface. The silylated material was used to anchor $VO(acac)_2$, followed by calcination in air at 450 °C resulting in a hydrophobic material with an improved stability towards leaching and the V^{5+} centers still accessible to water adsorption.

In the work by Kevan and co-workers [150,151], it was found that the surface VO_x species undergo strong interactions with surface Ti centers (or surface Zr centers) but not with Si or Al centers in V/MCM-41 or V/Al-MCM-41. Vanadium is monoatomically dispersed at $V/Ti < 0.17$ and forms clusters at higher vanadium loading. Calcination causes this critical V/Ti ratio to increase to 0.33, thus, enhances the V dispersion.

2.2.3. *Zirconium oxide*

Zirconium oxide supported on MCM-41 was prepared by impregnation [155] with $Zr(iPrO)_4$ or with Cp_2ZrCl_2 following in the latter case the technique describes in [137]. These catalysts once calcined were found active for the oxidation of cholesterol with a product distribution comparable to the homogeneous process using $Zr(iPrO)_4$ as the catalyst. A similar procedure was used in [156] for the grafting of Zr oxide over MCM-48 using $Zr(OPr)_4$. This technique was found to yield a higher Zr dispersion compared to incipient wetness with zirconylnitrate solutions. It was argued that MCM-48 supported Zr would be a better catalyst than hydrothermally prepared Zr-MCM-48.

Essentially, monolayer dispersion of ZrO_2 in MCM-41 obtained by incipient wetness with an acidic solution of urea and $ZrOCl_2$ was reported in [157]. Using a still undisclosed impregnation procedure, Peden obtained a 42 wt.% ZrO_2 loading in MCM-41, the monolayer coverage of which would correspond to 45 wt.%. The new method yields no Zr extraphase until the solid is heated to 850 °C. When calcination is below this temperature, the surface charge measurements allow to show essentially full coverage of the silica surface [158].

2.2.4. *Iron oxide*

Iron oxide has been deposited on M41 S materials by incipient wetness of iron(III) nitrate solutions. All reports indicate the production of nanoparticles of Fe_2O_3 by this technique. UV–VIS spectroscopy results indicate that compared to the 4.1 eV band gap of bulk Fe_2O_3, these nanoparticles display a significant quantum size effect which yields a band gap reduced to 2.1 eV [159,160]. Similar materials have been found active in the benzylation of benzene by benzylchloride [161] suggesting the formation of surface acid sites. This result would be in line with the observations in [162] according to which the formation of Fe_2O_3 nanoparticles encapsulated in the pore lattice of MCM-41 and MCM-48 is accompanied by the substitution of some trivalent iron in the silicate framework. In [157], it was shown that very high Fe_2O_3 loading can be reached without crystallization or mesopore blockage.

A detailed study of MCM-48 multiply impregnated with aqueous solutions of $Fe(NO_3)_3$ is reported in [163]. It involves a combination of XANES, EXAFS, HRTEM, selected area electron diffraction (SAED) and nitrogen adsorption/desorption measurements. Nanoparticles of hematite were found to decorate the inner walls of MCM-48. These particles showed, however, some structural disorder. No tetracoordinated iron was observed but the hexacoordinated iron(III) ions are less strongly held together than in bulk crystalline hematite. This phase is randomly distributed in the pore lattice and not in a crystalline state even at loadings as high as 42.5 wt.% of Fe_2O_3.

2.2.5. Cobalt, nickel, molybdenum and tungsten oxides

These oxides are lumped together here as they enter into the composition of the oxidic precursors which once sulfided constitute the active phase of HDS catalysts (see Section 3.1). Relatively, few studies have been devoted to MMS's supported oxides of these four metals. Cheng et al. [164] prepared Al-MCM-41 supported MO materials by first exchanging the support with NH_4NO_3 and impregnating the resulting solid with ammonium heptamolybdate. The dried and calcined catalyst was tested in the hydrodemetallation of nickel tetraphenylporphyrin. The conversion was shown to depend on both the Al content of the support and the pore diameter.

Morey et al. made a detailed study of Mo and W oxides supported on MCM-48 and produced by the reactions of surface silanols with $Mo_2(OEt)_{10}$ and $W(OEt)_5$, respectively, followed by calcination [165]. The maximum loading before appearance of bulk metal oxide clusters is 7.4 mol% (0.37 atom nm^{-2}) for W and 2.1 mol% (0.15 atom nm^{-2}) for Mo much lower than for Zr, Ti and V deposited using similar approaches. In both cases the UV–VIS spectra show two peaks at 216 and 260 nm assigned to isolated tetrahedra and isolated octahedra, respectively. The photoacoustic FT-IR spectra show lines at 931 and 921 cm^{-1}, respectively, assigned to Mo–O–Si and W–O–Si asymmetric stretching vibrations. Both solids were found to be active for the peroxidative bromination of a large organic substrate, phenol red.

Brégeault et al. proposed a new approach to the grafting of tungsten oxo (peroxo) species in MCM-41. They used oxoperoxophosphatotungstates $Q_2[(HPO_4)\{W_2O_2(\mu\text{-}O_2)_2(O_2)_2\}]$ denoted PW_2, for electrostatic anchoring on silica MCM-41 ($Q = NR_4^+$ or H_3O^+) [166]. The technique provides well dispersed isolated oxo species largely separated from one another with no WO_3 phase segregation. The 8.2 wt.% W catalyst prepared with this technique was found to be extremely active and selective in the epoxidation of cyclooctene by H_2O_2 at room temperature [166].

Hartmann et al. succeeded in stabilizing Ni(I) at the surface of MCM-41. They first ion-exchanged Ni(II) ions by liquid (L) and solid state reactions (S) of $NiCl_2$ with MCM-41 and Al-MCM-41. They found by ESR that stable Ni(I) can be generated by thermal or hydrogen reduction as well as by γ-irradiation at 77 K of (L) NiAl-MCM-41 [167]. Similarly prepared solids were used as catalysts for ethylene dimerization, isolated Ni(I) was identified as active species. A sample prepared by introducing $NiCl_2$ in the synthesis gel of MCM-41 was, however, more active [168,169].

Lensveld et al. have compared the deposition of Ni oxide over MCM-41 by incipient wetness impregnation with nickel nitrate and citrate [170]. From this comparison, it is concluded that impregnation with a nickel citrate solution is an excellent method allowing to graft up to 10 wt.% Ni in MCM-41 with a high dispersion.

2.2.6. Chromium oxide

Highly dispersed supported Cr oxides are used as commercial catalysts for polymerization (see Section 3.3), dehydrogenation and selective catalytic reduction of NO_x. An ethylene polymerization catalyst was obtained by grafting Al-MCM-41 with $Cr(acac)_3$ from a methanol solution followed by calcining at 500 °C [171]. Before calcination DRS and ESR investigations showed signals typical of Cr^{3+} in strongly distorted complex. These signals do not disappear entirely upon calcination. Cr^{6+} and some Cr^{5+} appear but the oxidation is incomplete suggesting the presence of small clusters of Cr_2O_3 in the calcined material.

In a recent study, Zhu et al. discussed the immobilization of Cr oxides in Me-MCM-41, Me standing for Al, Ti or Zr [172]. The solids were prepared by incipient wetness impregnation with aqueous Cr_2O_3 at a loading of 2 wt.% Cr. It was found that Cr interacted strongly with the surface Ti centers of Ti-MCM-41 so that Cr(VI) and Cr(V) were highly dispersed on this support whereas Cr_2O_3 appeared in (Zr, Al, Si)MCM-41.

2.2.7. Zinc oxide

Zhang et al. have synthesized ZnO nanoparticles using MCM-41 as the host material [173]. To this end they functionalized the pore surface with ethylenediamine groups which they used as adsorption centers for Zn^{2+} from zinc acetate solutions. ZnO particles were obtained after calcination of the resulting (Zn-ED-MCM-41) material at 600 °C. Up to ZnO loading of 9.3 wt.% they could observe high blue shifts in the DR-UV–VIS spectra corresponding to quantum size effects and photoluminescence ascribed to oxygen vacancies centres. The method was said to be also applicable to the deposition of Co oxide.

Another method was utilized by Kowalak et al. [174]. They impregnated MCM-41, HMS and SBA-3 silica with an ethanol solution of $Zn(acac)_2$, yielding Zn/Si ratio as high as 0.15. After solvent evaporation, the modified samples were calcined at 530 °C. HMS and SBA-3 better retained their structure after Zn modification by this technique than MCM-41. The Zn modified materials have acquired ion-exchange properties, and some catalytic activity in 2-propanol dehydration reflecting the presence of acid sites associated with tetragonal Zn.

2.2.8. Manganese oxide

Excellent propene and CO oxidation catalysts were obtained by Burch and co-workers [175–177] by supporting Mn oxide on MCM-41. The preparation technique involved the adsorption from gas phase of bulky $Mn_2(CO)_{10}$ carbonyl followed by calcination at 300 °C. IR analysis showed the presence of surface grafted carbonyl species which disappeared upon calcination. At 8.5 wt.% Mn loading no crystallized Mn oxides were present and change was observed in the lattice parameters of the MCM-41 support. EXAFS studies of this material suggest that the Mn-oxo species are tetracoordinated and of MnO_4^-, Mn_2O_7 or $Mn_2O_6^{2-}$ structure.

2.2.9. Copper oxide

Zecchina et al. studied a series of catalysts prepared by impregnation of MCM-41 with an aqueous solution of $Cu(NO_3)_2$ [178]. A thermal treatment at 600 °C in vacuum allowed to produce Cu_2O/MCM-41 by self reduction of the CuO deposit formed by thermolysis of the copper nitrate. The Cu_2O loading was up to 10 wt.%. A FT-IR study of CO adsorbed on these solids allowed to conclude that at low loading coordinatively unsaturated Cu(I) ions are atomically dispersed and anchored to the framework. At higher loading, Cu_2O aggregates into microcrystals.

2.2.10. Rare earth metal oxides

van Bekkum and co-workers [179,180] introduced La oxide layers in Cs/MCM-41 materials which they had found to be of poor regenerability as reflected by a loss in surface area and by clustering of the Cs_2O particles [181,182]. The mixed La, Cs oxide materials were prepared by evaporation of a methanol solution of cesium acetate and lanthanum nitrate containing a suspension of MCM-41 or HMS particles and calcination at 500 °C. The mixed oxides were found much more stable. TPD of CO_2 showed an increased capacity of adsorption upon addition of the La (equimolar Cs/La and 5 wt.% La) but the metal/CO_2 ratio remains essentially unchanged. By contrast TPD of NH_3 showed a high increase in NH_3/metal ratio due to the stronger Lewis acid character of La_2O_3. These catalysts were found active in a variety of base catalyzed reactions including isomerization of phenylalkanols and their aldol condensation, Michael additions of ethyl cyanoacetate to unsaturated esters, and its Knoevenagel condensation to benzaldehyde.

Schueth et al. [157] have reported that rare earth oxides including La oxides can be introduced by incipient wetness of nitrate solutions in MCM-41 and SBA-15 up to 50 wt.% oxide loading with a high dispersion.

2.3. Acid catalysts

2.3.1. Acidic properties by atomic substitution

All siliceous mesoporous materials present a very low acidity only due to the silanol groups on the surface. Just like in zeolites, substitution of silica by trivalent atoms in the inorganic framework of mesoporous molecular sieves was performed in order to create acidity. Incorporation of heteroatoms in MCM-41 and HMS has been extensively discussed, by Tuel [183]. In this section, interest is restricted to the substitution of trivalent cations for silicon, including Al^{3+}, B^{3+}, Ga^{3+}, Fe^{3+}, in mesoporous silica. Boron-substituted MCM-41 was, for example, synthesized by Trong On and co-workers [184,185]. The effect of different treatments and various cations on the state of boron and the stability of the MCM-41 structure was studied. These materials are active for the Prins condensation of isobutylene with formaldehyde to isoprene with 100% selectivity [186]. Gallium-modified mesoporous materials were the object of a recent review [187], and will, therefore, not be dealt with here. Many studies have reported the activity in acid catalysis of Al-, Ga- and Fe-MCM-41 [188,189] or -MCM-48 [190] and indicate that the acid strength and catalytic activity decrease in the order Al $>$ Ga $>$ Fe. It was shown that Fe-MCM-41 presented weaker acidity essentially composed by Lewis acid sites. Similarly, Lewis acid sites were observed upon introduction of iron in MCM-48 [191] (also for vanadium-MCM-41 [192]). Most of framework iron was expelled during thermal treatment [193], but it was observed that extra-framework species enhanced the thermal and hydrothermal stability of the mesoporous host [194]. By contrast, insertion of aluminum induced the highest acidity with formation of both Brønsted and Lewis sites. In any case aluminum represents the best candidate for incorporation in the silica framework.

For the substitution of silicon atoms by aluminum, the protonic acid form is obtained by exchanges of the calcined MMS with ammonium salts followed by calcination or by direct synthesis for calcined amine templated HMS [195]. The state of aluminum may be observed by ^{27}Al MAS NMR, which evidences the tetra-coordinated framework species (Al(IV) observed at $\delta = 52$ ppm), generating Brønsted acid sites and octa-coordinated extra-framework species (Al(VI) observed at $\delta = 0$ ppm), generating Lewis acidity. In the case of zeolites, post-synthesis treatments, such as steaming permit to control the density and strength of acid sites. In amorphous MMS, the Si/Al molar ratio is only controlled by the concentration of aluminate species in the synthesis gel. A number of studies has dealt with characterization of MMS acidity [189,196–203]. In general, the acid sites number increases with the aluminum content, but the acid strength is very low and often compared to the ones in amorphous silica-alumina. Increasing aluminum amounts in the mesopore structure generate a decrease in the well defined hexagonal order, as observed by the worse definition of XRD bands [196,201,204] and a significant contraction of the pore diameter after calcination, indicative of the thermal instability. Al-MMS presents, therefore, a low thermal and hydrothermal stability strongly depending on the Si/Al ratio and the intra- or extra-structure location of aluminum [205]. Before calcination aluminum species are, predominantly tetra-coordinated but after thermal treatments part of them is extracted from the framework. Both, the limit of stability and of incorporation in the inorganic walls depend strongly on the aluminum source used at the synthesis [5,206–214]. For example, Trong On et al. reported the stability of Al-MCM-41 under different treatments, vapor treatment, acidic and basic conditions. Five-coordinated aluminum was observed in unusually large fraction in absence of extra-framework aluminum species [214]. Reddy and Song [208] studied the effects of four aluminum sources: sodium aluminate (SA), aluminum isopropoxide (AI), aluminum sulfate (AS) and pseudo boehmite (PB). The framework stability and acid strength are related to incorporation in the inorganic framework (tetrahedral species) in the following order: SA $>$ AI $>$ AS $>$ PB. The non-suitability of PB as aluminum source had been reported previously [196]. Most often, the studies evidenced a better incorporation of aluminum when using monomeric species (like sodium aluminate) than oligomeric ones (like aluminum sulphate) in the synthesis gel. In this sense, Badamali et al. [212] reported that the differences in the isomorphous substitution of Al in the silicate matrix had to be correlated with the reactive species generated in the alkali solution. Using monomeric species the same Si/Al ratio was observed in the synthesis gel and the final material. Si/Al molar ratios as low as one were reported in [215–217], the Loewenstein rule was respected and aluminate and silicate species alternated in the polymerized amorphous structure. Reddy and Song claimed the acidities of Al-MCM-41 comparable to H-Y zeolite, when the aluminum source was chosen correctly [209]. As discussed above, Al(IV) species represent exchanged Brønsted acid site. The proton may be exchanged by other cations. Yiu and Brown [218] reported that H^+, and Al^{3+} both generate Brønsted acidity and that Fe^{3+} generates more Lewis acidity. Consequently, H^+-AlMMS and Al^{3+}-AlMMS were active in the alkylation of toluene with benzyl alcohol catalyzed by Brønsted sites. Fe^{3+}-MCM-41 showed, however, activity for alkylation of toluene with benzyl chloride which is known to be catalyzed by Lewis sites. Enhancement of MMS hydrothermal resistance by chemical modifications [219–223], salts effects [224–226], post-synthesis restructuration [227,228] or pH adjustments [200,229–231] was reported. All the methods involving limited thermal treatment permitted to improve the stability of the alumino-silicates: elimination of exchange post-synthesis thermal operations to obtain the protonic form [195,232], template extraction instead of calcination or partial condensation during the cationic exchange in acidic media [233].

Recently, Kan et al. [234] reported the formation of mesoporous materials from aluminosilicates and gallosilicates of Kanemite structure. The acidity observed on these aluminosilicates type materials was similar to the ones in Al-MCM.

Introduction of aluminum by direct synthesis in SBA-15 mesoporous materials yielded a much higher stability to thermal and hydrothermal treatment than Al-MCM-41 [235–237]. Aluminum was incorporated essentially in the inorganic structure creating a high catalytic activity for cumene cracking. It must be underlined that this reaction was performed in steaming conditions for which MCM-41 type materials were not resistant enough [238].

A new class of acidic porous clay heterostructures (PCH) has been proposed by Pinnavaia and co-workers [239–242] as mesoporous acidic catalysts. These materials are obtained by surfactant-directed assembly of open framework silica within the two-dimensional interlamellar galleries of clays. PCH materials exhibit regular porosity in the supermicropore to small mesopore range (15–25 Å) and a very high thermal stability. Consequently, Pinnavaia and co-workers foresee promising application in acidic catalysis.

2.3.2. Acid phase deposition

2.3.2.1. Aluminum. In order to preserve the thermal stability of all silica MMS while creating high acidity, efforts have been made for post-synthesis alumination of all silica mesoporous materials [243–251]. The aluminum was deposited by impregnation (aluminum isopropoxide, $Al(NO_3)_3$, aluminum chlorohydrate). For example, impregnation with $Al(NO_3)_3$ [250] has yielded both Lewis and Brønsted acid sites with a mild acid strength and the number of both types of acid sites increased with decreasing Si/Al molar ratio. This method improved accessibility since acids are only located on the surface (not in the walls) and the uniformly hexagonal framework of MCM-41 was effectively maintained. Some authors even reported the enhancement of hydrothermal and mechanical stability of aluminum impregnated MMS compared to all silica ones [245,251]. In the case of aluminum isopropoxide impregnated siliceous MMS [244], it was demonstrated by ^{27}Al MAS NMR that, after the thermal treatment, part of the aluminum was anchored in tetrahedral coordination (Al(IV)) and part had formed Al(VI) species. Increasing the aluminum content resulted in an increase in framework aluminum species and consequently in a higher Brønsted acidity. Same conclusions were reported for the post-synthesis alumination of SBA-15 with trimethylaluminum, in this case AlSBA-15 displayed a higher density of Brønsted acid sites than Al-MCM-41 obtained in the same manner [252]. Hamaguchi and Hattori [253] made a similar study for FSM-16 and reported the formation of alumina particles at high aluminum content. Aluminum chlorhydrate (ACH) impregnated from aqueous media [245,247] induced an increase in wall thickness resulting in a higher mechanical and hydrothermal stability. Enhanced Brønsted acidity and steaming resistance were observed even under the severe conditions of regeneration in FCC [246]. ACH grafted materials presented a higher catalytic activity than $AlCl_3$. $AlCl_3$ grafted MMS were, however, efficient acid catalysts in less demanding reactions such as alkylation (see Section 3.2).

In summary, grafted ACH-MMS generated stable mesoporous materials showing high Brønsted acidity. Mokaya even claimed a reinsertion of extra-framework species upon treatment with an aqueous NH_4OH solution [248]. Attention must also be paid to the accessibility of tetrahedral aluminum species. Indeed, Luan et al. [254] evidenced that, for a complete incorporation of aluminum species in siliceous SBA-15, part of Al was inaccessible within the pore walls. Recently, Mokaya [255] reported the enhancement of steaming stability when the siliceous mesoporous host possesses thick pore walls. In general, it is not possible to reach a perfect control of the type of surface acid site generated but it was found that alumination by chemisorption of $AlMe_3$ on the surface of MCM-41 yielded purely Lewis acid sites [256].

2.3.2.2. Heteropoly acids (HPA). Heteropoly acids (HPA) having Keggin structure present a high acidity, particularly the 12-tungstophosphoric acid

($H_3PW_{12}O_{40}$ or HPW) [257], but their use as acid catalysts is limited by a very low surface area (below $10\,m^2\,g^{-1}$). MMS represent, therefore, excellent supports for the dispersion of HPA. HPA have been supported on silica MMS enhancing their catalytic activity [258–260], but the dispersion and stability of the acidic phase were not perfectly controlled. Introducing HPA can induce structure distortion and even framework destruction at high loading [261]. Blasco et al. [262] have reported the formation of clusters at high HPA loading which partially blocked the pores and as a consequence the catalytic activity in alkylation reactions decreased. The problem has been partially resolved by increasing the pore diameter from 40 to 66 Å, but the cluster formation was not eliminated. The authors concluded then that in order to increase the catalytic performance of HPA supported over MMS, the dispersion had to be controlled. Jalil et al. [263] have underlined the importance of the impregnation solvent to obtain better dispersions. To this end, Peden and co-workers proposed a very promising new way to obtain a high dispersion on mesoporous hosts [264–267]. Metal cationic salts ($CsCO_3$) are first deposited on the mesoporous surface, forming a first precursor impregnated support. This material was calcined to graft the alkali metal over the support by creating a covalent bond. The heteropoly acid, dissolved in a solvent having a limited potential for dissolution of the first precursor, interacted with the primary deposited phase and formed the metal heteropoly acid salt ($Cs_xH_{3-x}PW_{12}O_{40}$). This acidic phase was insoluble in polar solvent and consequently presented a high stability to leaching and limited cluster formation by mobile species. It was clearly demonstrated by TEM that the previous method led to the formation of clusters whereas a good HPA dispersion was obtained with the new method [268]. The authors tested these new materials in acid catalyzed alkylation (see Section 3.2) in which very promising results were obtained.

2.3.3. *Acidic properties by organic grafting*

This approach was initiated by earlier developments of selective adsorbants for heavy metals. To this end alkylthiols had been grafted over Montrillonite clay [269] due to their ability to bind heavy metals and to form monolayers [270–274]. The grafting is performed by silanation, for example, by 3-mercaptopropyltrimethoxysilane (MPTMS). In this search for higher trapping capacity, alkylthiols were grafted over porous clay heterostructure (PCH) [275], MCM-41 [275,276], HMS [275,277], SBA-15 [278] and MSU [279] mesoporous materials and encouraging results were obtained in trapping mercury. The possibility to oxidize the thiol groups (SH) into the corresponding sulfonic acid (SO_3H) in H_2O_2 solution or HNO_3, opened a new class of Brønsted acidic organic–inorganic mesoporous materials [280–288]. Van Rhijn et al. summarized (Fig. 1) the various preparation procedures [282].

- By co-condensation: the alkylthiol molecules are introduced in the synthesis gels, and the hybrid materials are obtained directly. In general, this co-condensation method is used when the template can be eliminated by solvent extraction. It was reported that this synthesis method permits to graft a higher content of MPTMS.
- By post-synthesis silylation over the calcined mesoporous material.
- By coating for which the calcined surface was hydrated before proceeding to the grafting step. A MPTMS monolayer surface coverage of 76% was reported [276,289].

Another method, not shown in Fig. 1, which consists in the grafting of the alkoxysilane during template extraction was also proposed [290–292].

By co-condensation, a better three bond grafting of MPTMS was expected, but recently Diaz et al. [287] evidenced that the molecules are anchored by only two Si–O condensation bonds, like in the post-synthesis method. In co-condensation, synthesis of the hybrid material in basic media showed a higher thiol loading (4–5 $mmol\,g^{-1}$ of silica) than the other methods (1–2 $meq\,g^{-1}$ of silica). After the oxidative treatment, only a small fraction of the grafted molecules presented acidic properties [280–283]. For example, Lim et al. [280], for their direct synthesis of the hybrid MCM-type material with an initial loading of 4.7 $mmol\,g^{-1}$ of silica, reported that after oxidation with an aqueous solution of 20% HNO_3, the proton exchanged capacity was only 1.76 $meq\,g^{-1}$ of catalyst.

Margolese et al. [288] reported the co-condensation of the same thiol molecules during acidic synthesis of

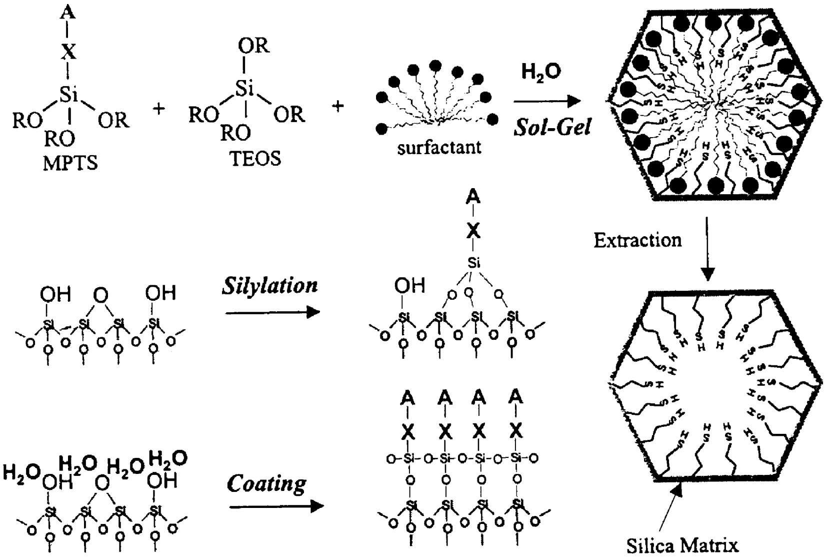

Fig. 1. Mercaptopropyl encapsulation into mesoporous materials by direct synthesis or post-synthesis pathways [282].

non-ionic templated mesoporous materials (SBA-15). Nearly all the thiol molecules were oxidized and represented acid sites after oxidation (H_2O_2), but the mesoporous silica was partially destroyed. The authors proposed then to proceed during the synthesis and added H_2O_2 in the gel. A better conservation of the mesoporous long range order was observed. Co-condensation of two functional groups was already proposed in [293] (phenyl or methyl alkoxysilane). Mori and Pinnavaia [294] have reported recently the optimization of 3-mercaptopropyl-functionalized HMS with nearly three times more grafted molecules per unit mass of silicon compared to MCM-41 or SBA-15 mesostructures. Some of these materials present very interesting activities in esterification of D-sorbitol, hydroxylation–condensation of methylfuran with acetone [282], esterification of glycerol for monoglycerides synthesis [283,287]. For microporous materials, Jones and co-workers [295–297] have developed organic functionalized molecular sieves (OFMS) as new hybrid organic–inorganic acidic materials. Phenyltrimethoxysilane was introduced in the synthesis gel of a pure-silica zeolite beta. The phenyl groups were easily sulfonated by SO_3 in vapour phase to form acid sites. This method can represent another approach for the synthesis of acidic hybrid mesoporous materials. The synthesis of phenyl-functionalized mesoporous materials was already proposed in [293,298,299].

2.3.4. Mesoporous zeolitic materials

The hydrothermal instability and mild acidity of related mesoporous alumosilicate molecular sieves compared to those of zeolites is due to their amorphous character. This limits their potential applications in petroleum refining and fine chemical synthesis [20]. Therefore, to upgrade the performances of mesoporous molecular sieves and zeolites, much effort has been undertaken to synthesize a new type of materials, which would combine the advantages of these two kinds of molecular sieves. Recent studies have shown that the walls of mesostructured silica-alumina can be converted to a zeolitic product, but the microporous zeolite phase is separated from the mesostructure, giving rise to FAU/MCM-41 and ZSM-5/MCM-41 composites containing inter-connected mesopore and micropore lattice [300–303]. These composites, however, exhibited an enhanced acidity for hydrocarbon cracking in comparison to mechanical mixtures of ZSM-5 and MCM-41 and an improvement in steam stability for purely siliceous composition [302]. The synthesis of a partially crystalline bimodal pore system with combined micro- and mesopores, designated as ITQ, has been achieved by delaminating the layered zeolite MCM-22 and ferrierite (FER) [304, 305].

Entrapped unit cells of ZSM-5 contained in Al-MCM-41 and Al-HMS were prepared by ion-exchanging the mesoporous aluminosilicates with tetrapropylammonium cation (TPA^+) as a MFI structure-directing agent and then digesting the mesopore structures in glycerol at 120 °C [306]. Pinnavaia and co-workers [307,308] recently reported an approach to more acidic and hydrothermally stable mesostructures based on the direct assembly of nanoclustered aluminosilicate precursors that normally nucleate zeolite crystallization. The assembly of zeolite seeds such as ZSM-5, FAU and beta seeds under hydrothermal conditions in the presence of cetyltrimethylammonium ions afforded hexagonal MSU-S structures. The resulting mesoporous materials are highly acidic and remarkably steam stable. A similar zeolite beta type of materials was also prepared from silica and sodium aluminate in the presence of co-templates of tetraethylammonium hydroxide and cetyltrimethylammonium bromide [309]. In the later cases, the XRD patterns did not show crystalline features, however, further evidence for the retention of protozeolite units cells was provided by IR spectroscopy and the acid catalytic activity of these materials toward cumene cracking.

Very recently, we described a new general methodology for the production of a new type of materials with semi-crystalline zeolitic mesopore walls. This procedure involves a templated solid-state secondary crystallization of zeolites starting from the amorphous SBA-15. These materials are designated as UL-zeolites [310–313]. The zeolite phase in UL-zeolite was characterized upon crystallization by wide-angle XRD diffractograms indicating that the initially amorphous walls of the mesoporous material are progressively transformed into crystalline nanoparticles. Furthermore, the bright- and dark-field TEM images recorded on the same area of UL-ZSM-5 indicate that nanocrystals are embedded in the continuous amorphous inorganic matrix to form semicrystalline wall structures while preserving the mesoporous structure. This indicates that the pore walls consist of nanocrystals of this zeolite. These materials have much stronger acidity compared to those of the corresponding amorphous alumosilicates and a much improved hydrothermal stability. These features open new possibilities for using this type of materials as acid catalysts.

2.4. Base catalysts

Basic heterogeneous mesoporous materials were less discussed than acidic ones. Nevertheless the first studies have shown a promising perspective in using basic MMS as catalysts. Mesoporous materials can be imparted basic properties by: (i) cation-exchange (Na^+, Cs^+, ...) [180–182,314]; (ii) impregnation [180,182,315,316]; (iii) functionalization with organic molecules (like amines) by post-synthesis treatment [316–328] or direct introduction in the synthesis gel [329–333].

As discussed in Section 2.3, introducing aluminum in the MMS framework induces negative charges, which generate acidity when compensated by a proton. Then a simple cationic exchange with alkali salts permits to create basic properties. Kloetstra and co-workers first proposed to cation-exchange acid sites with Na^+ or Cs^+ on calcined samples in aqueous solutions of alkali salts [180,181]. These authors also proposed to impregnate MMS with a concentrated solution of Cs acetate, which was then eliminated by high temperature decomposition. The basic strength of these materials was studied by CO_2 temperature programmed desorption (TPD) [182] (Fig. 2). This analysis pointed out that CO_2 desorbed at higher temperature from impregnated materials than from exchanged ones, which is indicative of a higher basic strength. Moreover, incorporation of basic species by cationic exchange is limited by the exchange capacity of the support. Increasing the aluminum framework content results in an increase of the exchange level and this goes with a basic strength increase, a phenomenon well known in zeolites [334–337]. The XRD characterization of Cs-MCM-41 showed a loss of long-range order with increasing Cs loading. A drastic decrease in specific surface area and pore volume was also observed by adsorption/desorption of nitrogen. The authors first interpreted these observations by a structure collapse. However, they underlined that the decrease in specific surface area, mesopore volume and diameter can also be associated with oxide inclusion in the internal mesoporosity [180]. The instability of the Cs species was indeed evidenced by ^{133}Cs NMR. The hydrated Cs ions are very mo-

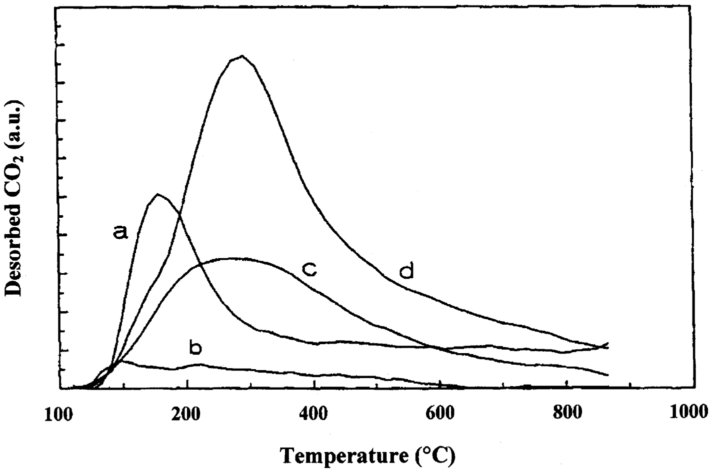

Fig. 2. CO_2 TPD plots of alkali containing MCM-41 with Si/Al = 12.5: (a) Na-MCM-41 exchanged; (b) Cs-MCM-41 exchanged; (c) Cs-MCM-41 impregnated (19.2 wt.% Cs); (d) Cs-MCM-41 impregnated (27.5 wt.% Cs) [182].

bile in both exchanged and impregnated samples. In the latter case, after hydration and dehydration, a reorganization of Cs species was observed, which is probably due to oxide clusters formation. Then the leaching of the basic particles in aqueous solution cannot be excluded. Kloetstra et al. [180] impregnated MMS simultaneously with Cs and La. The composite phase showed a stronger interaction through an eventual La–O bond with the inorganic framework. This permitted a stabilization of the basic catalysts, which were found unaffected by hydration. It is important to note that the solvent used for exchanges or impregnations must be chosen taking into account the instability of the silica structure in the presence of basic solutions. Therefore, this work provides a key example of stabilizing the basic active phase by the grafting of additional supported oxide on the silica support.

Brunel et al. [317] have presented the first works on the functionalization of MMS surface by alkoxysilanes and particularly amine terminated ones. The basic phase was bound covalently to the inorganic surface. The fonctionalisation process consists in a grafting of the organic basic molecule over the calcined MMS in anhydrous refluxing solvent (toluene) under an inert atmosphere. Hydrolysis and condensation of alkoxysilanes with silanol surface groups result in a covalent linkage between the organic and inorganic phase yielding the formation of hybrid materials (Fig. 3, pathway 1). Introducing organic molecules inside the pore lattice involves a decrease in mesopore volume, surface area and diameter as demonstrated by adsorption/desorption measurements (Fig. 4 and Table 1). In Table 1, the BET parameter C values are representative of the interaction between the adsorbed nitrogen molecule and the material surface. Changes in this parameter mean changes of this interaction, which reflects a modification in surface polarity. In this case, the decrease in C value reflects an increase in the surface hydrophobicity induced by grafted organic molecules. This new lipophile character will facilitate the introduction of the organic reactants during catalytic reaction. A really judicious approach, employed by these authors in their synthesis of new basic mesoporous materials, is the two-step functionalization reported in Fig. 3. First, 3-chloropropyltriethoxysilane molecules were grafted (pathway 1) and the resulting Cl-MMS was treated again in an appropriate solvent with an excess of tertiary amine, piperidine for example, to modify the chloro functional group in a 3-piperidinopropylsilylated-MMS. By the first pathway primary amines [319,320] and diamines [328] can be grafted over the MMS surface. By the second pathway, the modification of the chloro group through the partial nucleophilic displacement of the chlorine, can be done with tertiary piperidines [319,320] and very strongly basic guanidines like 1,5,7-triazobicyclo[4.4.0] dec-5-ene (TBD) [321]. The latter compound can be employed for catalytic re-

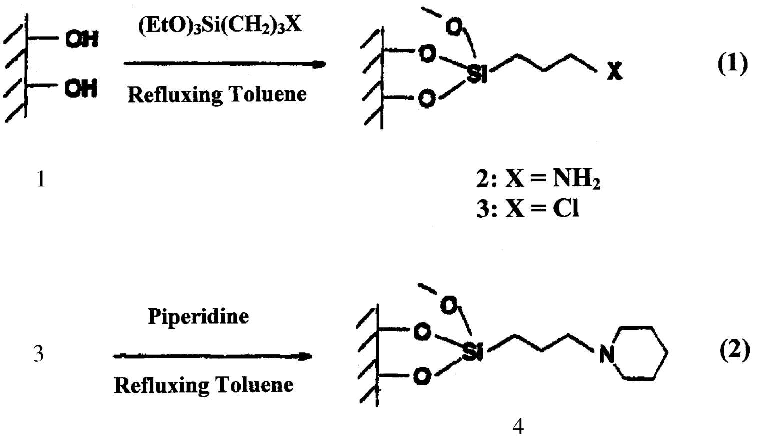

Fig. 3. One-step amine (1) or two-step piperidine (2) grafting of MMS calcined surface [319].

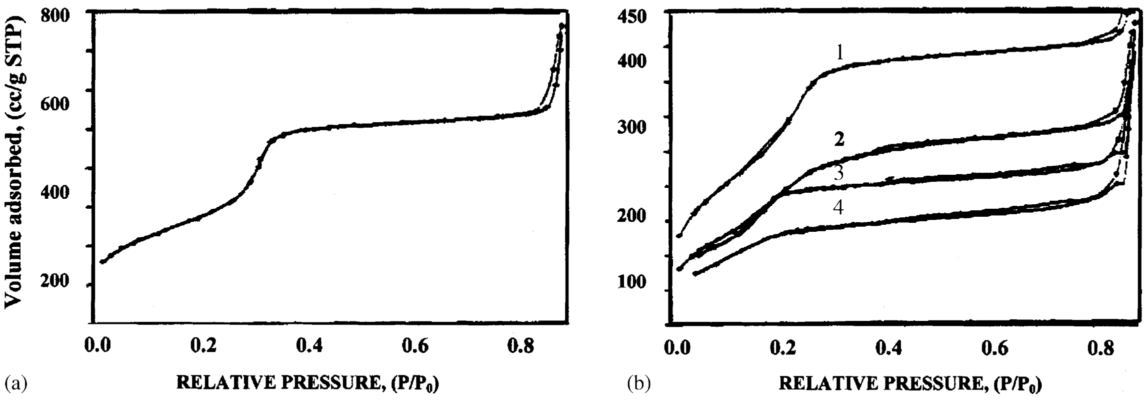

Fig. 4. Nitrogen sorption isotherms at 77 K of (a) calcined MMS; (b): (1) 3-chloropropylsilylated-MMS; (2) 3-(2-pyridinomethyl)aminopropylsilylated-MMS; (3) 3-(bis-[3-salicyliden-amino)propyl]carbamatopropylsilylated-MMS; (4) 3-(2-isonicotinamidoethyl)aminopropylsilylated-MMS [317].

Table 1
Textural and thermodynamic parameters deduced from nitrogen sorption isotherms [317]

Materials	Surface area ($m^2 g^{-1}$)	Mesoporous volume ($ml\,g^{-1}$)	Diameter (Å)	BET parameter C
MMS[a]	920	0.76	33	100
Cl-MMS[b]	851	0.57	27	60
PyrMeN-MMS[c]	577	0.35	24	50
NH_2EtNH-MMS[d]	586	0.29	20	22
SalDPT-amino-MMS[e]	608	0.31	20	19
IsoNicEtN-MMS[f]	436	0.22	13	28

[a] Calcined support.

[b] 3-Chloropropylsilylated-MMS.

[c] 3-(2-Pyridinomethyl)aminopropylsilylated-MMS.

[d] 3-(2-Aminoethyl)aminopropylilylated-MMS.

[e] 3-(Bis-[3-salicyliden-amino)propyl]carbamatopropylsilylated-MMS.

[f] 3-(2-Isonicotinamidoethyl)aminopropylsilylated-MMS.

action requesting a strong basicity, like Michael reactions and transesterifications, where promising results were obtained. The displacement of the chloro group in a non-anhydrous solvent can, however, produce formation of HCl and this acid might poison the base sites. To prevent this phenomenon, Subba Rao et al. [338] proposed, in the case of TBD active phase, to use an other alkoxysilane molecule. The surface was covered with oxirane groups by reaction of the SiOH with 3-trimethoxysilylpropoxymethyloxirane. Then TBD reacts under remarkably mild conditions with epoxide groups without formation of any by-product. This is an important point for using these materials at commercial scale.

An important aspect of using these hybrid organic–inorganic basic catalysts stems from the elimination of surface silanols, which yields an inhibition of undesired surface activity. To this end, the samples were treated by hexamethyldisilazane, which is well known for his high reactivity towards OH groups of untreated silica surfaces [339,340]. This operation must be done before step 2 to eliminate hydrogen bond interaction between the OH and the basic site. As discussed in Section 3.2, the inhibition of surface hydroxyl groups improves the selectivity for base catalyzed reactions. The efficiency of this end-capping technique was, therefore, thoroughly discussed by Sutra et al. [324]. The authors evidenced by ^{29}Si and ^{13}C RMN MAS that the hexamethyldisilazane treatment did not eliminate all the hydroxyl groups from the MCM-41 surface.

All the above discussion deals with the active phase introduction by post-synthesis treatment. The alkoxysilane functional groups can also be introduced directly in the MMS synthesis gel. This kind of one pot synthesis was first proposed by Macquarrie [329]. This author prepared HMSs, by the neutral amine synthesis route, which permits elimination of the template by extraction with ethanol without degradation of the organic grafted molecules. In this way, loadings of primary amine up to 2.2–2.7 mmol g^{-1} were obtained, depending on the triethoxysilane/aminopropylsilane molar ratio of the synthesis gel [331], while maintaining the porosity [330]. By contrast, with post-modified MMS 1.9 mmol g^{-1} is achievable for primary amine loading [322], whereas the two step post-synthesis method does not permit to introduce more than 1 mmol g^{-1} of amines [316].

An original approach for the syntheses of basic mesoporous organic materials was proposed by Miller and co-workers [341,342], consisting in the formation of heterogeneous base catalysts through a cross-linked lyotropic liquid crystal (LLC). The monomers are constituted by carboxylate polar groups and polymerizable styryl lipophile groups. Co-polymerization with divinylbenzene permits the formation of a network while maintaining the nanoscale order of the original LLC phase. The close packing of the carboxylate charged groups inside the pores controls the basicity. These materials were tested in the heterogeneous base catalyzed Knoevenagel condensation of ethyl cyanoacetate with benzaldehyde.

As a general conclusion of the different syntheses of basic mesoporous silica, it must be reminded that the ion-exchange method results in mobile active species on the surface, which leads to an instability upon hydration of the catalysts. The same phenomenon is observed for impregnated MMS, with the exception of some composite materials such as the LaCs-MCM-41, which present a higher stability due to stronger interactions with the host material. The covalent binding of a base by grafting an organic amine yields an especially interesting technique. It permits to obtain very stable materials while maintaining the mesoporosity. The mechanism of grafting molecules over the silica surface is still a matter of discussion [325]. As developed in Section 3.2, the basic strength may be controlled by the choice of the grafted organic molecules.

2.5. Anchored metal complexes

The heterogenization of homogeneous catalysts on the channel walls of MMS, which is expected to combine the advantages of homogeneous catalysts with the easy product separation and catalyst recovery of heterogenous ones, constitutes a rapidly expanding research area. The larger pore diameter channels of MMS with a high surface concentration of silanol groups relative to that of microporous zeolites permits the fixation of entire chiral metal complexes and organometallic moieties onto the inner walls of these high surface area solids. This can be conducted using three principal approaches: (i) the direct grafting of organometallic complexes onto the inner MMS walls; (ii) the functionalization of MMS silanol groups with silane coupling agents followed by the anchoring of metal complexes to the surface; and (iii) the ship-in-a bottle immobilization of metal complexes, e.g. the complex is prepared inside mesopores by either ion-exchange or adsorption and immobilized by electrostatic attraction and sterical hindrance.

2.5.1. Direct grafting of metal complexes

The attachment of guests to the MMS walls can be achieved by the direct reaction of surface hydroxyl groups with reactive ligands. The direct grafting of titanocene dichloride onto the pendant SiOH groups of the MCM-41 inner walls via the reactive chloride ligands was first reported by Maschmeyer et al. [137]. The high dispersion of grafted complexes on the surface was achieved due to surface silanols activated by triethylamine. After calcination, four-coordinated titanium species were present as demonstrated by EXAFS spectroscopy. The resulting titanium centers showed a high catalytic activity for the epoxidation of alkenes. Recently, the authors [343] also described a simple grafting procedure of $Ti(OSiPh_3)_4$ onto the internal surface of MCM-41 to produce an epoxidation catalyst of high activity and selectivity. In addition, the presence of the phenyl groups on each titanium center of the catalyst increases the longevity of the activity of the catalytic centers towards attack from atmospheric moisture. This methodology is adaptable to many other oxides and related systems [147,153,171,175,243,344–351], including, for example, a catalyst designed for selective low-temperature oxidation of cyclohexane with anchored oxo-centered trimeric cobalt acetate [349]. Other examples such as vanadium-grafted MCM-41 using vanadylacetylacetonate or vanadium metallocene [344] and manganese-grafted MCM-41 via the surface immobilization of gaseous $Mn_2(CO)_{10}$ [175] as oxidation catalysts were demonstrated. Furthermore, iron(II)-phenanthroline, $[Fe(Phen)_3]Cl_2$, was grafted on the MCM-41 pore walls in alcohol, and shown to be active for phenol hydroxylation [345]. Chromium acetylacetonate complexes, $[Cr(acac)_3]$, were grafted on the surface of Al-MCM-41 and these materials were found to be active for polymerization of ethylene [171]. Another example was reported by O'Brien et al.: by means of the ring-opening reaction of the strained metallocenophane, $[Fe\{(\eta\text{-}C_5H_4)_2SiMe_2\}]$, the anchoring of ferrocenyl end groups inside the mesopore channels can be achieved [350]. The bimetallic $Me_3SnMo(CO)_3Cp$ complex was also introduced into the MCM-41 channels; this complex was anchored via the oxophilic trimethyl tin component to the mesopore walls [351].

2.5.2. Indirect grafting

A number of studies involving surface MMS modification and functionalization have been carried out to develop new adsorbents/catalysts [152,153,219,220, 290–292]. There are three types of SiOH groups over siliceous MCM-41 surface [219,220], e.g. isolated single, hydrogen bonded and geminal SiOH groups, of which only the single and geminal SiOH groups are responsible for active silylation. Trimethylsilylated MCM-41 exhibit more hydrophobic surface properties. The anchoring of organometallic complexes onto the porous walls of MMS by grafting a silane neutral ligand through covalent Si–O–Si can be achieved. The neutral ligands are mainly amine or phosphine functions directly grafted to the silica surface by a silylation procedure. These types of ligands permit attachment of complexes through a coordination bond with metal centers [352,353]. For example, Cauvel et al. [319] functionalized MCM-41, with 3-chloropropyltriethoxysilane and demonstrated the generalized synthesis method described in Section 2.4 to introduce organic bases (such as primary and tertiary aminofunctions). Functionalized silica MCM-41 was obtained through the treatment with a toluene solution containing the respective 3-aminopropyl- or 3-chloropropyl-silane coupling agent. The chloropropyl sample was subsequently treated with a piperidine solution to yield grafted tertiary amino groups, i.e. the 3-piperidinopropyl moiety (Pip-MMS). The resulting materials were subsequently treated with hexamethyldisilazane vapor at 453 K in order to selectively poison the residual OH groups [340]. These new hybrid MMS showed high activity and regioselectivity for glycidol ring-opening with fatty acids under mild reaction condition. With the same approach, Sutra and Brunel [318] and Brunel et al. [354] prepared MCM-bonded manganese(III) Schiff-base complexes. The chloro atoms of MCM-41 coupled 3-chloropropyl-triethoxysilane were replaced by the pentadentate ligand 3-[*N*,*N*-bis-3-(3,5-di-*tert*-butylsalicylidenamino)-propylamine (salpr). The introduction of Mn atoms was achieved by reacting surface *t*-salpr ligands with $Mn(acac)_2$. Both activity and stability of these immobilized complexes were also studied in the styrene epoxidation using different oxidants [355]. Covalently anchored Mn(II) salen complexes on MMS were also prepared by ensembling step-wise salen entities and subsequent complexation with Mn and directly condensing silylated prefabricated Mn(II) salen complex onto MCM-41 [356]. Furthermore, manganese(II) 2,2′-bi-pyridine complex incorporated in MCM-41 exhibited higher catalytic activity for the oxidation of styrene than the corresponding homogeneous catalyst [357]. Additionally, copper(II) and manganese(II) phenanthroline complexes grafted onto MCM-41 modified with 3-aminopropyl were also described [358]. Recently, heterogeneous Grubbs' type catalysts were prepared by ligand exchange reaction between Ru–alkylidene complexes (Grubbs' type) and a phosphinated mesoporous matrix (P-MCM-41) [359]. These catalysts exhibited high catalytic activity for both ring opening metathesis polymerization (ROMP) towards norbornene and ring closing metathesis (RCM) of diallylamine and diethyldiallylmalonate. Zhang et al. [360] and Zhang and Ying [361] introduced transition metal dopants into the MCM-41 silicate framework to provide distinct sites for covalent bonding with the intentionally chosen NH_2 substituents on porphyrin macrocycles. This strategy effectively fixates the porphyrins without engaging their metal centers, leaving the later accessible as active sites for oxidation catalysis. Chiral salen Co(III) (Oac) catalysts were also prepared through multi-step anchoring and exhibited high enantioselectivity of epoxides to diols [362]. Additionally, various transition metal complexes (e.g. Mn, Cu, Co) in functionalized MMS and their catalytic activity in the oxidation of aromatic amines was also demonstrated [363]. Furthermore, the grafting of rare-earth silylamide complexes, $[\mathrm{Ln}\{\mathrm{N(SiHMe_2)_2}\}_3(\mathrm{thf})_x]$ ($\mathrm{Ln} = \mathrm{Sc, Y, La, Nd, Er}$ or Lu), onto Al-MCM-41 via surface organometallic chemistry was achieved. $AlMe_3$-directed desolvation and alkylation reactions were also discussed [347,364].

Various organometallic chiral catalysts may be tethered by functionalizing the MMS surface with organic groups such as amines, carboxyls and phosphines. This opens routes to the preparation of novel catalysts consisting of large concentrations of accessible, well-spaced and structurally well-defined active sites (Fig. 5) [365,366]. The key concept in this approach is the interaction of the substrate with both the pore wall and the chiral directing groups. The confinement of the substrate in the mesopore channel should lead to a larger influence of the chiral directing group on the orientation of the substrate relative to the reactive catalytic center as compared to the situation in solution. This is not only the case for enantioselective reactions but also for regioselective ones.

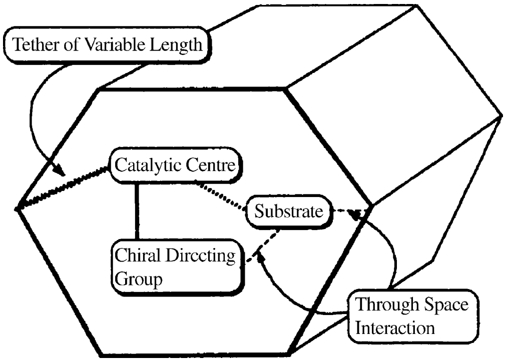

Fig. 5. Schematic representation of the confinement concept [365,366].

For example, the chiral ligands based on bis-diphenyl-phosphinoferrocen (BPPFA) would be particularly attractive for tethering into MMS, because their planar chirality never undergoes racemization, they are synthetically very accessible [367]. Furthermore, these chiral chelate ligands possess functionalities suitable for reaction with pore-bound tethers. The opportunities for variations of the R groups and hence, the steric/electronic characteristics for both metal complexation and tailoring of the chiral environment offer great scope. The homogeneous transition metal complexes of BPPFA are active for a variety of stereoselective reactions. Thus, with the chiral MMS derivatives, catalytic regio- and enantio-selective syntheses might be explored in the fashion typified by Corma et al. [368] in the rhodium/USY system, where an increase in enantiomeric selectivity from 75 to 95% could be achieved and is thought to have been caused by the additional substrate-pore wall interaction as shown in Fig. 5. Shephard and co-workers [366,369] have developed an interesting methodology to anchor various transition metal complexes to the internal surface of the MCM-41 support. The exterior surface of the MMS support was first deactivated by reacting the pendant silanols with an appropriate amount of Ph_2SiCl_2 under non-diffusive conditions. The chiral catalysts were obtained from the ligand 1,1′-bis(diphenyl-phosphino) ferrocene (dppf) anchored to the inner walls of the materials and co-ordinated to Pd(II). This chiral catalyst showed a higher regioselectivity and enantioselectivity in the allylic amination of cinnamyl acetate (so-called Trost–Tsuji reaction) and in the hydrogenation of ethyl nicotinate to ethyl nipecotinate than the one prepared using a non-porous silica as the support and than the corresponding homogeneous catalyst [369,370]. Furthermore, the same research group [371] presented a useful TEM method for directly imaging the position of functional tethers grafted onto the MCM-41 surface. They examined two MCM-41 samples, on which bulky clusters, $[Ru_6C(CO)_{14}(\mu^6\text{-}C_6H_4C_{10}H_{20}O_6)]$, were anchored without and with poisoning of the external silanol groups with Ph_2SiCl_2 before the multi-step modification. A HR-TEM micrograph of the former sample showed clusters bound predominantly to the outer surface of the derivatized MCM-41 particles. In contrast the latter sample showed uniformly distributed clusters within the MCM-41 channels (dark spots) and little or no contrast at the outer surface of the particles. This indicates that with the poisoning treatment, the tethers were forced to bind almost entirely to the internal surface of MCM-41. These results provided a foundation for the future examination of the effects of mesopore confinement on catalysts.

The capacity of chiral phosphines to bind the platinum group metals has led to an enormous diversity in the metals/reaction available to such sites. It would be possible to insert not only, similarly to Hayashi and co-workers [372,373], gold (aldol cyclization), palladium (Trost–Tsuji reaction) and platinum (hydroformylation), but also a further set of metal centers, source from various ruthenium cluster species which potentially allows an assessment of catalyst dispersion [373]. The addition of group VIII and IX metals would allow access to asymmetric hydrogenation [374], hydroformylation [375] and carbamate synthesis [376].

Finally, the various developments in the area of confined chiral catalysts and the related discussion of possibilities in mesopore derivatizations with chiral, catalytically active dppf complexes, highlight an exciting area of chemistry in which the mesoporous dimension has significant potential to make an impact.

2.5.3. Ion-exchange

When hexagonal ordered mesoporous materials are synthesized using cationic surfactants, these surfactants are organized in the form of a cylindrical micellar structure with hydrophilic positive ends coulombically interacting with silica pore surfaces. The weak Coulombic interaction can be easily broken and the cationic surfactant replaced by another cation through ion-exchange. In fact, this exchange reaction was employed to remove surfactant molecules from the ordered inorganic materials synthesized through an ionic surfactant templating method. For example, Bonneviot and co-workers [377,378] developed a new methodology for the surface functionalization of as-synthesized mesoporous silica prepared by cationic surfactant through the ion-exchange reaction between cationic surfactant molecules (e.g. cetyltrimethylammonium, CTA^+) and cationic coating complexes (e.g. cobalt complexes). The positively charged complexes may efficiently replace the positively charged surfactant molecules through ion-exchange (Fig. 6) and characterized by XANES, extended EXAFS and UV–VIS spectroscopies [377,378]. This method allows to create highly reactive silanolato groups and to introduce a variety of types of transition metal complexes without loss of mesopore structure. Following the same approach, Dai et al. [379] described a new method to increase the concentration of the functional ligands coated on the mesopore surface; $Cu(aapts)_2{}^{2+}$ and $UO_2(aapts)_2{}^{2+}$, [aapts = 3-(2-aminoethylamino) propyltrimethoxysilane] were first exchanged with cationic surfactant molecules (CTA^+) and followed by a removal of Cu^{2+} or $UO_2{}^{2+}$ cations from surface complexes using a 1N nitric acid wash solution. The loading of resulting functional ligands (s-aapts = surface-bonded aapts ligand) by this method is higher than those of the conventional coating method [379].

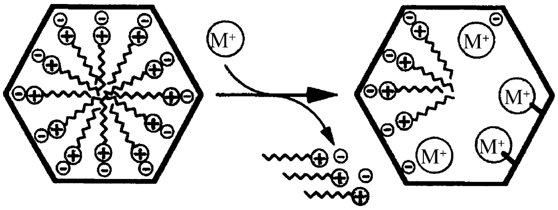

Fig. 6. Ion exchange process between hydrophilic heads of CTA^+ surfactant and transition metal complex ions allowing to introduce metal complex ion at the MCM-41 surface [377,378].

Simultaneous surfactant extraction and surface silylation on MCM-41 prepared by either the alkaline route or the acidic route were also achieved in an exchange process with organosilanes replacing surfactants [290,291,380]. Lin et al. also [380] found that the surfactant-silyl exchange is greatly favored for mesoporous material prepared by the acid route compared to that by the alkaline route. This indicates that in the acidic route, the surfactant/silicate interaction is weaker; the weak hydrogen interactions between the silica wall and the surfactant ($S^+X^-I^0$, S^0I^0) would facilitate extraction of the surfactant by polar solvents under mild conditions. In contrast, this exchange process is slow for alkaline-synthesized M41S mesoporous materials due to the strong electrostatic interactions between surfactant cations and silicates (S^+I^-).

Several researchers have exploited the direct ion-exchange of cationic metal complexes toward either hydroxyl groups or charge-compensating cations such as Na^+, H^+ on the calcined MMS alumino-silicate surface [345,381,382]. For example, Liu et al. [345] treated ion-exchanged MCM-41 silica with phenanthrolineiron(II) chloride and were able to immobilize this complex. A higher activity for the oxidation of phenol with H_2O_2 was obtained with the immobilized ion complex than with the corresponding homogeneous catalyst. However, a significant leaching was noted. This could be overcome when the metal complexes were anchored onto the walls of MCM-41 silica with an organic linker. Furthermore, Kim et al. [381] reported the immobilization of Mn(II) bipyridine complexe cations, $[Mn(bpy)^2]^{2+}$, in Al containing MCM-41 channels by ion-exchange. This immobilized complex catalyst exhibited a higher catalytic activity for styrene oxidation than the corresponding homogeneous catalyst and showed no significant loss of catalytic activity when recycled. In addition, chiral Mn(salen) [382] and Co(salen) [383] complexes were ion-exchanged by charge-compensating Na^+ and immobilized on Al-MCM-41 and Al-FSM-16. The chiral Mn(salen) catalyst exhibited high enantioselectivity in the asymmetric epoxidation of styrene without any leaching.

Finally, the immobilization of enzymes to form heterogeneous bio-catalysts is an exciting goal. In this context, the embedding of enzymes such as cytochrome c, papain and trypsin by physical adsorption was reported and showed a clear dependence on enzyme size. Silanation of the mesopore opening after enzyme adsorption enhanced its stability and minimized leaching of enzyme into solution at high pH. The entrapped trypsin enzyme exhibited some activity in the hydrolysis of *N*-benzoyl-a-DL-arginine-4-nitroanilide. Although its stability was also enhanced by immobilization, it was less active than the corresponding homogeneous catalyst [137,317,384–405].

2.6. Non-siliceous mesoporous metal oxides

MMS type materials composed of transition metal oxides are attractive heterogeneous catalysts, catalyst supports and nanocomposite host materials for a wide range of applications. Several reviews [20,21,406] and a number of publications [8,46,134,135,397,407–475] were devoted to this type of materials. We, therefore, outline here only the major synthesis pathways and refer the reader to these reviews for further information. Several mesostructured metal oxides, such as oxides of Sb, Fe, Zn, Pb, W and Mo, were prepared first by Huo and co-workers [8,407] through a generalized electrostatic approach. Unfortunately, most mesophases collapsed upon surfactant removal either by solvent extraction or by calcination. This could be due to the lack of complete condensation of the inorganic framework.

Through a number of alternative surfactant-assisted synthesis approaches, non-silicate mesoporous metal oxides were achieved using low molecular weight surfactants, e.g. titania [408–412], niobia [397,413], tantala [414–416], alumina [46,417–424], tin oxide [425] manganese oxide [426,427], ceria [428] and zirconia [429–440], vanadium oxide [441,442] aluminophosphates [443–459], vanadophosphates [460–464] and doped materials [134,135,465–472], etc. However, these mesoporous transition metal oxides are somewhat less satisfactory than M41S in terms of thermal stability. Bagshaw and Pinnavaia [46] used non-ionic surfactants to synthesize mesoporous alumina in neutral media and suggested that the resulting mesoporous materials with wormhole-like channels are assembled by hydrogen-bonding interaction of the inorganic species with the surfactant agents. Antonelli and Ying [408] prepared mesoporous TiO_2 using a modified sol–gel method, in which a titanium alkoxide was hydrolyzed in the presence of an alkyl phosphate surfactant. The authors reasoned that the hydrolysis and condensation rates were controlled using a chelating agent such as acetylacetone. A surface area of about 200 $m^2 g^{-1}$ was achieved. However, phosphorus from the surfactant was bound so strongly to the molecular sieve that it could not be removed by either calcination or solvent extraction. The residual phosphorus could poison the catalytic surface sites [411]. This limits the use of these materials as catalysts and catalyst supports. On the other hand, Trong On [412] reported an effective route for the synthesis of mesostructured lamellar and hexagonal phosphorus-free titania using a modified sol–gel method in conjunction with the cationic surfactant, cetyltrimethylammonium chloride ($C_{16}TMA^+Cl^-$), and soluble peroxytitanates as the source of titanium. Hexagonal mesoporous TiO_2 after calcination at 300 °C possessed a narrow pore-size distribution and a surface area of 310 $m^2 g^{-1}$. This strategy, thus, obviates the presence of phosphorus in mesoporous titania as well as the use of acetylacetone and other chelating agents to control the condensation reaction. Additionally, Antonelli and co-workers [397,413,414] developed the so-called ligand-assisted synthesis. The mechanism is based on the fact that bonds are formed between the inorganic species and the surfactant amine headgroups (S–I). Following this approach, mesostructured niobium [397,413] and tantalum oxides [414] were prepared. Suib and co-workers [426,427] prepared mixed-valent semiconducting mesoporous manganese oxide with hexagonal and cubic structures and showed that these materials are catalytically active.

Mesoporous zirconium oxides are of particular interest for acid catalysis. Zirconium oxide contains both weakly acidic and basic surface sites providing for high activity in reaction requiring acid–base bifunctional catalysts. Several synthesis routes, leading to mesostructured zirconia were described, which are based on two main synthesis pathways, a templating and a scaffolding mechanism. The main difference is that the templated materials are distinguished by their ordered pore system, while the ones made via scaffolding have a disordered pore arrangement, however, the materials were found to collapse upon calcinations. Furthermore, Ciesla and co-workers [431,432] reported that ordered mesostructured zirconia could be thermally stabilized by the existence of an appreciable amount of sulfate or phosphate groups. In addition, Huang et al. [433] prepared a spongelike mesoporous zirconia with some degree of pore wall crystallinity and found that the crystallization of the zirconia resulted in collapse of the mesoporous structure. Stable and well-defined mesoporous zirconias were also prepared through a one-pot synthesis with anionic and cationic surfactants and depend highly, however, on the nature of the headgroup [434,435]. It is noted that by introducing dopants such as phosphates and sulfates, modified zirconia were not only improved in terms of thermal stability, but also exhibited higher acid strength and acidity for acid catalyzed reactions; for example, phosphated zirconia is mildly acidic and sulfated zirconia is strongly acidic or even superacidic [436]. Mesoporous metal oxides had improved stability and catalytic performance by introducing a variety of metal dopants such as Y, Pt, La, Co, W, Mo, Cr, Cu, Ti [134,135,465–472]; for example, Ozin et al. used cetyltrimethylammonium bromide as a template to synthesize mesoporous yttria–zirconia and (nickel/platinum)–yttria–zirconia with a high surface area and a high thermal stability [465,466]. For all of the above non-silica materials prepared using low molecular weight surfactants, the resulting mesoporous materials have, therefore, generally small pore sizes (∼4 nm) and their channel walls exclusively amorphous. Furthermore, most of the above syntheses were carried out in aqueous solution using metal alkoxides as inorganic precursors.

As discussed in Section 1, Yang et al. [473,474] proposed a general synthesis procedure involving amphiphilic poly(alkylene oxide) block copolymers in non-aqueous solutions as structure-directing agents which may be applied to the preparation of a variety of non-siliceous mesostructured metal oxides. This procedure was indeed used in the preparation of well ordered large pore (up to 14 nm) mesoporous TiO_2, ZrO_2, Nb_2O_5, Ta_2O_5, Al_2O_3, SnO_2, WO_3, HfO_2 and several mixed oxides [473–475]. These mesoporous metal oxides are thermally stable and have robust inorganic frameworks and thick pore walls, within which a high density of nanocrystallites can be nucleated and grown. These mesoporous metal oxides, therefore, can be produced with semicrystalline channel walls, which are expected to provide new opportunities for modifying their properties.

2.7. Transition metal cation-substituted mesoporous silica

Substitution of transition metal cations such as vanadium, titanium, chromium, zirconium for silicon in microporous molecular sieves framework generated catalytically active materials. In particular, silica analogs of zeolites ZSM-5, ZSM-11 and beta modified by substitution of Si by one of these cations yielded remarkable liquid phase partial oxidation catalysts using peroxides as the oxidant. The pore diameter of these materials is, however, limited to 5–6 Å which imposes severe restrictions to the size of the reactant molecules [476,477].

To solve this steric limitation, many researchers have emphasized the synthesis of large- and ultralarge-pore transitional cation modified mesoporous silica (MS) molecular sieves in order to oxidize bulky substrates.

2.7.1. Titanium

The preparation procedures of Ti-MMS materials are based on the direct introduction of precursors such as tetraethylorthotitanate (TEOT) [478,479], titanium isopropoxide ($Ti(\textit{iso}OC_3H_7)_4$) [40,48,143], titanium butoxide ($Ti(OBu)_4$) [480,481], Ti(IV) bis(ethyl acetoacetato) diisopropoxide [46,482] or titanium sulfate ($(Ti(IV)OSO_4)$) [483] in the synthetic gel. The matching of the rates of hydrolysis/condensation of titanium and silica precursors governs the use of various titanium sources [46,482]. This allows to avoid phase segregation or anatase formation. Mixture of fumed silica [480,481,484,485] and TMA silicate solution [480,481] or TEOS [486,487] were used as silica precursors. The latter silica source is of frequent use.

2.7.1.1. Ti-MCM-41/MCM-48. Corma et al. [487] were the first to report the synthesis and use of Ti-MCM-41 (the SiO_2/TiO_2 molar ratio was of 60 and surface area of $936\,m^2\,g^{-1}$) as catalyst for selective hydrocarbons oxidations. These catalysts with pore size of about 2–3 nm were active for olefin epoxidation and sulfide oxidation to sulfoxides and sulfones. However, they remain less active for small olefins epoxidation than TS-1 and Ti-β but they are interesting as catalysts to oxidize large molecules which cannot access the internal active sites of titanium zeolites [487]. Recently, the highest titanium content ($Si/Ti = 1.9$) incorporated into MCM-41 using complexing agents (titanatrane and silatrane) without subsequent phase segregation was reported [488]. Much work was done concerning Ti-MCM-41 catalysts but only a few on titanium incorporated in MCM-48 (Ti-MCM-48) [489–492]. These Ti-MCM-48 catalysts have their catalytic properties improved owing to the three-dimensional geometry of their pore network compared to hexagonal Ti-MCM-41 which facilitates the diffusion of large molecules [492].

2.7.1.2. Ti-HMS. The synthesis and catalytic applications of titanium-substituted HMS (Ti-HMS) were reported [11,40,41,48,493–496] as well as the detailed description of their physicochemical properties [494]. The Ti-HMS catalyst first prepared (the SiO_2/TiO_2 molar ratio was of 100) by Tanev et al. [40] showed a better activity in various oxidation reactions such as aromatic compounds oxidation. For example, the comparison of activities for 2,6-di-*tert*-butylphenol (2,6-DTBP) oxidation with Ti-MCM-41 and Ti-HMS revealed the higher efficiency of Ti-HMS [487]. Other advantages of Ti-HMS materials are their preparation made at room temperature, their simple solvent extraction of template due to the neutral templating route used. Their pore sizes are comparable to those of Ti-MCM-41, even though the neutral surfactant ($C_{12}H_{25}NH_2$) used to assemble Ti-HMS (1.0 mol% Ti) is smaller than the ionic one ($C_{16}H_{33}N(CH_3)_3{}^+$) in Ti-MCM-41 (1.0 mol% Ti) [48]. Pinnavaia and Zhang [48] reported the good selectivity of Ti-HMS and Ti-MCM-41 for benzene hydroxylation to phenol compared to TS-1. They also showed the higher activity of Ti-HMS than Ti-MCM-41 for the liquid phase oxidations of large substrates (see Table 2, [48]). The Ti-HMS materials exhibit higher effective diffusivities compared to Ti-MCM-41 materials because of their large particle mesopore volume ($1.11\,cm^3\,g^{-1}$ in the 10–30 nm range) compared to Ti-MCM-41 ($0.03\,cm^3\,g^{-1}$). The opposite effect was observed by Trong On et al. [493] for α-pinene epoxidation using *tert*-butylhydroperoxide as the oxidizing agent with similar epoxide selectivities. The textural mesoporosity plays a key role in the catalytic reactivity enhancement and its presence depends on the synthesis conditions especially when a water-rich solvent is used [43]. In absence of textural mesoporosity, activities of both Ti-HMS and Ti-MCM-41 remain

Table 2
Catalytic activity of Ti-substituted (2 mol%) mesoporous molecular sieve silica [48]

Catalyst		TS-1	Ti-MCM-41 (S^+I^-)	Ti-MCM-41 ($S^+X^-I^+$)	Ti-HMS (S^0I^0)
MMA oxidation	Conversion (mol%)	2.5	4.0	6.2	6.8
	MPV[a] selectivity (mol%)	78	93	93	93
Styrene oxidation	Conversion (mol%)	8.4	10	23	28
	PhCHO selectivity (mol%)	71	82	78	77
	Epoxide selectivity (mol%)	14	6.2	4.1	4.7
	Diol selectivity (mol%)	4.5	3.8	8.2	9.6
2,6-DTBP oxidation	Conversion (mol%)	5.0	39	22	55
	Quinone[b] selectivity (mol%)		91	90	91

[a] MPV is methyl pyruvate.

[b] Quinone selectivity is expressed as the cumulative selectivity of monomer and dimer quinone. MMA and DTBP stand for methyl metacrylate and di-*tert*-butylphenol, respectively. Non-ionic [(S^0I^0)] and ionic [(S^+I^-), ($S^+X^-I^+$)] templating pathways.

similar for aniline oxidation as reported by Gontier and Tuel [496] and are lower than that of TS-1 for linear olefins oxidation.

2.7.1.3. Ti-, V-, and Zr-MSU. The idea to control the rates of Ti-alkoxide and TEOS hydrolysis leads to the synthesis and catalytic application of titanium-substituted MSU materials [46,482]. Bagshaw et al. [483] reported the synthesis in acidic and basic media of well-defined mesoporous metallosilicate [M]-MSU-*x*; where M stands for Ti, V and Zr and *x* designates the non-ionic surfactant used as template. They emphasized the importance of the solubility of metal oxy-hydroxy cationic precursors and the control of the simultaneous condensation of metal oxo-salts and TEOS under acidic and basic conditions. These two new pathways were complementary to those described by Attard et al. [497] and Zhao et al. [49] under acidic conditions. According to them, these syntheses could still be improved. In this line, the [M]-MSU-*x* pore morphology improvement using post-synthesis hydrothermal treatment was reported [498].

2.7.1.4. Ti-SBA-15. Corma [19] noted that for substrates sizes above 1.2 nm the pore diameters can affect the activity and selectivity of transition metal substituted MMS in liquid phase processes. This may have prompted for the synthesis of transition ions modified SBA-15 materials. In fact, Luan et al. [143] reported the use of incipient-wetness impregnation (see Section 2.2) to insert titanium species into SBA-15 due to the difficulty of the direct incorporation in the framework under strong acidic media (2 M HCl). The maximum concentration of titanium obtained was of about 6 at.% relative to silicon [143]. Higher titanium loadings yield titanium dioxide (anatase) which reduces the pore diameter [143].

Ti-MMS were also reported to be excellent photocatalysts for CO_2 reduction (Ti-MCM-41/48) [499] and for acetic acid decomposition (Ti-MCM-41) (39 times higher than commercial anatase) [500]. Recently, Ti-MMS were used as nanoflask for polymerization reaction (see Section 3.3) [501].

2.7.2. Vanadium

Vanadium MS were synthesized using vanadate salts such as ammonium vanadate (NH_4VO_3) [502], vanadyl sulfate ($VOSO_4{\cdot}5H_2O$) [484,485,503] or vanadium chloride (VCl_4) [502].

Vanadium incorporation in MCM-41 framework yield efficient catalysts for partial oxidation of cyclododecanol, and 1-naphtol [484]. V-MCM-41 and V-HMS materials were active for the hydroxylation of 2,6-DTBP to the corresponding benzoquinone using H_2O_2 as oxidant [504]. In addition, V-HMS catalysts are more active for phenol, naphthalene and cyclododecanol oxidations with H_2O_2 or *tert*-butyl hydroperoxide as the oxidizing agent [504] compared to Ti-HMS [505]. In both gas and liquid phase reactions, the catalytic performance is far below that of titanium- or vanadium-silicalites [506]. Morey et al. [490] reported the synthesis of V-SBA-3 (Si/V $<$ 18) and the possible obtention of V-SBA-1 with Si/V ratio larger than 18. Recently, a new synthesis of well ordered cubic V-SBA-1 (Si/V < 20) under highly acidic conditions was reported [502]. These V-SBA-1 materials have a bimodal pore system (≈2 nm and ≈4 nm diameters). In addition, the three-dimensional structure of the pore network is also advantageous for diffusion of reactants and products [502]. Luca and co-workers [442,507] demonstrated the dependence of surface area on the synthesis medium for their V-MMS materials. These surface areas increase from 270 to 1100 $m^2 g^{-1}$ with a decrease in vanadium content from 32 to 8 at.% using ethanolic medium. V-MMS like Ti-MMS were also active and selective catalytic materials for decomposition, reduction and oxidation reactions as reported by Raimondi et al. [508] for group IV transition metal incorporated MMS.

2.7.3. Zirconium

Zirconium-substituted MMS [481,509,510] can be produced using Zr precursors such as zirconyl nitrate ($ZrO(NO_3)_2 \cdot 2H_2O$) [511], zirconium *n*-propoxide [512], zirconium isopropoxide [481], Zr(IV)OCl_2 [483]. Tuel et al. [481] and Occelli and Biz [512] showed opposite effects of increasing Zr content in MMS framework on MMS surface areas using non-ionic and ionic routes, respectively. According to Occelli and Biz [512], the surface area, pore volume and average pore diameter of their Zr-MMS decreases from 1136 to 482 $m^2 g^{-1}$ with the SiO_2/ZrO_2 ratios from 26.0 to 3.2 while these properties are not dependent on Zr content as reported by Tuel et al. [481]. This variation of properties was shown to be also dependent on pH as observed by Jones et al. [510] for their materials. For example, Zr-MMS (with same Si/Zr ratio of 50) synthesized one in basic and the other in acid conditions gave Zr-MMS with different surface areas of 1302 and 1140 $m^2 g^{-1}$, respectively, for the same average pore diameter of 2.8 nm. Nevertheless, the Zr-MS catalysts were shown to be active and selective for the oxidation of various substrates such as norbonylene, aniline, cyclohexane using both H_2O_2 and TBHP as oxidizing agents and remained less selective than Ti-MMS for epoxidation reactions [481,509,510]. According to Tuel and co-workers [481,509] and Jones et al. [510], this can be related to the strong Lewis acidity of Zr^{4+} cation. Independently, Wang et al. [511] reported the presence of both Lewis and Brönsted acidities in their synthesized Zr-MCM-41 materials by a near neutral route. This acid strength is in linear correlation with the Zr content and acid site density [510]. The solids can be used in acid catalysis [511]. Zr-MMS was used as support for chromium species for the oxidation of CH_2Cl_2 [513].

2.7.4. Iron

Fe-containing MS can be prepared using iron salts such as iron nitrate [$Fe(NO_3)_3 \cdot 9H_2O$] as iron source [486,514–516]. Modification of MMS (MCM-41, MCM-48 or HMS) by incorporation of transitional ions (Fe^{3+} ion for example) is well documented [183,194,486,514–516]. The major problem with iron atoms is the formation of extraframework iron species during template removal by calcination [194,518]. The synthesis of Fe-MMS with maximum incorporation of Fe (Si/Fe ratio of about 10) was performed in neutral conditions using primary amines [183]. Using solvent extraction for the removal of the organic template (compared to conventional thermal treatment) preserves both the mesopore structure and the tetrahedral coordination of the cation in the framework [183,517].

These Fe-MMS were also found to be very active and selective catalysts (100%) for the benzylation of benzene [161]. They were used for oxidation (hydroxylation of aromatic compounds and epoxidation of olefins) [519], polymerization [45,520] reactions and oligomerization of propene [183,517]. Unfortunately, the activity of these oligomerization catalysts could not be enhanced by decreasing the Si/Fe ratio below 200 when prepared in basic medium [194,518].

2.7.5. Other elements

Recently, the synthesis and characterization of MMS (MCM-41, HMS, MCM-48) modified by Sn [521,522], Mo [45], Mn [523] or Cr [45,489,490,520] were reported. For example, chromium salts such as chromium nitrate ($Cr(NO_3)_3 \cdot 9H_2O$) [161] were used as Cr source in Cr-MMS preparation. Zhang and Pinnavaia [489] showed that unlike Ti, the leaching of Cr from the sample when washed with diluted acetic acid is of about half the amount of Cr. However, this does not exclude the use of this catalyst (Cr-MCM-41) for the oxidation of phenol, 1-naphtol and aniline with dilute H_2O_2 solution [520]. A synthesized chromium modified MCM-48 (Cr-MCM-8) showed an excellent catalytic activity (100% conversion at 350 °C) and catalytic stability toward oxidative depletion of trichloroethylene [477]. This Cr-MCM-48 was also used for the oxidation of methyl methacrylate and styrene with H_2O_2 [489]. More recently, Pak and Haller reported the synthesis and characterization of Cr and V modified KIT [524] but no catalytic application was reported.

The selective oxidation of aromatics as well as the hydroxylation of phenol and 1-naphtol were carried out using Sn-MCM-41 [521] while Sn-HMS catalyses lactide ring opening and its polymerization and the hydroxylation of benzene [522]. Ziolek et al. [525] reported the potential catalytic application of niobium-incorporated MCM-41 (Nb-MCM-41) for the decomposition of NO, the reduction of NO with NH_3 and the oxidation of thioethers with H_2O_2. Tsai et al. [526] showed the efficiency of Cu(II)-substituted MCM-41 in the oxidation of trimethylphenol (TMP) to the corresponding trimethylbenzoquinone (TMBQ) under mild reaction conditions.

Lanthanum (La) and cerium (Ce) incorporated MCM-41 materials are active acid catalysts and the cerium incorporation improves the thermal and hydrothermal stability as well as the catalytic performance of MMS material [527]. Dai et al. [528] reported the synthesis and the highest catalytic performance of Mo-substituted SBA-1 for the partial oxidation of methane compared to Mo-impregnated pure siliceous SBA-1 and amorphous silica.

2.7.6. H_2O_2 decomposition

Transition metal ion-substituted silica MMS are amorphous and possess a large density of surface silanol groups. These silanol groups were shown to be responsible for the low efficiency of hydrogen peroxide in partial oxidation reactions as demonstrated by Carvalho et al. [529] using a series of redox mesoporous catalysts M-MCM-41 (where M = Fe, Ti, V, Cr, Mn or Co). They concluded that the low hydrophobicity of M-MCM-41 materials compared to TS-1 yields a higher adsorption of H_2O_2 followed by its decomposition (see also [530]). Same observations were made by Zhang et al. [44] using various oxidation catalysts with same titanium loading (2 mol%) which were synthesized by different templating mechanisms (Table 3, [44]). They also showed that the highest H_2O_2 decomposition rate is obtained with anatase and the lowest ones with TS-1 and Ti-HMS. They noted that H_2O_2 decomposition is dependent on the templating mechanism which is also correlated with the silanol group density [44]. Hence, the selectivity in catalytic oxidation can be improved by decreasing the density of surface silanol groups. This improvement can be reached by an appropriate choice of catalysts preparation (Table 4) [44], template removal method [219] or by chemical modifications of surface silanols (silylation or organic modification to increase the catalyst hydrophobicity) [531,532].

Table 3
H_2O_2 decomposition on various titanium-sustituted MMS [44][a]

Catalysts	H_2O_2 decomposition (mol% conversion)
TS-1	2.7
Ti-HMS (S^0I^0)	2.2
Ti-MCM-41 (S^+I^-)	3.8
Ti-MCM-41 ($S^+X^-I^+$)	6.1
Anatase	13

[a] Reaction conditions: 30 mg of catalyst and 30 mmol of H_2O_2 (30 wt.%). Temperature of 321 K for 2 h.

Table 4
^{29}Si MAS NMR results for pure mesoporous titanium modified (2 mol%) silica synthesized at room temperature [44][a]

Synthesis conditions	Catalysts	Q^2	Q^3	Q^4
$S^+X^-I^+$	MCM-41	4	52	44
	Ti-MCM-41	3	40	57
S^+I^-	MCM-41	4	55	41
	Ti-MCM-41	1	42	57
S^0I^0	HMS	0	27	72
	Ti-HMS	0	25	75

[a] $Q^n = Si(SiO)_n(OH)_{4-n}$ (n = 2–4 in the table).

3. Some examples of MMS catalytic applications

3.1. Hydrotreatment

Hydrotreatment of petroleum fractions which involves hydrodesulfurization (HDS), hydrodenitrogenation (HDN), mild hydrocracking (MHC) of heavy feeds and hydrogenation of aromatics in different distillates, is an example of a process for which the need for converting increasingly large molecules has been long recognized [533,534]. There are two good reasons for this, firstly, the refiners have to treat increasingly heavier crude oils which have, therefore, increasingly higher contents of sulfur and nitrogen as well as vanadium, nickel and iron [535] and secondly, the universal environmental concerns are reflected into more and more stringent regulations [536] which impose lower levels of sulfur and other heteroatoms in the refined products. This potential significance of the application of MMS as supports for hydrotreatment catalysts is vividly reflected by the patent literature [26,537–543].

MMS's with their high surface area predominantly localized in uniformly distributed large diameter pores represent a clear new opportunity for the design of hydrotreatment catalysts. An early work by Corma compared a NiMo/MCM-41 catalyst with a NiMo/SiO_2-Al_2O_3 and a NiMo/USY in the simultaneous one step HDS, HDN and MHC of a vacuum gas oil at temperatures ranging from 350 to 450 °C [238]. A secondary hydrocracking of the hydrotreated products of the same feed was also studied. The three catalysts had the same 12 wt.% MoO_3 and 3 wt.% NiO but largely different Al contents and acid sites. The three supports had specific surface areas of 648, 268 and 551 $m^2\,g^{-1}$ and average pore diameters of 3.3, 4.6 and 2.1 nm, respectively. Upon impregnation the specific surface area of the three catalysts was decreased whereas the average pore diameter was increased. Feed A was a vacuum gas oil with 2.53 wt.% S, 2900 ppm N and a distillation range between 181 and 559 °C with 90 wt.% boiling above 360 °C. Table 5 shows some of the results of this study, giving the first order kinetic rate constants for HDS and HDN at 400 °C as well as the distribution of the products boiling below 360 °C at about 50% MHC conversion.

These results indicate the superior activity of the MCM-41 supported catalyst in both HDS and HDN. A higher activity was also observed in MHC but the data in Table 5 illustrate the better selectivity toward middle distillates of this catalyst. The authors relate the high HDS/HDN activity to extraframework aluminum species formed upon calcination of the MCM-41 alumino-silicate support. Interaction of Ni and Mo with these species would yield Ni–Mo films comparable to those present in γ-Al_2O_3 based catalysts.

It may, therefore, be of interest to prepare MMS supports having various extraframework Al oxide overlayers and to vary the Ni–Mo contents. The 12% MoO_3–3% NiO content is indeed optimized to the monolayer coverage of a γ-Al_2O_3 support with specific surface area on the order of 200 $m^2\,g^{-1}$. Schueth et al. have, for example, produced layers of La_2O_3 in silica MMS's with 50 wt.% content [157]. It may, thus, be expected that higher monolayered Ni–Mo contents could be reached with appropriate MMS supports.

The MHC selectivity results shown in Table 5 as well as some other results also reported in [238] for the simulated two steps hydrocracking of feed A over the same catalysts indicate that the mild acidity of the MCM-41 support which is comparable to the one of the amorphous SiO_2–Al_2O_3 support allows to avoid the overcracking observed with USY. It is also believed that the large pores of MCM-41 allowing a fast diffusion of the products out of the pore lattice would also contribute to avoiding overcracking. This illustrates once again the need to consider the various effects of internal diffusion and efficiency factors in dealing with the performances of MMS's derived catalysts.

Table 5
First order kinetic constants for HDS and HDN of feed A at 400 °C and distribution of products boiling below 360 °C determined at about 50% MHC conversion of feed A [238]

Catalyst	Rate constants ($cm^3\,g^{-1}\,h^{-1}$)		Distribution of products boiling below 360 °C (wt%)		
	k_{HDS}	k_{HDN}	C_1–C_4	Naphta[a]	MD[b]
Ni-Mo/MCM-41	3.34	0.93	16.2	25.8	58.0
Ni-Mo/SiO_2-Al_2O_3	2.51	0.56	18.9	23.1	57.9
Ni-Mo/USY	1.34	0.48	19.7	27.3	52.0

[a] Naphta: C_5^+ with bp < 195 °C.

[b] MD: middle distillate, 195 < bp < 360 °C.

Vartuli et al. have examined the demetallation and asphaltene removal of residuum oil over a series of Ni–Mo/MCM-41 of diameters ranging between 30 and 80 Å. The 80 Å pore catalyst was more active than a conventional demetallation catalyst [33].

Song et al. compared two CoMo/MCM-41 catalysts with two CoMo/γ-Al_2O_3 with normal (13.5 wt.% MoO_3, 2.9 wt.% CoO) and high (27 wt.% MoO_3; 5.8 wt.% CoO) metal loadings, in the hydrotreating of dibenzothiophene [544,545]. Increasing the metal loading in MCM-41 yielded close to three-fold increases in conversion specially associated with an increased hydrocracking/hydrogenation as well as HDS of the hydrogenated products. No such increase was observed upon increasing the metal loading over the alumina support. This result indeed underlines the ability of MMS supports to generate large surface area thin films of supported oxides which once sulfided yield very active catalysts. When tested in hydrotreating of atmospheric and vacuum resids, the CoMo/MCM-41 catalyst was found to have activities comparable to commercial CoMo/γ-Al_2O_3 and to sulfided ammonium tetrathiomolybdate (ATTM) [546]. The authors suggest that this is due to the not large enough pores of the MCM-41 support (BJH diameter: 28 Å) which did not allow to convert asphaltene molecules.

Klemt et al. [547] have shown that the MCM-41 support preparation technique is critical in controlling the product distribution in n-decane hydrocracking. Two NiMo/MCM-41 catalysts with similar (10 wt.% MoO_3; 2.3 wt.% NiO) metal loadings were prepared on two alumino-silica MCM-41 supports. The first one was prepared by calcination of the template followed by ion-exchange in 0.1N NH_4NO_3 aqueous solution whereas the second one was extracted by a NH_4NO_3 ethanol solution. The template removal by extraction stabilized the mesoporous structure and led to an enhanced acid site density tempered by an enhanced dealumination. The induced electron deficiency state of the metals led to a decreased hydrogenolysis and in particular a decreased methane generation in the hydrocracking of *n*-decane.

Klimova et al. studied Mo and NiMo HDS catalysts supported on γ-Al_2O_3 to which various amounts (up to 30 wt.%) of an MCM-41 material (Si/Al: 6.7) were added [548]. Surprisingly, the NiMo catalyst had a higher thiophene HDS activity when the MCM-41 content of the support was increased. As discussed above, it might be suggested that this increased activity is associated with a NiMo phase interacting with highly dispersed extraframework oxyaluminum species in the MCM-41 sieve. In a further work, the same group tested a series of CoMo catalysts supported on a mixture of γ-Al_2O_3 with up to 70 wt.% of MCM-41 (Si/Al = 200, BJH pore diameter 35.8 Å) [549]. These catalysts were found to have dibenzothiophene HDS activity which increased with the MCM-41 content of the support. The observed increased content in acid site density upon increasing the MCM-41 in the support also suggests that the activity is associated with an aluminum containing phase highly dispersed in the MCM-41 pore lattice.

HDS of dibenzothiophene over Co–Mo/MCM-41 was the object of a recent study by Wang et al. [550]. The support was purely siliceous with a BET surface area exceeding 1000 $m^2\,g^{-1}$ and a BJH pore diameter of 4.6 nm. Introducing Mo and Co led to substantial decreases in surface area and pore volume. The effects of loading on catalytic performance were studied up to CoO and MoO_3 loadings of 20 wt.%, respectively. Unfortunately loading and Co/Mo ratio were varied simultaneously. An optimum HDS rate due to optimal hydrogenolysis to biphenyl and hydrogenation to cyclohexylbenzene as well as a minimal hydrocracking (to benzene and cyclohexane) were observed at a Co/Mo of 0.75. This optimal ratio is usually much lower when the support is γ-Al_2O_3. No comparison is, however, otherwise reported with Co–Mo on any other supports so that the advantages of the MCM-41 support are not really discussed in this paper.

Pinnavaia has emphasized the beneficial aspect of a wormhole-like structure like the one of HMS's in conducting catalytic reactions of large molecules likely to present diffusional limitations [48]. Yue et al. were the first to use the disordered mesoporous KIT-1 as a support for HDS catalysts [551]. The same group had previously studied Ni/MCM-41, Mo/MCM-41 and NiMo/MCM-41 in HDS of thiophene and found Mo/MCM-41 the most active owing to a better Mo dispersion in the silica MCM-41 support [552]. Comparing also Ni/KIT-1, Mo/KIT-1 and NiMo/KIT-1 led to a similar conclusion, namely that highly dispersed Mo/KIT-1 containing up to 20 wt.% MoO_3 was very active and much more so than similar MCM-41 supported catalysts. The authors ascribe this good result to the disordered mesopore structure of KIT-1 allowing an easier access of the reactants to the catalytic sites.

An unusual catalyst was prepared by Halachev et al. and shown to be very active in HDS of dibenzothiophene [553]. It was made by modification of a Ti-HMS material (SSA: 800 $m^2 g^{-1}$, BJH pore diameter: 85 Å) by addition of H_3PO_4 (yielding 0–1.5 wt.% P_2O_5) and deposition by incipient wetness of 4.6 wt.% Ni and 10.6 wt.% Mo. The presence of phosphorus is said to yield a better reducibility (sulfidation) of the supported metals and corresponds to an enhanced activity. These catalysts showed a higher HDS activity than a commercial NiMo/Al_2O_3 catalyst. The same group has also reported a study of the hydrogenation of naphthalene over similar catalysts namely NiMo/Ti-HMS, P-NiMo/Ti-HMS, NiW/Ti-HMS, P-NiW/Ti-HMS, NiW/Al_2O_3 and P-NiW/Al_2O_3. Very high conversion to *cis* and *trans* decalines was reported for both P promoted and non-promoted NiW/Ti-HMS [554].

Murali Dhar and Prasada Rao have just published an especially interesting study of thiophene HDS and cyclohexene hydrogenation over HMS and Al-HMS supported W, Ni-W, Co-W, Mo, Ni-Mo and Co-Mo catalysts [555]. They performed oxygen chemisorption at −78 °C over the sulfided catalysts and found that over W/Al-HMS the O_2 uptake varied linearly with the W loading up to 21 wt.%. Interestingly, the BET surface area expressed in $m^2 g^{-1}$ of support was essentially unchanged up to this loading, indicating a very high dispersion of WS_2 microcrystals. The rates of both HDS and hydrogenation were found to vary proportionally to the O_2 uptake. Very high rates were reached with Ni or Co promoted W and Mo catalysts when supported on Al-HMS compared to alumina supported catalysts.

These results must be considered as very promising but, as underlined by the authors, the commercial utility of such catalysts cannot be assessed until high pressure studies with heavier model compounds and real feeds are performed.

The problem of the long term stability must also be addressed. Corma underlined (review [556]) that hydrotreatment catalysts need not be as hydrothermally resistant as cracking catalysts which must withstand the high temperature and steam content of the FCC regenerator. Still hydrotreatment catalysts are usually regenerated by ex situ calcination which requires thermal and hydrothermal stability as well.

As a conclusion it seems that MMSs and especially the wormhole like structured ones are superior supports for hydrotreatment catalysts. The mesostructured aluminas of MSU type (see Section 2.6) should, therefore, be interesting supports provided their hydrothermal resistance is meeting the requirements of the process, but HDS catalysts supported on such materials have not been discussed in the open literature yet.

3.2. Alkylation

Friedel–Crafts reactions, such as alkylations and acylations, are performed in liquid phase with homogeneous acid catalysts like $AlCl_3$, BF_3 and H_2SO_4. The corresponding industrial processes present severe environmental impact and often lack selectivity toward the targeted products. Thus, heterogenizing the catalyst is highly desirable. MMS offer the opportunity to apply heterogeneous catalysis to these organic reactions for bulky substrates, while maintaining the easy product diffusion from the catalytic site obtained in homogeneous catalysis. Indeed, low product diffusivity would favor secondary reactions and/or catalyst deactivation.

In his 1997 review paper, Corma [19] underlined the interest of MMS as catalysts supports for these reactions and in particular he discussed the very interesting results obtained by Armengol et al. [557] for the alkylation of 2,4 di-*tert*-butylphenol with cinnamyl alcohol over H-MCM-41 catalyst. Compared to large pore HY zeolite, mesoporous materials present high activity and selectivity. On HY, diffusional limitations of the reactant through the zeolite pore opening impose that the reaction takes place only on the external surface of the crystals yielding low activity and selectivity.

Since these early works, many studies dealt with the liquid phase alkylation of aromatics over MMS with alcohols [228,558–562], benzyl chloride [161, 563–568] or olefins [103,207,264–267,569–577].

In the case of aromatics alkylation with alcohols the relationship between acid strength and isomer selectivity is well established. Sakthivel et al. [578]

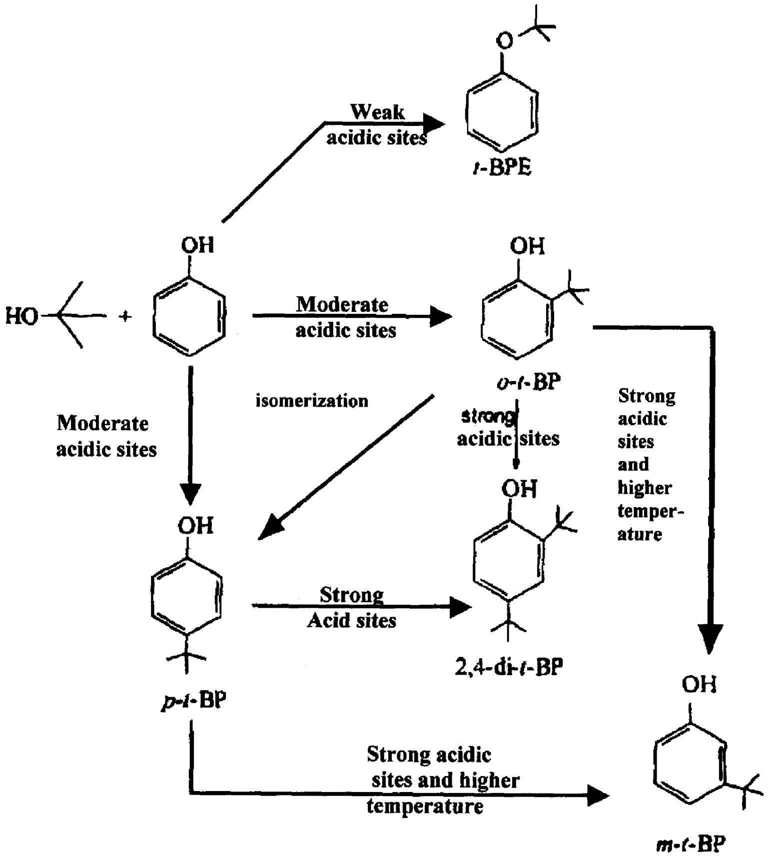

Fig. 7. Effect of acid sites on alkylation of phenol with *t*-butylalcohol [578].

summarized the effect of acid strength on the alkylation of phenol with *t*-butyl alcohol as shown in Fig. 7. Consequently, from the knowledge of the acid strength distribution it will be possible to predict the isomer selectivity. These authors used HAl-MCM-41, known for its moderate acidity (see above), for the vapour phase *t*-butylation of phenol and observed a high para selectivity, 84,6% at a conversion of 31% under optimum conditions (phenol: *t*-butyl alcohol = 2:1, $T = 448\,\mathrm{K}$, WHSV = $4.8\,\mathrm{h}^{-1}$). In agreement with Fig. 7, the selectivities depend highly on the synthesis conditions. The acidic properties of HAl-MCM-41 are strongly linked with the aluminum source employed and so does the catalytic activity [212]. When a large amount of aluminum is incorporated in the framework as tetrahedral species (sodium silicate) the activity is higher (higher conversion) but less selectivity in para isomer is observed. Comparable results have been obtained for the moderate acid catalyst HFe-MCM-41 for phenol:*t*-butyl alcohol = 1:4, $T = 448\,\mathrm{K}$, WHSV = $4.8\,\mathrm{h}^{-1}$. At a conversion of 21%, a para selectivity of 88% was observed [579]. The acid strength is obviously not the only factor influencing the selectivity for a shape selective catalyst. The most important parameter is the pore dimension. For example, Wang et al. [265] demonstrated a shape selective effect in the catalytic alkylation of 4-*t*-butylphenol (TBP) by styrene, which leads to very bulky molecules: 2-(1-phenylethyl)-4-*t*-butylphenol (product 1) and 2,6-bis-(1-phenylethyl)-4-*t*-butylphenol (product 2) over PW (tungstophosphoric acid) dispersed on three mesoporous silicas with uniform pore diameter distributions of 18, 30 and 100 Å. The reaction is schematized below.

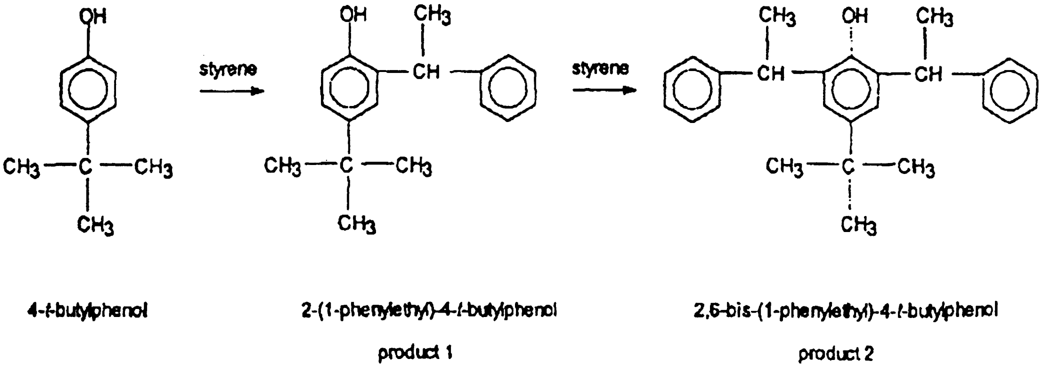

The dialkylated product 2 is a very bulky molecule with a kinetic diameter of 20 Å, so this experiment yields a clear test of shape selectivity.

Selectivities at 90% conversion are summarized in Table 6. It can be seen that the selectivity in product 1 is higher over the mesostructured silica with 30 Å pore diameters than over the one at 100 Å. The authors take into account the kinetic diameter of product 2, which is nearly 20 Å, and explain the better selectivity in product 1 by a transition state hindrance for the formation of the dialkylated product 2 in the 30 Å diameter pores.

Similar conclusions are reported in the case of *O*-methylation of 2-naphtol for the formation of 2-methoxynaphthalene where the best selective catalyst is a HAl-MCM-41 with a pore diameter of 40 Å, compared to 64 Å, 80 Å [580]. It is important to note that in this study, results obtained over SAPO molecular sieve (pore diameter = 7.3 Å) were comparable to those of MMS for 40 Å pore diameters. In our opinion, the low selectivity in intermediate product observed at high mesopore diameters cannot be explained by shape selectivity. We believe that the observed change in selectivity should rather correspond to a decrease primary reaction rate due to a lower surface concentration of acid sites. Indeed, in the same conditions the conversion of 2-naphthol decreases from 83.7–76.1 and 50% for pore diameters, respectively, equal to 40, 80 and 100 Å.

Table 6
Selectivities in 2-(1-phenylethyl)-4-*t*-butylphenol (product 1) and 2,6-bis-(1-phenylehtyl)-4-*t*-butylphenol (product 2) at 90% conversion of 4-*t*-butylphenol [265]

Catalyst	Product 1 (%)	Product 2 (%)
PW	46	45
50% PW/amorphous SiO_2	54	38
50% PW/30 Å SiO_2	80	13
50% PW/100 Å SiO_2	61	32

As discussed above, MMS permit the alkylation of bulk molecules for which the microporosity of zeolites imposes limitations to the reaction. For example, the benzylation of benzene with benzyl chloride (benzylation) has been discussed extensively. The first reported research used Fe-containing catalysts, supposedly in reference to the good results obtained with iron pillared clays catalysts (FePILCs), producing quantitative conversions with greatly reduced amounts of catalysts at short reaction time and low temperature [581]. He et al. [563] compared the activity of different mesoporous and microporous materials in this catalytic reaction. The authors showed no activity for Si-MCM-41, Al-MCM-41 (without exchange) and a very low activity for HAl-MCM-41. In the same conditions, a high activity was observed over Fe-MCM-41, 98% of conversion after 1 h at 60 °C but the catalyst presents no activity at 40 °C. This is the highest activities obtained compared to other catalysts, even when iron is deposited over HY zeolite. It is important to note the high catalyst stability, tested for more than 1 year, as opposed to the instability of iron species in FePILCs, for which redistribution of iron can be observed after 3 months at room temperature. A lower activity for Fe-HMS catalysts was observed in the same reaction. The authors explained that the lower pore size of the HMS sample (25 Å) hindered a good distribution of iron species unlike Fe-MCM-41 (33 Å) [161]. Interesting results were obtained by deposition of In or Ga active phases [564,568]. Very high conversions (90%) are observed after only a few

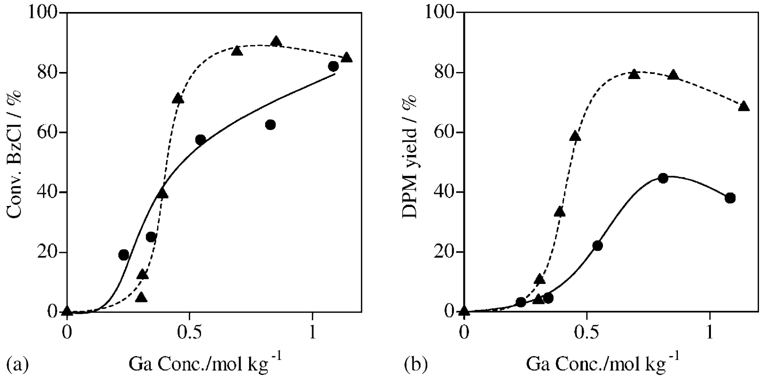

Fig. 8. Dependence of the (a) conversion of benzyl chloride and (b) yield of diphenylmethane (DPM) as a function of Ga content. (●) Ga-MCM-41 (introduced in the synthesis gel); and (▲) Ga/MCM-41 (impregnated) [567].

minutes at 80 °C. It would have been interesting to perform the catalytic tests at the same low temperature than the previous experiments (40 and 60 °C). Results presented by Okumura et al. [567], who introduced gallium species in MCM-41, show a highly active catalyst at temperature as low as 40 °C. In Fig. 8(a), the evolution of conversion as a function of the Ga content is reported. Independently of the method of active phase introduction, the activity increases considerably until 0.4 mol kg^{-1} of Ga loading and then decreases. The authors evidenced by NH_3 TPD the presence of weak acid sites, generated from agglomerated Ga_2O_3 species. At Ga content higher than 0.4 mol kg^{-1}, the molecular ratio acid site/Ga decreases due to aggregate formation, which can explain the activity decrease. In Fig. 8, it is shown that the impregnation of Ga generates higher activity and selectivity than the direct synthesis. In the latter case, it is important to underline the instability of Ga species during the template elimination by calcination at high temperature, which generates extra framework aggregates.

Yahav et al. [565] have developed a completely different approach by using sulfated zirconia deposited over HMS. The very high catalytic activity of this material is evidenced in several tests. A very interesting one is the benzene and toluene benzylation with benzyl chloride at 45 °C. For a molecular ratio of 1:5 (benzene or toluene:benzyl chloride), after only 40 min, 100% conversion is obtained with no side products formation.

The use of MMS as shape selective catalysts for bulk molecules in alkylation reactions must be stressed. As it is the case with microporous materials, in mesoporous molecular sieves the reaction can also take place outside the pore lattice, on the external surface. Price et al. [570,571] proposed a way to eliminate the active sites outside the mesopore in order to improve the selectivity. These authors studied the alkylation of benzene with different chain length olefins over $AlCl_3$ active phase grafted on two HMS materials with 16 and 24 Å pore diameters. They claimed a better selectivity for the small pore catalyst before as well as after deactivation of the external surface. Indeed, a difference in selectivity, with a maximum of 5%, was observed. It will be interesting to show porosity characterization, which could put in evidence the external site inhibition. It is a little surprising that the external surface, which is very low compared to the internal one, was only deactivated and that no changes in the porosity was observed after the introduction of bulk poisoning molecules like triphenylsilane. By contrast, the authors tested the akylation of benzene with different chain length olefins over the same catalyst and showed an increase in monoalkylated products with an increase in the olefins chain length. The same results were obtained in other similar studies [573,574]. For example, Hu et al. [573] grafted $AlCl_3$ molecules onto MMS surface and studied the selectivity in this alkylation type reaction, with different olefins chain length on one mesoporous catalyst and also by changing the catalyst pore diameters with one olefin (octene). In both cases, these authors demonstrated an increase in selectivity in monoalkylated products due to increased steric

Table 7
Selectivity and products distribution for the reaction of 1-octene with benzene catalyzed by $AlCl_3$ supported on MCM-41 with different pore sizes [573]

Catalyst	Pore diameter (Å)	1-Octene conversion (%)	Monoalkylated benzene (%)	Dialkylated benzene (%)
$AlCl_x$/MCM-41 [18][a]	39.2	100	75.2	24.8
$AlCl_x$/MCM-41 [16][a]	33.4	100	79.7	20.3
$AlCl_x$/MCM-41 [14][a]	30.9	100	83.3	16.7
$AlCl_x$/MCM-41 [12][a]	26.0	100	84.2	15.8
$AlCl_x$/MCM-41 [10][a]	22.5	100	89.7	11.3
$AlCl_x$/ZSM-5	5.5	5	78.2	21.8

[a] [*n*]: number of carbon atom in the surfactant chain.

hindrance for the secondary products formation. A good selectivity in monoalkylated benzene for alkylation of benzene with octene (benzene:alkene = 2:1) was performed by adjusting the pore diameter. The authors showed, that for a constant conversion of 100%, the selectivity to monoalkylated benzene increased from 75.2 to 89.7% when the pore diameter decreased from 39.2 to 22.5 Å. Consequently the selectivity in dialkylated benzene decreases in the same time (Table 7). As a general rule, increasing the pore diameter enhances the diffusivity of both reactants and products. Thus, the probability for secondary reactions should decrease, and therefore, a higher selectivity for the primary product should be observed at constant substrate conversion. In this study, the inverse effect was observed. A possible explanation would, therefore, be that the shape selectivity effect observed is associated with transitions state hindrance of the secondary alkylation, which of course would correspond to a decrease in the rate of formation of the dialkylated product. In the same conditions, for a microporous material like zeolite ZSM-5, the conversion and selectivity are very low because the reaction cannot take place inside the too small micropores and occurs only on the external surface, with unhindered secondary alkylation. An interesting point of this paper is the comparison of heterogeneous $AlCl_x$/MCM-41 and homogeneous $AlCl_3$ results for the catalyzed reaction. The authors put in evidence that the heterogeneous catalysts activity is comparable to the homogeneous one and that they are more selective towards monoalkylbenzene (Table 8).

In conclusion, acidic mesoporous molecular sieves are good candidates for alkylation reactions. In order to get high activity and selectivity, it is important to control both the porosity and the acidity. Deposition of a Lewis acid phase like $AlCl_3$ can induce catalytic activity comparable to homogeneous catalysts and in some examples better than microporous zeolites, with a much-enhanced selectivity for primary products. The acidity generated by lattice aluminum is in some cases insufficient, as it was, for example, observed in trimethylbenzene disproportionation [577] and for the cymene synthesis by transalkylation [572]. In this case, mesoporous materials can be used as catalyst supports. Deposition of very acidic molecules such as HPA (heteropolyanion) allows obtaining a higher activity. It is important to note that

Table 8
Selectivity for the alkylation of benzene with 1-alkenes in the homogeneously (free $AlCl_3$) and heterogeneously (MCM-41 supported $AlCl_3$) catalyzed reactions [573]

Alkene	Catalyst[a]	Selectivity toward alkylbenzenes[b] (%)		
		Mono[c]	Di	Tri
1-Hexene	Homog.	58.6	31.1	10.3
1-Hexene	Heterog.	79.9	20.1	–
1-Octene	Homog.	66.0	24.3	9.7
1-Octene	Heterog.	79.7	20.3	–
1-Decene	Homog.	68.5	22.5	9.0
1-Decene	Heterog.	91.1	8.9	–
1-Dodecene	Homog.	72.5	27.5	–[d]
1-Dodecene	Heterog.	96.2	3.8	–
1-Tetradecene	Homog.	70.1	29.9	–[d]
1-Tetradecene	Heterog.	98.5	1.5	–
1-Hexadecene	Homog.	77.5	22.5	–[d]
1-Hexadecene	Heterog.	>99.0	<1.0	–

[a] Homog.: homogeneous catalysis with $AlCl_3$ (0.15 mmol); Heterog.: over $AlCl_x$-MCM-41 (0.1 g of catalyst containing 0.15 mmol of $AlCl_x$).

[b] Determined by GC of the product mixture.

[c] Exclusively linear alkyl benzenes.

[d] Non-volatile product, not analyzed by GC.

Table 9
Influence of alumina in the MCM-41 framework and the Al_{MAO}/Zr ratio (carrier) on the polymerization activity, molecular weight, molecular weight distribution and microstructure[a] of polypropenes with $[Me_2C(Cp)(Flu)]ZrCl_2$/MAO/MCM-41 catalyst system[b]

Si/Al in MCM-41	Al_{MAO}/Zr	Act.[c]	M_η[d] (kg mol^{-1})	D	T_m (°C)	[mmmm] (%)	[mmmr] (%)	[rmmr] (%)	[mmrr] (%)	[rmrr] [mrmm] (%)	[rrrr] (%)	[rrrm] (in %)
12												
	270	13	102	2.0	141							
12	100	7	116	2.0	136	3	1	2	4	5	76	9
12	40	4	94	2.0	138	9	3	3	5	6	64	10
∞	40	26	98	2.1	145	0	0	1	3	3	87	6

[a] [mrrm] = 0,[mrmr] = 0.

[b] Polymerization conditions: $V = 300$ ml toluene, $T = 30\,°C$, $t = 2$ h, [propene] = 1.29 mol l^{-1}, 1×10^{-2} mol TIBA, 3.3×10^{-5} mol $[Me_2C(Cp)(Flu)]ZrCl_2$ [591].

[c] Activity in (kg sPP (mol Zr h $c_{propene}$)$^{-1}$).

[d] M_η: viscosity-average molecular weigth.

the dispersion of HPA over MTS is not well controlled and the pores can be partially blocked [262]. Some efforts have been done on this point and the dispersion and stability of these acids are now nearly mastered [264,267]. It must be remembered that even though product diffusion in the pore lattice is critical for selectivity, it can also be affected by the external diffusion between particles [560] and therefore by the particules morphology [561].

3.3. Polymerization

Mesoporous molecular sieves were proposed as catalyst supports for the synthesis of polymers having controlled molecular weight and narrow polydispersity. These characteristics are of both fondamental interest and practical importance [582–585].

Metallocene complexes of various metals including Al, B, Zr, and Ti which are known to be very active catalysts for olefins polymerizations can be attached onto the inner surface of mesoporous molecular sieves [586–591]. Mesoporous molecular sieves may play a key role in accomodating the larger metallocenes and polymerizing larger monomers such as propylene due to their controlable pore size, pore volume and high surface areas. These new materials allow to anchor more of the active complexes, the co-catalyst species (e.g. MAO) and favor the active sites to be accessed by bulky monomers polymerization compared with microporous zeolites.

For example, mesoporous silica MCM-41 materials supported metallocene $[Me_2C(Cp)(Flu)]\ ZrCl_2$ (Flu stands for fluorenyl group) were indeed used by Kaminsky et al. [591] for syndiospecific propene polymerization with higher syndiotacticity and higher melting points than achieved when using homogeneous systems or supported systems based on ordinary silica (Table 9, [591]).

The efficiency of supported metallocene or metallocene amides catalysts activated with methylalumoxane species (MAO) as co-catalysts was reported by many authors for olefins polymerization [587,592–598]. Most of the time, large amounts of these activated species (e.g. MAO) are required and the large surface areas of mesoporous molecular sieves provide for their high dispersion onto the inner walls [595] in addition to the high surface coverage of the metallocenes used. Van Looveren et al. [587] reported the syndiospecific propene polymerization and the co-oligomerization of ethylene using methylalumoxane (MAO) MCM-41 supported metallocene catalysts $[\{C_2H_4(1\text{-indenyl})(2)\}Zr(CH_3)_2]$. Schneider et al. [598] also reported ethylene and propylene polymerization using η^5-cyclopentadienyltris(dimethylamido)-zirconium $[CpZr(NMe_2)_3]$ catalyst immobilized on a chlorosilane- and hexamethyl-disilazane (HMDS)-modified mesoporous silica surface. This heterogenization process is absolutely necessary to make the homogeneous metallocene catalysts useful for industrial applications in order to avoid the “fouling” generated by polymer precipitation onto internal reactor surface, as the polymer precipitates instead onto the catalyst surface [595] or to reduce side reactions [598].

Köppl et al. [599] demonstrated that the silanols groups lined on the mesoporous materials surface

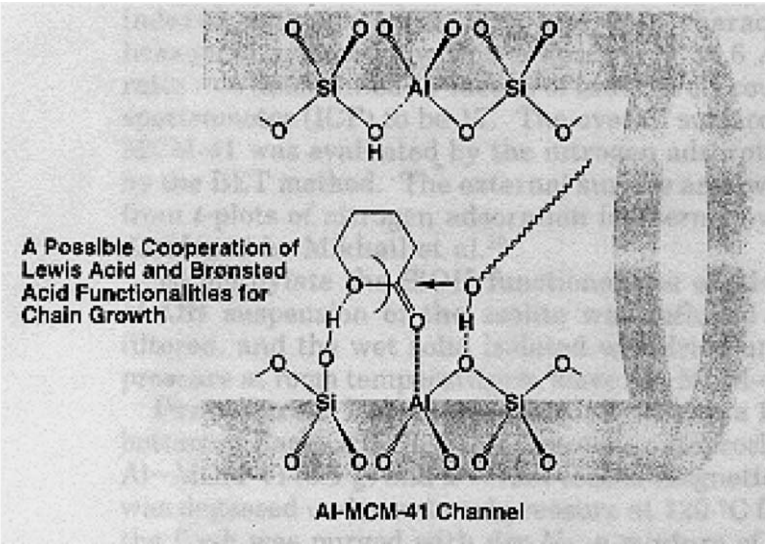

Fig. 9. Proposed mechanism for the polymerization of δ-valerolactone (VL) with alcohol in the presence of an aluminosilicate mesoporous molecular sieve (Al-MCM-41) [603].

(for example, MCM-41 material [587]) can be used to modify the properties of the solid support and ultimately its catalytic performance via the in situ hydrolysis of trimethylaluminum species ($AlMe_3$) into MAO species. This process followed by the reaction of the MAO species with metallocene complexes had been proposed earlier to design microporous silica supported polymerization catalysts [600,601]. These MAO species can also be used to provide chirality to the attached metallocene active species [587–594,602]. The chirality can derive from an appropriate control of channels size [595] which may impose a specific environment sometimes in conjunction with the various kinds of silanol groups (geminal, vicinal, isolated silanol groups) on the inner surface of the mesoporous materials including those associated with heteroatoms present in their framework [587–594,602]. A precise control of polyolefin stereochemistry can be obtained in that way [597].

In some of these polymerization catalysts, atoms such as Ti, Zr (and Al) used as initiators can be incorporated directly in the matrix of the inorganic support [172,603] in conjunction or not with methylalumoxane species (MAO) as co-catalyst. These heteroatoms were also used to enhance the thermal stability of the attached active metallocene complexes on the solid support compared to the heteroatom free MMS [604–607]. Coles and Jordan [608] showed that the insertion of aluminum species in mesoporous molecular sieves framework creates electrophilic cationic Al centers which may be used for ethylene polymerization. It was also reported by Kageyama et al. [609] that mesoporous materials such as Al-MCM-41 with a Lewis-acidic aluminosilicate framework catalyze living-opening polymerization of cyclic esters (Fig. 9 [603]) whereas those of Ti-MCM-41 type, allow the ring-opening of delta-valerolactone to give high molecular weight polyesters. The later kind of polymerization reaction was also demonstrated by Moriya et al. [610] with epsilon-caprolactone using silica gel organically modified with the stannyl ester of silicic acid and chlorosilane. Abdel-Fattah and Pinnavaia [522] reported the highest activity of Sn-HMS in the ring opening polymerization of L-lactide dimer to poly(L-lacid acid) at 130 °C compared to Ti-, Fe-, Y-, and La-HMS derivatives and pure HMS silica, as well as Sn-doped silica gel (1.0 mol% Sn) and pure SnO_2 (Table 10, [522]). Kim and Inui [516] reported that metal (Al, Ga, Fe)-incorporated mesoporous crystalline silicates are effective catalysts for oligomerization of propene. Weckhuysen et al. [607] showed that chromium acetyl acetonate [Cr(acac)(3)]

Table 10
Lactide polymerization over heterogeneous catalysts[a] [522]

Catalyst	Conversion (%)	PLA molecular mass
Sn-HMS	82	36000
Ti-HMS	15	808
Fe-HMS	2	583
Y-HMS	0	–
La-HMS	0	–
HMS	0	–
Sn-doped Silica	22	3200
SnO_2	73	17800

[a] Reaction conditions: 2.00 g (13.9 mmol) lactide dimer; 0.1 g catalyst (except for SnO_2, where 0.001 g was used); $T = 130\,^{\circ}C$; reaction time 72 h. All catalysts were calcined at 550 °C prior to use.

complexes grafted onto the surface of either pure silica MCM-41 or Al-containing silica (Si/Al ratio of 27) were effective catalysts in the gas-phase and slurry-phase polymerization of ethylene at 100 °C (Table 11 [607]). The formation of polyethylene nanofibers took place within the hexagonal channels of the mesoporous crystalline aluminosilicates. Optimal activity was observed at 1 wt.% Cr over the Al containing MCM-41. Increasing the calcination temperature from 550 to 720 °C still enhanced this activity. The authors also demonstrated that aluminum atoms incorporated in the framework of the mesoporous molecular sieves provide more thermal stability to deposited chromium acetyl acetonate complexes compared to the aluminum free one [607].

Table 11
Gas-phase polymerization of ethylene over $[Cr(acac)_3]$-MCM-41 catalysts: effect of the support composition, calcination temperature and Cr loading[a] [607]

Catalyst	Activity[b] ($g_{PE}\,g_{cat.}^{-1}\,h^{-1}$)
0.00-Al-C	7.80
0.50-Al-C	15.36
0.75-Al-C	25.62
1.00-Al-C	26.10
1.50-Al-C	7.44
2.00-Al-C	10.74
1.00-Al-C720	31.60
0.00-Si-C	6.00
1.00-Si-C	13.00

[a] Sample pre-treatment = 550 °C or 720 °C for 2 h; amount of catalyst = 0.3 g; initial ethylene pressure = 2.2 bar; reaction temperature = 100 °C; reaction time = 2 h.

[b] The activity is determined from the amount ethylene consumed during the whole ethylene polymerization run.

It is interesting to note that in the above discussed work of Kaminsky et al. [591] a higher activity in syndiotactic propylene polymerization over supported zirconocene $[Me_2C(Cp)(Flu)]ZrCl_2$/MAO was obtained when the MCM-41 support contained no framework Al. It is, therefore, clear that the Lewis acid sites generated by this aluminum species affect the nature of the grafted complexe. In this particular work it is shown that the introduction of Al in the framework converts the catalytic site from one which yields syndiotactic polypropylene to an isotactic polymer producing site.

Another concept was proposed by Moller et al. [602] who showed that 3-methacroylpropyl species grafted onto the surface of mesoporous materials act as seeds for the polymerization of these monomers leading to the formation of polymethacrylate/mesoporous composite materials. Ng et al. have studied the radicalar polymerization of methyl methacrylate (MMA) in the presence of such initiators as 2,2′-azoisobutyronitrile (AIBN) or benzoyl peroxide (BPO) within the channels of a MCM-41 silicate of about 2.7 nm in diameter. They showed that the average molecular weight of polymethyl methacrylate (PMMA) varied linearly with the monomer/initiator ratio whereas the polydispersity was not affected. This indicates that conducting the polymerization within the channels allows to control bimolecular chain termination while maintaining a good diffusivity of monomers and initiator to the reaction site. As a result very high molecular weights are obtained [611].

Kageyama et al. [612] made especially interesting observations using hexagonal MMS's in the form of mesoporous silica fibers (MSF) as support for ethylene polymerization catalysts. Dichlorotitanocene (Cp_2TiCl_2, where Cp stands for cyclopentadienyl ligand) and MAO were grafted on an MSF support having a mesopore diameter of 2.7 nm.

In order to explain the observed formation of crystalline polyethylene fibers with a diameter of 30–50 nm, they proposed that linear nanofibers of polyethylene with ultrahigh molecular weight are produced through an "extrusion polymerization mechanism" as described in Fig. 10 [612]. This new concept of using the morphology of mesoporous molecular sieve to provide oriented nanomolds for the

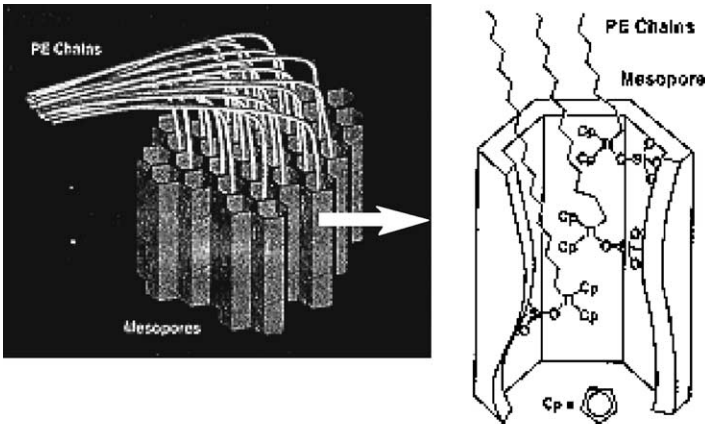

Fig. 10. Conceptual scheme for the growth of crystalline fibers of polyethylene by mesoporous silica-assisted extrusion polymerization [612].

synthesis of crystalline polymer fibers is likely to be of very general application. Unfortunately, crystalline fibers of polyethylene is already a commercial product so that it would be preferable to demonstrate this concept with other polymeric materials. This polymer morphology related to the channels inherent to the mesoporous materials compared to ordinary amorphous silica [613] was used by Spange et al. [614] to obtain a uniform distribution of polymer diameter upon cationic polymerization of cyclohexyl vinyl ether (CHVE) within MCM-41 channels yielding host–guest hybrid materials.

Using mesoporous hosts in the form of fibrous materials may indeed lead to other examples of fibrous polymers with unprecedented properties.

3.4. *Immobilized enzymes and enzymatic activity*

Mesoporous molecular sieves (MMSs), which have large surface area, adjustable uniform pore diameters, hydrophobic/hydrophilic behavior and electrostatic interactions [1,4], hold great promise for use as supports to immobilize proteins including enzymes, such as peroxidase, trypsin, papain and cytochrome. MMS may then find applications in the development of novel biosensors, biocatalysts, and bio-molecule separation systems [384–396]. Materials such as sol–gel display similar stability as MMS and have been used to encapsulate proteins for use as biosensors. However, a disadvantage in the use of sol–gel is their variability in pore size. They cannot, therefore, be tailored to isolate specific proteins and prevent the enzyme from leaking out of its cage.

Owing to the narrowly defined pore diameter of MMS, it is possible to design the specificity of these materials as hosts to particular enzymes with given characteristics such as size and charge, by varying the pore size and by modifying MMS with various functional groups, which enable electrostatic attraction or repulsion between MMS and the proteins of interest to be maximized [387–390]. For example, Han et al. [387] reported the sequestration of ionic proteins from aqueous solutions by MMS (e.g. SBA-15 and mesostructured cellular foams MCF) and the release of the sequestered proteins by increasing the ionic strength.

3.4.1. *Enzyme–support Interaction*

3.4.1.1. Surface polarization. The surface polarization of host and guest (e.g. support and enzyme) is a major factor in the adsorption process depending on the isoelectric points (IEP) of both the support and enzyme. Fig. 11 shows a schematic representation of the surface polarization of a solid particle as a function of the solution buffer pH. An oxide or an enzyme in contact with a buffer solution whose pH is below its IEP tends to polarize positively and favors anion adsorption; whereas the surface is negatively charged and favours cation adsorption while a pH is above its IEP [393]. Furthermore, the enzyme–support interactions can also be altered by changes in the enzyme

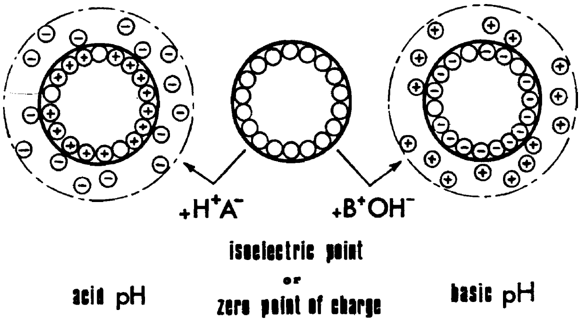

Fig. 11. Schematic representation of the surface polarization of an oxide particle or an enzyme as a function of the buffer solution pH [393].

buffer solution pH, which might make the adsorption process reversible.

The enzyme adsorption studies are conducted to determine the optimum pH at which the enzyme–support interactions are favored. For example, using the same support, MCM-41 with the pore diameter of 40 Å noted as MCM-41/40 (the number on the right hand of the designated sample is the pore diameter), the adsorption of papain was favored at pH 6 and the amount of papain adsorded decreased significantly from pH 6 to 9. However, cytochrome c adsorption was less susceptible to the pH 6–9 of the buffer solution. It is important to note that the isoelectric point of silica is low at pH 1–2, therefore, in the pH 6–9 range studied, the silica surface is negatively charged and favors the enzyme immobilization to silica MCM-41 by means of accessible silanols in the support. The distinct adsorption behavior between cytochrome c and papain could be attributed to the difference in their isoelectric points (see Table 12). In the range of pH 6–9, cytochrome c is below its isoelectric point (at pH 10); a positive charge in the surface of the enzyme would favor immobilization to the negative charge of the silica surface. At pH 9, papain is past its isoelectric point (at pH 8.75); consequently, the nature of the surface charge has changed resulting in a very low loading capacity of papain into the silica support [385].

3.4.1.2. Nature of the MMS surface. To study the effects of the preparation methods on the nature of surface, Takahashi et al. [388,389] prepared two types of mesoporous materials; one was prepared using a cationic surfactant, e.g. MCM-41/50 and FSM-16/51 and the other using a non-ionic poly(alkylene oxide) triblock copolymer, e.g. SBA-15/50. This study shows that even though the mesopore size is over the molecular diameters of the enzymes, a much larger adsorption capacity of the enzyme on MCM-41/50 and FSM-16/51 is obtained compared to that on SBA-15/50. This may be due to the different nature of the mesopore surface between two types of materials.

To clarify this point, the adsorbed amounts of cationic and anionic pigments were also measured for these materials. This study shows that the adsorbed amounts of cationic methylene blue (MB) for the FSM-16 and MCM-41 materials were larger than those of the SBA-15 and silica gel. However, using anionic sodium anthraquinone-2-sulfonic acid (ASS) as an anionic adsorbent, the adsorbed amount is almost the same for the three types of mesoporous materials. Furthermore, a two to three time higher adsorbed amount of MB (cationic) is obtained compared to that of ASS (anionic) for FSM-16 and MCM-41, while no significant difference in the adsorbed amounts were observed between MB and ASS for SBA-15 and silica gel. This indicates that FSM-16 and MCM-41 tend to adsorb larger amounts of cationic molecules

Table 12
Physical properties of some free enzymes and supports used for MMS immobilization [385,393]

Enzyme and support	Molecular mass, M_W	Isoelectric point pH (IEP)	Partial specific volume (cm^3 g^{-1})	Spherical molecular diameter (Å)
Cytochrome c	12300	10.0	0.72	30
Papain	20700	8.75	0.724	36
Trypsin	23400	10.5	0.73	38
Peroxidase	44000	∼6	0.699	46
SiO_2	–	1–2	–	–
Al_2O_3	–	6–7	–	–
TiO_2	–	∼6	–	–

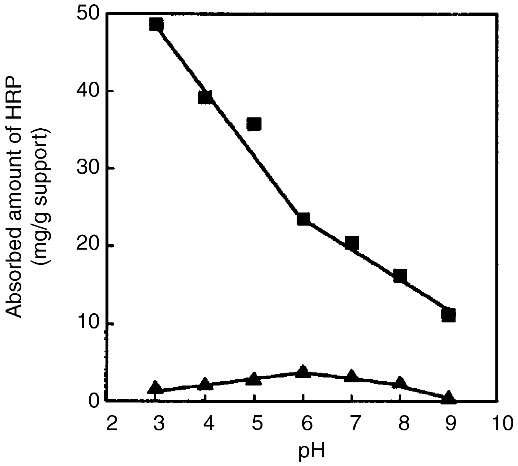

Fig. 12. pH profiles of HRP adsorption onto FSM-16/51 (■) and SBA-15/50 (▲) with almost the same mesopore diameter (51 and 50 Å, respectively) [388,389].

and this propriety may be related to the methods of synthesis. The use of a cationic surfactant may lead to enhancement of the anionic potential of the silanol groups on the surface and facilitate adsorption of cationic molecules, as compared to that of a non-ionic surfactant. Fig. 12 presents the amount of adsorbed horseradish peroxidase (HRP) as a function of buffer solution pH. A similar observation was also reported by Washmon et al. for the immobilized cytochrome c into silica MCM-41 and SBA-15 [390]. These results suggest that the ionic characteristics of material surfaces determine their adsorptive selectivity for ionic compounds, as enzymes many of which have positively charged (cationic) residues on their surface [384–389].

3.4.2. Effect of enzyme size

Immobilization of different enzymes in silica MCM-41/40 was performed by Diaz and Balkus [385]. The goal of this study was to enhance stability while exploiting the catalytic activity of these hybrids. The effect of enzymes size on enzyme immobilization capacity was evaluated using phosphate as an enzyme buffer solution at pH 6. Fig. 13 shows the capacity of adsorbed enzymes as a function of their molecular mass. A clear correlation between enzyme size and molar loading was reported. Due to the large size of the enzyme peroxidase (M_W: 44000), only a small quantity of this enzyme was adsorbed, as compared to the smaller size enzymes trypsin (M_W: 23400), papain (M_W: 20700) and cytochrome (M_W: 12300) (see Table 12). This suggests that peroxidase was adsorbed on the outer surface of the MCM-41 particles while the other enzymes which are smaller penetrate into the MCM-41 mesopore system and the adsorption capacity for these enzymes is therefore much higher.

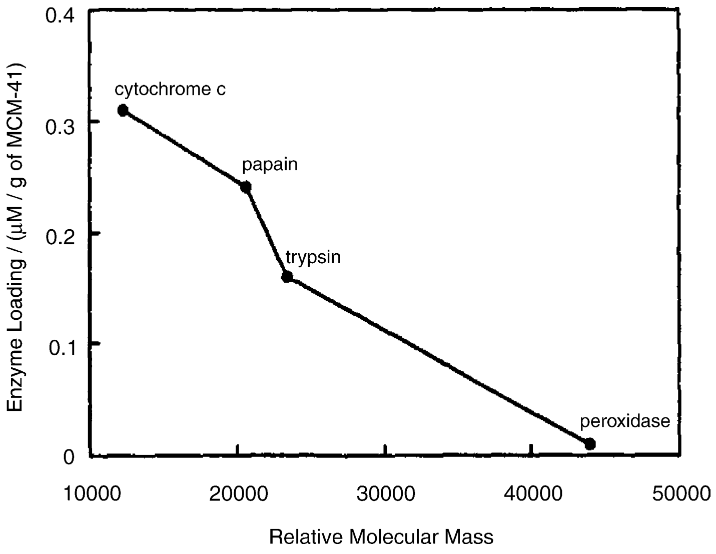

Fig. 13. Effect of enzyme size on the immobilization efficiency of the MCM-41/40 host with the average pore diameter of 40 Å [385].

3.4.3. Effect of mesopore size

Takahashi et al. [388,389] used horseradish peroxidase (HRP) and subtilisin (having kinetic diameters of 48 and 43 Å, respectively) immobilized on the mesoporous silica FSM-16 with various pore diameters; e.g. 27, 51 and 89 Å (FSM-16/27, FSM16/51 and FSM16/91). For FSM-16/51 and FSM-16/91, whose pore diameter is over that of the enzyme, the adsorbed HRP amounts increased with increasing the mesopore diameter. The adsorbed HRP amount reached over 80 and 180 mg g^{-1} support for FSM-16/51 and FSM-16/91, respectively. In contrast, only a small amount of enzyme, e.g. 35 mg g^{-1} support, was adsorbed on FSM-16/27. The pore volume of FSM-16/27 was essentially the same before and after enzyme adsorption indicating that the enzyme molecules did not essentially occupy the mesopore space and were adsorbed to the outer surface of particles. Fig. 14 presents model images of HRP immobilized in mesoporous molecular sieves with various pore sizes using computer schematic models. The enzymatic activity of HRP immobilized in mesoporous silica with various pore sizes was evaluated by the oxidative reaction of 1,2-diaminobenzene in an organic solvent. A native HRP was used as the reference. The immobilized enzymes exhibited relatively high enzymatic activities compared with the native enzyme activity. The authors also indicated that the immobilized enzyme in mesoporous silica, the pore size of which matched the enzyme kinetic diameter, exhibited the highest activity. The enzyme immobilized in mesoporous silica and silica gel, which have pore sizes larger than that of the enzyme, showed however, medium activities. The lowest catalytic activity was observed for the enzyme immobilized on the outer surface (e.g. FSM-16/27).

To study the effect of pore size on thermal stability, the immobilized enzymes were treated at 70 °C in the buffer solution followed by the phenol polymerization reaction [388,389]. The residual enzymatic activity after thermal treatment also showed a clear dependence on pore size. An immobilized enzyme is thermally stable when the average mesopore size matches the enzyme kinetic diameter; and it is less stable when the pore diameter is larger or smaller than that of the enzyme kinetic diameter. For example, HRP immobilized in FSM-16/51 was quite stable; its enzymatic activity was decreased by only 20% after 120 min of

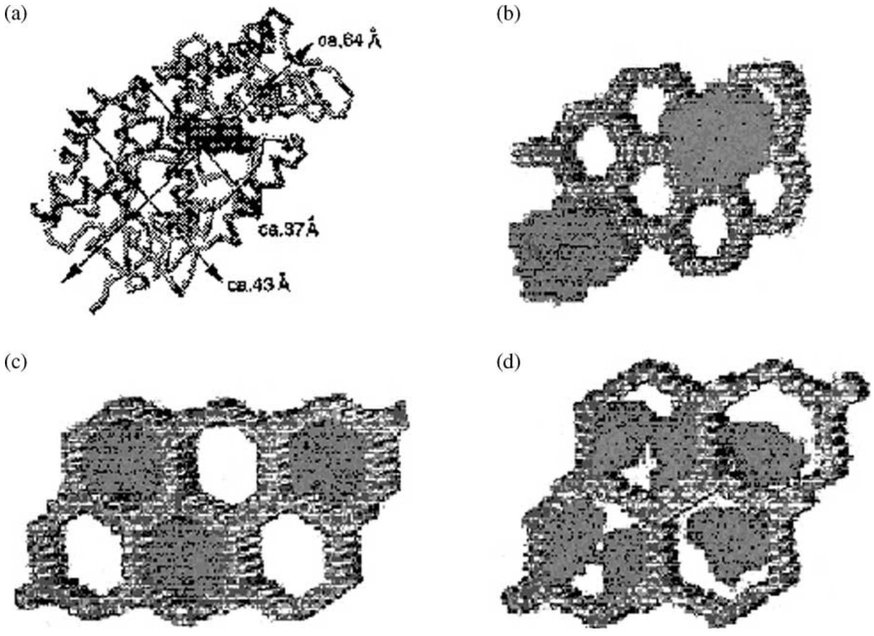

Fig. 14. Structural model of an HRP molecule (a) and image models of immobilized HRP in FSM-16 with various pore sizes, e.g. 30, 50 and 90 Å for models (b–d), using a computer schematic model [388,389].

treatment, while 40% for FSM-16/89 after 120 min and more than 50% of deactivation after only 60 min of treatment for FSM-16/27 were observed. FSM-16/27 was drastically deactivated within 60 min of thermal treatment when the enzyme was adsorbed on the outer surface of the FSM-16 particles.

3.4.4. *Effect of the mesopore structure*

The immobilization into silica MCM-41 improved enzyme stability, however, the observed catalytic activity of enzymes, such as trypsin and papain, was not dramatically improved as compared to other supports [385]. This could be due to the one-dimensional MCM-41 pore system where access to the occluded bio-molecules may be limited to the ends of the channels. For this reason, the enzyme immobilization into a variety of mesoporous molecular sieves was studied [390,391]. Washmon et al. [390] examined the adsorption of cytochrome c into various mesoporous materials with almost the same average mesopore diameter, such as three-dimensional silica MCM-48/34 and one-dimensional hexagonal structure: silica MCM-41/32, Al-MCM-41/32 [1,4] and Nb-TMS1/33 [397]. These materials have different compositions and/or structure. A greater enzyme adsorption loading was observed for MCM-48 compared to MCM-41 and Nb-TMS1. One may expect the highest loading in MCM-48 due to the three-dimensional pore structure. Furthermore, the effect of pH on cytochrome c adsorption into these materials was also examined. The order of stability in terms of enzyme retention is silica MCM-48 $\sim$ silica MCM-41 $>$ Nb-TMS1 $>$ silica Al-MCM-41. On the other hand, Yiu et al. [391] studied trypsin immobilized in three types of mesoporous materials (MCM-41/30, MCM-48/24 and SBA-15/59) and commercially available porous silica gel was chosen for comparison. Hydrolysis of *N*-α-benzoyl-DL-arginine-4-nitroanilide (BAPNA) was applied to assess the activity of the immobilized enzymes. A lower activity was reported for trysin supported on mesostructured materials compared to trysin on silica gel [391]. This could be explained by the tight fit of this enzyme in the mesopore system. The catalytic activity would depend on the orientation of the enzyme when it was originally adsorbed. The evaluation of enzymatic activity using larger pore channels and tri-dimensional structures might resolve this issue. This would allow better enzyme mobility within the channels, and permit enzyme–substrate interactions regardless of enzyme orientation.

3.4.5. *Entrapment of MMS immobilized enzyme*

Leakage of adsorbed enzyme into solution is a common disadvantage of the adsorption immobilization. The desorption of immobilized enzyme from supports is noted at high pH. For example, at pH 9.0, a large fraction of papain immobilized in silica MCM-41/40, e.g. 70%, leaks into solution after 24 h, compared to 15% in pH 6.0 buffer [385]. Reduction of the pore size through silanation would restrict enzyme movement and avoid diffusion into the bulk solution even for extended exposure to high pH buffer solution. However, the organosilanes employed for pore reduction should not be expected to react with the adsorbed enzyme. Diaz and Balkus [385] also showed that the MCM-41/40 entrapped trypsin using 3-aminopropyltriethoxysilane (APS) did not leak into solution when the material was immersed in pH 9.0 buffer, which would normally release ∼90% of the enzyme after 24 h. This could be explained by the fact that the ∼6 Å long APS chain was reducing the pore opening by ∼12 Å [317]. It is also noted that no significant leakage was detected for cytochrome c immobilized in silica MCM-41/40 at the pH 6–9 range. It is logical that cytochrome c which is a smaller enzyme can migrate deeper into the pore system and contact with the pore walls of the silica MCM-41 host, which improves the retention of the enzyme.

Furthermore, the movement of trypsin, which causes autolysis in solution, is restricted by immobilization. No significant activity loss was observed after incubation of MCM-41/40 entrapped trypsin at 25 °C for a week, compared to the total deactivation of free trypsin in solution after 24 h [385,390,391]. The entrapment of FSM-16-immobilized HRP with various pore diameters was also studied by Li and Takahashi. The leakage level and the oxidative activity of 1,2-diaminobenzene in an organic solvent showed a similar trend [392]. Several procedures have been developed to improve the stability and catalytic activity of enzymes immobilized in MMS [398–405].

Finally, the active enzyme in MMS probably has a preferred orientation dictated by the size of the channels. This would be an important advantage over sol–gel entrapment, for which the average pore size precludes interaction with large polymeric substrates, as the enzymes could be randomly oriented with respect to the pore openings.

3.5. Catalysis by anchored complexes

3.5.1. Enantioselective alkylation

Chiral secondary alcohols are important intermediates for the construction of active chiral natural products and biologically active compounds. Diorganozinc reagents act as ideal alkyl donors to aldehydes for catalytic asymmetric alkylation. β-Aminoalcohols are the chiral auxiliaries most commonly used in the catalytic process [615–617]. Extremely high enantiometric excess (ee) has been reported in homogeneous reaction employing a variety of aminoalcohol ligands (ee is defined as follows: $\text{ee} = [R] - [S]/([R] + [S])$; where $[R]$ is the concentration of enatiomer Rectus and $[S]$ the concentration of enatiomer Sinister). Taking into account environmental and economical considerations, immobilization of chiral ligands onto supports presents many advantages such as easier separation and recovery, etc. MMSs have been successfully employed as supports for various chiral catalysts.

The pioneering work for chiral heterogeneous catalysts reported by Soai and co-workers [616,617] deals with an anchoring of ephedrine onto silica and alumina surfaces, used in the enantioselective alkylation of benzaldehyde with diethylzinc; low activity and enantioselectivity were observed. Furthermore, using the same methodology, Laspéras and co-workers [618,619] prepared a chiral heterogeneous catalysts from β-aminoalcohol, the (−)-(1*R*, 2*S*)- or (+)-(1*S*, 2*R*)-ephedrine immobilized on the MMS surface (Table 13). This is expected to improve the catalytic performance for the same type of reaction. In both cases, however, the enantiomeric excesses were far lower than the ones obtained with the corresponding homogeneous catalysts. In connection with the low enantioselectivity, several issues should be addressed such as employment of a more selective ligand, suppressing undesired catalytic activity on the silica surface, changing silica mesopore size and addition of extra metal reagent. Bae et al. [620] developed a new chiral heterogeneous catalyst system using a proline-derived ligand immobilized on MCM-41 (pore diameter (p.d.), 31 Å) and SBA-15 (p.d., 89 Å). The reaction enantioselectivity for diethylzinc addition to benzaldehyde was found to be largely dependent upon the MMS pore size, capping of free silanol moieties with trimethylsilyl groups and employment of butyl lithium as extra-metal reagent. It is noted that catalysts based upon SBA-15 (p.d., 89 Å) consistently gave higher enantioselectivity than that of MCM-41 (p.d., 31 Å). In both MCM-41 and SBA-15 systems, TMS-capping as well as the employment of butyl lithium improved the enantioselectivity significantly. Product of the highest ee (75%) was obtained for TMS-capped SBA-15 based catalyst utilized after treatment with butyl lithium.

In recent works [621,622], MCM-41 was functionlized by a new sol–gel method involving prehydrolysis of the alkoxy groups of the silylating agent and control of the condensation reaction between monolayer-packed silylating agents. This method afforded high surface coverage that limits the undesirable activity of the uncovered support surface. This new generation of catalysts demonstrated remarkable enantioselectivity for diethylzinc addition to benzaldehyde at the level of the homogeneous catalyst.

Table 13
Asymmetric addition of diethylzinc to benzaldehyde using various chiral catalysts

Mineral support	β-Aminoalcohol	Enantiomeric excess (ee)[a]		References
		Heterogeneous (%)	Homogeneous (%)	
Silica	Ephedrine	37	76	[616,617]
MCM-41	Ephedrine	56	76	[618,619]
Al-MCM-41	Ephedrine	64	76	[621]
MCM-41	Prolinol	72	93	[620]
SBA-15	Prolinol	75	93	[620]

[a] $\text{ee} = [R] - [S]/([R] + [S])$, where $[R]$ is the concentration of enantiomer Rectus and $[S]$ the concentration of enantiomer Sinister.

3.5.2. Enantioselective hydrogenation

The enantioselective synthesis of chiral saturated ring systems involving piperidine or cyclohexane is of considerable practical interest. As detailed elsewhere [369,370,623], chiral chelate ligands based on 1,1′-bis(diphenylphosphino)ferrocene (dppf) are particularly attractive for tethering onto mesoporous silica and the superior performance of the chiral heterogenized catalyst compared to the unconfined homogeneous analogue was established. Recently, Thomas and co-workers [369,370] demonstrated that the chiral catalyst, which is derived from 1,1′-bis(diphenylphosphino) ferrocene (dppf) bonded to an active metal center (in this case Pd(II)) tethered to the MMS inner walls, displays remarkable increases in both enantioselectivity and activity in the one-step hydrogenation of ethyl nicotinate to ethyl nipecotinate, when compared to either the homogeneous counterpart or the non-porous carbosil-bound catalyst (Table 14). The effective enantioselectivity of the confined catalyst for the direct hydrogenation of ethyl nicotinate, with an enantiomeric excess (ee) of 17% and conversion in excess of 50%, while no enantioselectivity and low activity observed for the homogeneous alkyl silsequioxane with the same tethered, indicates the profound importance of confinement in catalysis. The confined catalyst also displayed a higher degree of activity (TON = 291) compared to the homogeneous form (TON = 98), after a reaction time of 72 h. and is remarkably stable. This kind of confined dppf catalyst also exhibited a degree of regioselectivity and enantiomeric excess in the allylic amination of cinamylacetate, which is far superior to that of its homogeneous counterpart or that of a surface-bound analogue attached to a non-porous silica.

3.5.3. Hydrogenation

Ichikawa and co-workers [624,625] developed an interesting methodology to prepare an active hydrogenation catalyst, in which Pt clusters of the type $[Pt_{15}(CO)_{30}]_2$-$[R_4NX]_2$ (R = Me, Et, Bu and hexyl and X = Cl, Br and OH) were immobilized in the ordered hexagonal channels of FSM-16. These catalysts exhibited much higher activity (20–100 times) for the water-gas-shift (WGS) reaction compared to $[Pt_{12}(CO)_{24}]^{2-}$ and $[Pt_9(CO)_{18}]^{2-}$ restricted in NaY and a conventional Pt/Al_2O_3 catalyst (4 wt.% Pt). Additionally, the clusters remained unchanged after immobilization. The CO-ligand sheath could be removed by heat treatment at 333–473 K under high vacuum, leading to particle sintering and resulting in 50–60 atom aggregates. Thus, the unsaturated Pt aggregates exhibited a good catalytic activity in the hydrogenation of ethylene and butadiene [626]. Furthermore, Thomas and co-workers [133,627] inserted mixed-metal cluster carbonylate salts such as $[Ru_6C(CO)_{16}]_2CuCl]_2$-$[PPN]_2$, where PPN stands for bis-(triphenylphosphino)iminium, into MCM-41 silica resulting in active hydrogenation catalysts. Contrary to the behavior of catalyst particles derived from Pt carbonyl clusters, these mixed-metal particles do not sinter upon thermal activation as confirmed by electron transmission microscopy. These bimetallic nanocatalysts exhibited high turnover frequencies for the hydrogenation of hex-1-ene, diphenylacetylene, stilbene, *cis*-cycloctene, D-limonene and 1,5,9-cyclododecatriene. Finally, a number of selective

Table 14
Conversion and enantiomeric excess of the different types of dppf-ferrocenyl-Pd catalysts for the direct hydrogenation of ethyl nicotinate to ethyl nipecotinate [369,370][a]

Dppf-ferrocenyl-diamine-Pd catalyst	Substrate (reactant)	*t* (h)	Conversion (%)	ee (%)
Homogeneous (I)	Ethyl nicotinate	72	15.9	–
		120	27.2	–
Tethered silica (II)	Ethyl nicotinate	72	12.6	2
		120	19.2	2
Tethered to MCM-41 and confined inside mesopore (III)	Ethyl nicotinate	48	35.5	17
		72	53.7	20

[a] Dppf-ferrocenylp-Pd-active center attached to a soluble silsesquioxane moiety(I), to a non-porous silica(II) and bound in a constrained manner inside mesoporous silica(III).

hydrogenation of polyenes such as 1,5,9-cyclododecatriene using a bimetallic Ru_6Sn nanoparticle catalyst has been highlighted [627,628].

3.5.4. Enantioselective epoxidation

One of the big challenges for catalytic chemists is the design of heterogeneous enantioselective oxidation catalysts; this is a topic that retains intense research interest and is, to date, significantly less advanced than the research into enantioselective hydrogenation catalysts. Hutching et al. [629] reported the synthesis of a heterogeneous enantioselective epoxidation catalyst by combining manganese(III) salen with the mesoporous Al-MCM-41. This catalyst is effective as an enantioselective epoxidation catalyst for *cis*-stilbene. The *trans* epoxide is formed with an ee of 70%, which is similar to that observed for the equivalent homogeneous reactions. The turnover rates based on the amount of Mn-salen for the heterogeneous catalyst were found to be higher (e.g. 26) than those for homogeneously catalyzed reaction (e.g. 7).

Recently, chromium(III) binaphthyl Schiff base complexes were immobilized onto the terminal NH_2 group of surface bound 3-aminopropyl tethering chains [630]. The asymmetric epoxidation of a series of unfunctionalized alkenes such as *p*-chlorostyrene, *cis*-methylstyrene, using PhIO as an oxydant was carried out in toluene. This catalyst exhibited significantly higher enantioselectivity than the same free complex. Its reusability was also examined. This catalyst could be reused at least two times without a decrease in activity and enantioselectivity. In contrast, the Mn-MCM-41-salen catalyst in [629] suffered from a loss of enantioselectivity of 40% ee when reused for the first time. The increase in the chiral recognition could arise from the enhanced stability of the chromium complex upon immobilization and from the unique spatial environment as suggested by Johnson et al. [369] and Maschmeyer [631].

Recently, Brunel and co-workers [632,633] reported the heterogeneization of a chiral macrocycle onto the MCM-41 surface, which had been previously grafted with 3-chloropropyl chains. The resulting material was followed by N-alkylation of the tetraazamacrocycle with propylene oxide and metalation with $Mn(II)Cl_2$. This MCM-41 grafted Mn(II) 2R,3R-cyclohexano-N,N',N'',N'''-tetrakis(2-hydroxypropyl)1,4,7,10-tetraazacyclododecane was evaluated in the epoxydation of *trans*-methylstyrene using iodosylbenzene as an oxygen donor. The *trans*-methylstyrene oxide was obtained with a relatively high enantioselectivity (76%) in comparison with other immobilized systems and although lower than that obtained with the homogeneous counterpart (94%). This can be explained by diffusion limitation of these species within the mesopore system. These primary results prompt further investigation to improve the selectivity in epoxide and the catalyst reusability [633].

As a conclusion, some degree of success in enantioselective heterogeneous catalysts was accomplished using functionalization of MMS supports. Owing to their unique textural and high surface areas, MMS are able to bring new interesting properties for the development of chiral heterogenized catalysts. A number of successful examples have been reported for enantioselective hydrogenation, epoxidation and alkylation. However, the stability and reactivity of this type of catalysts still deserve efforts to allow industrial application of such attractive materials.

3.6. Some examples of base catalyzed reactions

Base catalyzed reactions are useful for large organic molecule syntheses in the field of perfumes, pharmaceuticals and agro-chemicals. The large pore diameter, volume and surface area of MMS, which will permit to eliminate diffusional restrictions of reactants and products, should of course be beneficial in this area. Three reactions are essentially studied in the literature:

- *Knoevenagel condensations*;
- Monoglyceride syntheses;
- Michael additions.

Knoevenagel condensation is one of the oldest known reactions for carbon-carbon bond formation [634]. Weak bases like primary, secondary, tertiary amines, ammonium or ammonium salts under homogeneous conditions generally catalyze this reaction [634–636]. Heterogenizing these catalysts is providing operational simplicity, reusability and higher selectivity. To this end, MMS materials are new supports for these basic functionalities.

The most employed method for catalysts preparation is the grafting of amine molecules by post-synthesis treatment or by direct sol–gel process.

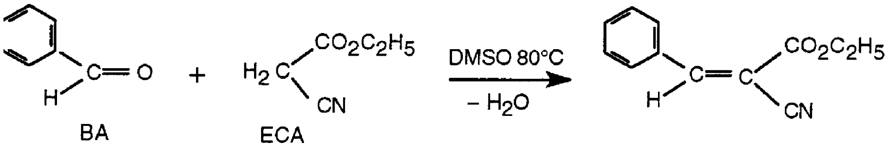

Fig. 15. Scheme of the Knoevenagel condensation of benzaldehyde (BA) with ethylcyanoacetate (ECA) in DMSO solution [320].

Primary amines were first immobilized over amorphous silica and showed a high activity in mild conditions [637], but the reaction mechanism was, however, not demonstrated. In this sense and for the first time, Lasperas et al. [320] studied the Knoevenagel condensation of benzaldehyde with ethylcyanoacetate in DMSO solution over amine grafted MCM-41 (Fig. 15). It must be underlined that the solvent is a main factor in this reaction for its influence on the catalytic activity, as reported in different studies, independently of the catalyst [328,330,638–640]. Lasperas et al. have used two active phases, a primary amine (3-aminopropyl triethoxysilane) and a tertiary piperidine. All samples yielded selectivities near 100% (<95%), but despite the fact that the piperidine basic strength is stronger than the one of the primary amine, the activity of the latter is higher. This was explained by assuming two different reaction mechanisms. The tertiary piperidine induced a classical base activation of the methylene group in ethyl cyanoacetate followed by nucleophilic attack of the carbonyl function in benzaldehyde. On the contrary, the primary amino group can activate the carbonyl group with imine formation followed by nucleophilic attack of the activated ethyl cyanoacetate (see Fig. 16). Under their heterogeneous conditions, the authors suggested a concerted mechanism. In this study, it was found that the reaction rate was proportional to the concentration of acid sites, which was changed by increasing the grafted function loading or by increasing the catalyst mass. This reflects the absence of internal diffusional limitation in the MMS large pores. Another important point is the stability of these basic catalysts, which can be regenerated by simple washing in an appropriated solvent. For example, in the case of amino-propyl groups the catalytic activity was maintained for several experiments after reactivation by washing in a methylene dichloride-di-ethyl ether blend. Choudary et al. [328] have also reported the stability of diamine function grafted over MMS materials, the catalyst was reused for several cycles without any reactivation and the reused catalyst gave identical yields with consistent rates compared to the fresh one.

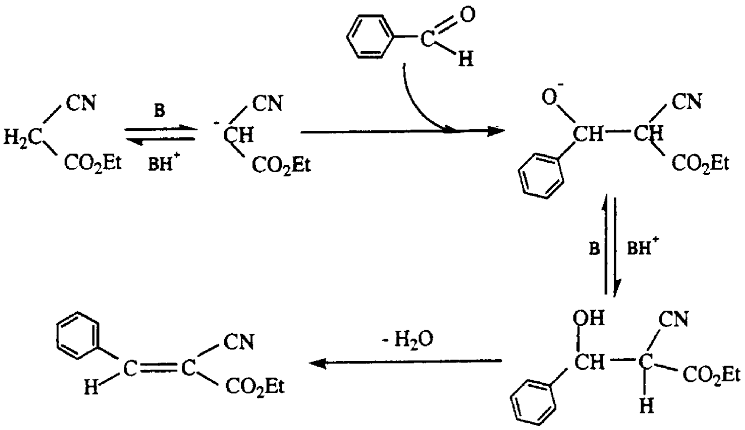

Fig. 16. Scheme of the catalytic mechanism of the Knoevenagel reaction with primary amino-groups. The primary amino-groups activate the carbonyl group by imine formation followed by nucleophilic attack of the activated ethyl cyanoacetate [322].

Table 15
Initial comparisons of the cross-linked lyotropic liquid crystal phase as based catalyst vs. Na-zeolite Y and Na-MCM-41 [342]

Base catalyst	Amount	Solvent	T (°C)	t (h)	Conversion (%).
Na-zeolite Y (wt.%)	20	None	140	2	19
Inv. Hex. network (mol%)	5	None	r.t.	2	70
Na-MCM-41 (mol%)	5	Water	100	3	90
Inv. Hex. network (mol%)	5	Water	100	0.25	94

The surface polarity is also an important parameter to improve the catalytic activity. Macquarrie [332] used the sol–gel process, proposed by Hall et al. [641], to graft at the same time two functional groups, an amino- and a neutral carbophylic one (such as phenyl group). In the case of phenyl addition, the activity was improved compared to the only amino-grafted catalyst. For example, in the reaction between ethyl cyanoacetate and cyclohexanone, the reaction was complete after 2 h with only amino groups, against 30 min with the bifunctional catalyst, for an equivalent loading of active amino sites. As described in Section 2.4, the basic strength of these grafted base catalysts depends of the molecule, in the same order as that established for the free organic bases.

In the case of cation-exchanged materials, Na-MCM-41 and Cs-MCM-41, the sodium form presents a good activity for the condensation of benzaldehyde with ethyl cyanoacetate, but its basic strength is insufficient to perform more demanding reactions such as the one with diethyl malonate. Cs^+-exchanged catalysts present stronger basicity and they were found more active than Na-MCM-41 [181]. The strongest activity was obtained for impregnated Cs active phase [180]. The composite phase Cs/La, which presents a high stability (see Section 2.4), represents a promising catalyst for this base catalyzed reactions [180]. In Knoevenagel condensation of benzaldehyde with ethyl cyanoacetate, 95% of conversion was obtained with a high selectivity (<95%) in α,β-unsaturated esters. These results were obtained in ethanol and the authors observed, as already reported, an important solvent effect.

Recently, Kubota et al. [642] presented as-synthesized MCM-41, still containing the quaternary ammonium template (hexadecyltrimethyl ammonium) as new basic catalysts. These materials have shown activity in surprising by mild conditions (20 °C, benzaldehyde 2.5 mmol, ethyl cyanoacetate 2.6 mmol, in benzene and 200 mg of solid catalyst) for the condensation of benzaldehyde with ethyl cyanoacetate. Yields of 82% in 1 h and 97% in 6 h were observed.

New organic mesoporous materials were tested as heterogeneous base catalysts for the Knoevenagel condensation reaction [341,342] (Table 15). The authors compared their basic material with two other catalysts, zeolite Y and MCM-41 in sodium form. The LLC heterogeneous catalyst presents a higher activity and a faster reactivity than the exchanged ones, which suggests promising applications of this organic mesoporous material.

One homogeneous catalysis method to *synthesize monoglycerides* is based on addition of fatty acids to glycidol and consists in using tertiary amines or ammonium salts catalysts. The difficulty in product recovery evidenced the need to heterogenize the catalyst. Cauvel et al. [319] proposed MMS functionalised with amino groups as catalyst for glycidol ring-opening with fatty acids under mild reaction conditions (120 °C). The authors have tested this reaction over an unmodified calcined MMS and two post-synthesis modified materials (grafted of primary and tertiary amino-groups). The calcined MMS has shown a complete transformation of glycidol without fatty acid conversion. This result reflected an undesirable activity of the silica surface, which catalyzed glycidol polymerization reactions. A better activity of tertiary amine compared to primary ones was attributed to a higher surface coverage due to the more overcrowded piperidyl function, which prevented diffusion towards the silanol surface groups. To eliminate the surface activity, materials were treated with hexamethyldisilazane. As expected the monoglyceride yields increased from 16 to 62% for the primary active phase and from 67 to 90% for the tertiary grafted base (in both case after 24 h). For the same reaction, Lin et al. [327] prefered to deactivate the surface silanol during the first steps of the catalytic test. The activity then increased progressively during the first runs. The strong tertiary base was an exception, in this case a very high primary activity was observed, which decreased progressively. This comportment was attributed to the formation of di- and triglycerides secondary compounds due to a stronger basicity. A high catalytic stability was reported, as evidenced by a very little loss of activity after 11 reaction cycles [316]. Despite this, the authors found that after using 24 h, the pore volume and surface area were considerably smaller and a weaker intensity of the XRD reflections was observed. This raises the problem of mesoporous stability during catalytic tests even if the activity is found unchanged.

Corma et al. [314] discussed the synthesis of monoglycerides by transesterification between glycerol and triglycerides in the presence of different heterogeneous basic catalysts such as MCM-41-Cs, high surface area MgO and hydrotalcites. The authors obtained the best results with MgO for which the conversion of triglyceride reached 97% after 5 h reaction at 513 K with monoglyceride selectivities up to 75%. However, it is important to note the more constraining conditions than exposed before, higher temperature and an excess of glycerol with a molar ratio glycerol to triglyceride 12:1, which induced a complex work-up procedure.

Derrien et al. [321] have also studied the transesterification reaction of ethyl propionate in *n*-butanol using MCM- 41 grafted MTBD and inhibition of the active surface silanols by end capping with hexamethyldisilazane. After 48 h at 100 °C, this catalyst has shown a conversion of 66% compared to 73% in homogeneous MTBD catalysis. This result evidenced the possibility of replacing homogeneous catalysts by these MMS basic materials for their high activity and good selectivity.

The use of MMS basic catalysts in *Michael addition* reactions was the subject of a few studies. This reaction demands a higher basic strength than Knoevenagel reactions. For example, a partially exchanged Na-MCM-41 catalyst was found inactive in the Michael addition of ethyl cyanoacetate to ethyl acrylate [180]. The presence of cesium oxide particles in over exchanged Cs-MCM-41 induces a strong basicity so that this solid is an interesting catalyst for this application [182]. Amines grafted by direct synthesis or post-synthesis treatment have therefore shown promising results in this more demanding reaction [331,338].

4. Conclusions

Mesostructured materials have certainly brought a new dimension to the design of catalysts. Their potential is currently under intense study in a very large variety of catalytic applications. These include both mature technologies like hydrotreating, alkylation or polymerization and newer fields of application such as supported enzyme catalysis, production of fine chemicals and the synthesis of chemicals of biological interest through heterogeneous catalysis.

One key issue for the applicability of MMS in catalysis is associated with the thermal and more importantly the hydrothermal stability. Even though many applications do not require high temperatures (several of them have been discussed in this review), the hydrothermal stability of the catalyst is still critical for such classical catalytic processes as cracking or hydrotreatment. In the latter case, for example, the regeneration of an HDS catalyst requires hydrothermal stability at 650 °C.

Hydrolysis of the Si–O–Si bridges leads to the pore lattice collapse. Therefore, structural stability is dependant on the level of condensation in walls (related to wall thickness) and to the surface density of silanol groups. This explains why thicker wall materials such as those synthesized using triblock copolymers as surfactants, exemplified by SBA-15, are more stable than M41S solids. Wormhole-like structured materials such as HMS and MSU-*x* are also more resistant.

In addition, several treatments, which lead to a decrease in silanol concentration, were found to enhance stability. Among these, silanation was discussed for some times. In spite of the low decomposition temperature of the organic moiety, thermal treatment of silanated silica MMS seems to induce condensation. Salt effects in some instances may also yield improvement in thermal stability. As discussed in Sections 2.2 and 2.3.2, the coating of MMS pore surface by oxide films is also a means of improving this stability. It is indeed remarkable that even post-synthesis alumination may yield such a result, whereas introducing Al ions in the silica lattice, which is the usual approach to making acidic catalysts, is detrimental to hydrothermal resistance.

Despite the significant improvement in structural integrity obtained over the last few years through direct assembly or post-synthesis treatments, the stability of MMS and their acidity are still inferior to conventional zeolites. As reported in Section 2.3.2, one might expect to improve both the stability and acidity of these materials if zeolite-like order could be introduced into the mesopore walls. For example, the use of zeolite seeds as precursors for the assembly of mesoporous aluminosilicates with high hydrothermal stability and acidity was reported by two independent research groups [307–309]. Recent results from our group showed the preparation of a new type of materials with semi-crystalline zeolitic mesopore walls based on a templated solid-state secondary crystallization of zeolites starting from amorphous SBA-15. The resulting materials have much stronger acidity and much improved hydrothermal stability [310–313]. Furthermore, another approach, also proposed by our group, involves the synthesis of zeolite coated mesoporous aluminosilicates (ZCMAS). Hydrothermally ultra-stable and highly acidic ZCMAS are achieved due to the nanocrystalline zeolitic nature of their thick pore walls [649,650].

The mechanical resistance of MMS lattices under high pressure or mechanical strains is also a topic of general relevance for practical applications as catalysts. As discussed in the introduction of Section 2, it seems that these lattices are very resistant especially in the as-synthesized form still containing the surfactant.

Another key issue for the applicability of MMS is associated with reactants and products mass transfer during catalytic reaction. Hexagonal MCM-41 or SBA-15 have long monodimensional (non-intersecting) pores which impose mass transfer limitations in the less accessible parts of these channels. Short intersecting pore framework and small domain size may well facilitate access to the active sites in a MMS structure. The wormhole-like structured materials such as HMS and MSU-*x* with highly interconnected pores and small domain sizes provide shorter diffusion paths for the reactants in the framework channels, leading to high effectiveness factors.

One can further expect to improve accessibility to the active sites in the mesopores by preparing hierarchically porous structures with modes in the macroscopic and mesoscopic scales. Several dual templating methods have been proposed recently for the preparation of such solids. They include macrotemplating with monodispersed latex beads [643–646], fibrous bacteria [647] and chitosan gels [648]. Indeed, structured solids with bimodal pore size distributions are of special interest in providing shorter diffusional pathways to bulkier molecules. This type of solids may, therefore, show great improvements with respect to internal diffusion limitations compared to conventional mesoporous molecular sieves. This is likely to be another exciting future development and a new degree of freedom in controlling catalytic materials properties.

Acknowledgements

The authors wish to thank Dr G. Xu for help in processing the manuscript.

References

[1] C.T. Kresge, M.E. Leonowicz, W.J. Roth, J.C. Vartuli, J.S. Beck, Nature 359 (1992) 710.

[2] T. Yanagisawa, T. Shimizu, K. Kuroda, C. Kato, Bull. Chem. Soc. Jpn. 63 (1990) 988.

[3] A. Monnier, F. Schueth, Q. Huo, D. Kumar, D. Margolese, R.S. Maxwell, G.D. Stucky, M. Krishnamurty, P.M. Petroff, A. Firouzi, M. Janicke, B.F. Chmelka, Science 261 (1993) 1299.

[4] J.S. Beck, J.C. Vartuli, W.J. Roth, M.E. Leonowicz, C.T. Kresge, K.D. Schmitt, C.T.W. Chu, D.H. Olson, E.W. Sheppard, S.B. McCullen, J.B. Higgins, J.L. Schlenker, J. Am. Chem. Soc. 114 (1992) 10834.

[5] C.Y. Chen, H.X. Li, M.E. Davis, Micropor. Mater. 2 (1993) 17.

[6] P. Behrens, Adv. Mater. 5 (1993) 127.

[7] P. Behrens, G.D. Stucky, Angew. Chem. Int. Ed. 32 (1993) 696.

[8] Q.S. Huo, D.I. Margolese, U. Ciesla, P.Y. Feng, T.E. Gier, P. Sieger, R. Leon, P.M. Petroff, F. Schueth, G.D. Stucky, Nature 368 (1994) 317.

[9] Q.S. Huo, D.I. Margolese, U. Ciesla, D.G. Demuth, P.Y. Feng, T.E. Gier, P. Sieger, A. Firouzi, B.F. Chmelka, F. Schueth, G.D. Stucky, Chem. Mater. 6 (1994) 1176.

[10] J.L. Casci, Stud. Surf. Sci. Catal. 85 (1994) 329.

[11] P.T. Tanev, T.J. Pinnavaia, in: T.J. Pinnavaia, M.F. Thorpe (Eds.), Access in Nanoporous Materials, Plenum Press, New York, 1995, p. 13.

[12] X.S. Zhao, G.Q. Lu, G.J. Millar, Ind. Eng. Chem. Res. 35 (1996) 2075.

[13] J.S. Beck, J.C. Vartuli, Curr. Opi. Solid State Mater. Sci. 1 (1996) 76.

[14] N.K. Raman, M.T. Anderson, C.J. Brinker, Chem. Mater. 8 (1996) 1682.

[15] D.M. Antonelli, J.Y. Ying, Curr. Opin. Solid State Mater. Sci. 1 (1996) 523.

[16] A. Sayari, P. Liu, Micropor. Mater. 12 (1997) 149.
[17] M. Ogawa, K. Kuroda, Bull. Soc. Chem. Jpn. 70 (1997) 2593.
[18] G.D. Stucky, Q.S. Huo, A. Firouzi, B.F. Chmelka, S. Schacht, I.G. Voigt-Martin, F. Schueth, Stud. Surf. Sci. Catal. 105 (1997) 3.
[19] A. Corma, Chem. Rev. 97 (1997) 2373.
[20] S. Biz, M.L. Occelli, Catal. Rev.-Sci. Eng. 40 (1998) 329.
[21] J.Y. Ying, C.P. Mehnert, M.S. Wong, Angew. Chem. Int. Ed. 38 (1999) 56.
[22] C.T. Kresge, M.E. Leonowicz, W.J. Roth, J.C. Vartuli, US Patent 5,098,684 (1992).
[23] J.S. Beck, C.T. Chu, I.D. Johnson, C.T. Kresge, M.E. Leonowicz, W.J. Roth, J.C. Vartuli, US Patent 5,108,725 (1992).
[24] J.S. Beck, D.C. Calabro, S.B. McMullen, B.P. Pelrine, K.D. Schmitt, J.C. Vartuli, US Patent 5,145,816 (1992).
[25] S.B. McCullen, J.C. Vartuli, US Patent 5,156,829 (1992).
[26] C.T. Kresge, M.E. Leonowicz, W.J. Roth, J.C. Vartuli, K.M. Keville, S.S. Shih, T.F. Degnan, F.G. Dwyer, M.E. Landis, US Patent 5,183,561 (1993).
[27] J.S. Beck, C.T. Kresge, M.E. Leonowicz, W.J. Roth, J.C. Vartuli, US Patent 5,264,203 (1993).
[28] J.S. Beck, K.D. Schmitt, J.C. Vartuli, US Patent 5,334,368 (1994).
[29] J.S. Beck, C.T. Kresge, S.B. McCullen, W.J. Roth, J.C. Vartuli, US Patent 5,370,785 (1994).
[30] J.S. Beck, J.C. Vartuli, G.J. Kennedy, C.T. Kresge, W.J. Roth, S.E. Schramm, Chem. Mater. 6 (1994) 1816.
[31] J.C. Vartuli, C.T. Kresge, M.E. Leonowicz, A.S. Chu, S.B. McCullen, I.D. Johnson, E.W. Sheppard, Chem. Mater. 6 (1994) 2070.
[32] J.C. Vartuli, K.D. Schmitt, G.J. Kennedy, C.T. Kresge, W.J. Roth, M.E. Leonowicz, S.B. McCullen, S.D. Hellring, J.S. Beck, J.L. Schlenker, D.H. Olson, E.W. Sheppard, Stud. Surf. Sci. Catal. 84 (1994) 53.
[33] J.C. Vartuli, S.S. Shih, C.T. Kresge, J.S. Beck, Stud. Surf. Sci. Catal. 117 (1998) 13.
[34] G.D. Stucky, A. Monnier, F. Schueth, Q. Huo, D.I. Margolese, D. Kumar, M. Krishnamurty, P. Petroff, A. Firouzi, M. Janicke, B.F. Chmelka, Mol. Cryst. Liq. Cryst. 240 (1994) 187.
[35] U. Ciesla, D. Demuth, R. Leon, P. Petroff, G.D. Stucky, K. Unger, F. Schueth, J. Chem. Soc., Chem. Commun. (1994) 1387.
[36] L. Bull, D. Kumar, S.P. Millar, T. Besier, M. Janicke, G.D. Stucky, B.F. Chmelka, Stud. Surf. Sci. Catal. 84 (1994) 429.
[37] Q. Huo, R. Leon, P. Petroff, G.D. Stucky, Science 268 (1995) 1324.
[38] A. Firouzi, D. Kumar, L.M. Bull, T. Besier, P. Sieger, Q. Huo, S.A. Walker, J. Zasadzinski, A.G. Glinka, J. Nicol, D. Margolese, G.D. Stucky, B.F. Chmelka, Science 267 (1995) 1138.
[39] Q. Huo, D.I. Margolese, G.D. Stucky, Chem. Mater. 8 (1996) 1147.
[40] P.T. Tanev, M. Chibwe, T.J. Pinnavaia, Nature 368 (1994) 321.
[41] P.T. Tanev, T.J. Pinnavaia, Science 167 (1995) 865.
[42] S.A. Bagshaw, E. Prouzet, T.J. Pinnavaia, Science 269 (1995) 1242.
[43] W. Zhang, T.R. Pauly, T.J. Pinnavaia, Chem. Mater. 9 (1997) 2491.
[44] W. Zhang, M. Froeba, J. Wang, P.T. Tanev, J. Wong, T.J. Pinnavaia, J. Am. Chem. Soc. 118 (1996) 9164.
[45] W. Zhang, J. Wang, P.T. Tanev, T.J. Pinnavaia, J. Chem. Soc., Chem. Commun. (1996) 979.
[46] S.A. Bagshaw, T.J. Pinnavaia, Angew. Chem. Int. Ed. 35 (1996) 1102.
[47] E. Prouzet, T.J. Pinnavaia, Angew. Chem. Int. Ed. 36 (1997) 516.
[48] T.J. Pinnavaia, W. Zhang, Stud. Surf. Sci. Catal. 117 (1998) 23.
[49] D. Zhao, J. Feng, Q. Huo, N. Melosh, G.H. Fredrickson, B.F. Chmelka, G.D. Stucky, Science 279 (1998) 548.
[50] D. Zhao, Q. Huo, J. Feng, B.F. Chmelka, G.D. Stucky, J. Am. Chem. Soc. 120 (1998) 6024.
[51] G.D. Stucky, D. Zhao, P. Yang, W. Lukens, N. Melosh, B.F. Chmelka, Stud. Surf. Sci. Catal. 117 (1998) 1.
[52] G.D. Studky, B.F. Chmelka, D. Zhao, N. Melosh, Q. Huo, J. Feng, P. Yang, D. Pine, D. Margolese, W. Lukens, G.H. Fredrickson, P. Schmidt-Winkel, Int. Patent WO99/37705 (July 1999).
[53] D.E. De Vos, B.F. Sels, P.A. Jacobs, Adv. Catal. 46 (2001) 1.
[54] K. Moller, T. Bein, Chem. Mater. 10 (1998) 2950.
[55] G.S. Attard, P.N. Bartlett, N.R.B. Coleman, J.M. Elliott, J.R. Owen, J.H. Wang, Science 278 (1997) 838.
[56] G.S. Attard, N.R.B. Coleman, J.M. Elliott, Stud. Surf. Sci. Catal. 117 (1998) 89.
[57] G.S. Attard, S.A.A. Leclerc, S. Maniguet, A.E. Russell, I. Nandha Kumar, B.R. Gollas, P.N. Bartlett, Micropor. Mesopor. Mater. 44–45 (2001) 159.
[58] S.H. Joo, S. Jun, R. Ryoo, Micropor. Mesopor. Mater. 44–45 (2001) 153.
[59] R. Ryoo, S.H. Joo, S. Jun, J. Phys. Chem. B 103 (1999) 7743.
[60] J. Lee, S. Yun, T. Hyeon, S.M. Oh, K.B. Kim, Chem. Commun. (1999) 2177.
[61] J. Lee, S. Yun, S.M. Oh, C.-H. Shin, T. Hyeon, Adv. Mater. 12 (2000) 359.
[62] S. Jun, S.H. Joo, R. Ryoo, M. Kruk, M. Jaroniec, Z. Liu, T. Ohsuma, O. Terasaki, J. Am. Chem. Soc. 43 (2000) 10712.
[63] M. Kruk, M. Jaroniec, R. Ryoo, S.H. Joo, Chem. Mater. 12 (2000) 1414.
[64] H.J. Shin, R. Ryoo, M. Kruk, M. Jaroniec, Chem. Commun. (2001) 349.
[65] H. Darmstadt, C. Roy, S. Kaliaguine, S. Choi, R. Ryoo. Carbon 2001, International Conference on Carbon, Lexington, Kentucky, 14–19 July 2001.
[66] S. Inagaki, S. Guan, Y. Fukishima, T. Ohsuna, O. Terasaki, J. Am. Chem. Soc. 121 (1999) 9611.
[67] B.J. Melde, B.T. Holland, C.F. Blanford, A. Stein, Chem. Mater. 11 (1999) 3302.
[68] T. Asefa, M.J. MacLachlan, N. Coombs, G.A. Ozin, Nature 402 (1999) 867.

[69] C. Yoshina-Ishii, T. Asefa, N. Coombs, M.J. MacLachlan, G.A. Ozin, Chem. Commun. (1999) 2539.

[70] T. Asefa, M.J. MacLachlann, H. Grondey, N. Coombs, G.A. Ozin, Angew. Chem. Int. Ed. 39 (2000) 1808.

[71] S. Guan, S. Inagaki, T. Ohsuna, T. Terasaki, J. Am. Chem. Soc. 122 (2000) 5660.

[72] Y. Lu, H. Fan, N. Doke, D.A. Loy, R.A. Assink, D.A. La Van, C.J. Brinker, J. Am. Chem. Soc. 122 (2000) 5258.

[73] A. Sayari, S. Hamoudi, Y. Yang, I. Moudrakovski, J.R. Ripmeester, Chem. Mater. 12 (2000) 3857.

[74] H. Fan, S. Reed, T. Baer, R. Shunk, G.P. Lopez, C.J. Brinker, Micropor. Mesopor. Mater. 44–45 (2001) 625.

[75] S. Guan, S. Inagaki, T. Ohsuna, O. Terasaki, Micropor. Mesopor. Mater. 44–45 (2001) 165.

[76] H. Yang, N. Coombs, G.A. Ozin, Nature 386 (1997) 692.

[77] G.A. Ozin, H. Yang, I. Sokolov, N. Coombs, Adv. Mater. 9 (1997) 662.

[78] N. Coombs, D. Khushalani, G.A. Ozin, S. Oliver, G.C. Shen, I. Sokolov, H. Yang, Dalton Trans. (1997) 3941.

[79] G.A. Ozin, C.T. Kresge, H. Yang, Stud. Surf. Sci. Catal. 117 (1998) 119.

[80] H. Yang, G. Vouk, N. Coombs, I. Sokolov, G.A. Ozin, J. Mater. Chem. 8 (1998) 743.

[81] S.M. Yang, H. Yang, N. Coombs, I. Sokolov, C.T. Kresge, G.A. Ozin, Adv. Mater. 11 (1999) 52.

[82] I. Sokolov, H. Yang, G.A. Ozin, C.T. Kresge, Adv. Mater. 11 (1999) 636.

[83] S.H. Tolbert, T.E. Schäffer, J. Feng, P.K. Hansma, G.D. Stucky, Chem. Mater. 9 (1997) 1962.

[84] Q. Huo, J. Feng, F. Schueth, G.D. Stucky, Chem. Mater. 9 (1997) 14.

[85] J. Feng, Q. Huo, G.D. Stucky, P.M. Petroff, Appl. Phys. Lett. 71 (1997) 620.

[86] Q. Huo, D. Zhao, J. Feng, K. Weston, S.K. Buratto, G.D. Stucky, S. Schacht, F. Schueth, Adv. Mater. 9 (1997) 974.

[87] D. Zhao, P. Yang, N. Melosh, J. Feng, B.F. Chmelka, G.M. Whitesides, G.D. Stucky, Adv. Mater. 10 (1998) 1380.

[88] P. Yang, D. Zhao, B.F. Chmelka, G.D. Stucky, Chem. Mater. 10 (1998) 2033.

[89] D. Zhao, P. Yang, B.F. Chmelka, G.D. Stucky, Chem. Mater. 11 (1999) 1174.

[90] D. Zhao, J. Sun, Q. Li, G.D. Stucky, Chem. Mater. 12 (2000) 275.

[91] S. Shio, A. Kimura, M. Yamaguchi, K. Yoshida, K. Kuroda, Chem. Commun. (1998) 742.

[92] H.P. Lin, C.Y. Mou, Science 273 (1996) 765.

[93] H.P. Lin, S. Cheng, C.Y. Mou, Micropor. Mater. 10 (1997) 111.

[94] H.P. Lin, S. Cheng, C.Y. Mou, Chem. Mater. 10 (1998) 581 and 3772.

[95] P. Tanev, Y. Liang, T.J. Pinnavaia, J. Am. Chem. Soc. 119 (1997) 8616.

[96] S.S. Kim, W. Zhang, T.J. Pinnavaia, Science 282 (1998) 1302.

[97] J.Wu, X. Liu, S.H. Tolbert, in: Proceedings of the 2nd International Symposium on Mesopprous Molecular Sieves, Quebec, 30 August–2 September 2000, Poster 119.

[98] J. Wu, X. Liu, S.H. Tolbert, J. Phys. Chem. B 104 (2001) 11837.

[99] J. Wu, M. Abu-Omar, S.H. Tolbert, NanoLett. 1 (2001) 27.

[100] D. Desplantier-Giscard, O. Collart, A. Galarneau, P. Van der Voort, F. Di Renzo, F. Fajula, Stud. Surf. Sci. Catal. 129 (2000) 665.

[101] A. Galarneau, D. Desplantier-Giscard, F. Di Renzo, F. Fajula, Catal. Today. 66 (2001) 73.

[102] U. Junges, W. Jacobs, I. Voight-Martin, B. Krutzsch, F. Schueth, J. Chem. Soc., Chem. Commun. (1995) 2283.

[103] K.M. Reddy, C. Song, Catal. Today 31 (1996) 137.

[104] R. Mokaya, W. Jones, S. Moreno, G. Poncelet, Catal. Lett. 49 (1997) 87.

[105] A. Corma, A. Martinez, V. Martinez-Soria, J. Catal. 169 (1997) 480.

[106] R. Ryoo, C.H. Ko, J.M. Kim, R. Howe, Catal. Lett. 37 (1996) 29.

[107] N. Yao, C. Pinckney, S. Lim, C. Pak, G.L. Haller, Micropor. Mesopor. Mater. 44–45 (2001) 377.

[108] B.H. Copper, B.B.L. Donnis, Appl. Catal. A137 (1995) 203.

[109] W.M.H. Sachtler, A.Tu. Stakheev, Catal. Today 12 (1992) 283.

[110] J. Heinerman, E. Vogt, WO 94/26846 (1994).

[111] K.M. Reddy, C. Song, Prepr. ACS, Div. Fuel Chem. 46 (1996) 906.

[112] T. Inui, J.B. Kim, M. Seno, Catal. Lett. 29 (1994) 271.

[113] Z. Liu, O. Terasaki, T. Ohsuna, R. Ryoo, Chem. Phys. Chem. 2 (2001) 229.

[114] H.J. Shin, C.H. Ko, R. Ryoo, J. Mater. Chem. 11 (2001) 260.

[115] H.J. Shin, R. Ryoo, Z. Liu, J. Am. Chem. Soc. 123 (2001) 1246.

[116] Z. Liu, Y. Sakamoto, T. Ohsuna, K. Hiraga, O. Terasaki, C.H. Ko, H.J. Shin, R. Ryoo, Angew. Chem. Int. Ed. 39 (2000) 3107.

[117] U. Junges, F. Schueth, G. Schmid, Y. Uchida, R. Schloegl, Berl Bunsenges. Phys. Chem. 101 (1997) 1631.

[118] U. Junges, S. Disser, G. Schmid, F. Schueth, Stud. Surf. Sci. Catal. 117 (1998) 391.

[119] C.P. Mehnert, J.Y. Ying, J. Chem. Soc. Chem. Commun. (1997) 2215.

[120] J.Y. Ying, Stud. Surf. Sci. Catal. 117 (1998) 85.

[121] W.S. Borghard, C.T. Chu, T.F. Degnan, S.S. Shih, US Patent 5,264,641 (1993).

[122] J.N. Armor, Appl. Catal. A: Gen. 112 (1994) N21.

[123] M. Kruk, M. Jaroniec, R. Ryoo, S.H. Joo, J. Phys. Chem. B 104 (2000) 7960.

[124] S. Coman, F. Cocu, J.F. Roux, V.J. Parvulescu, S. Kaliaguine, Stud. Surf. Sci. Catal. 117 (1998) 501.

[125] S. Coman, R. Caraba, F. Cocu, V.I. Parvulescu, H. Bönnemann, B. Tesche, C. Danumah, S. Kaliaguine, Stud. Surf. Sci. Catal. 130 (2000) 3471.

[126] S. Coman, V.I. Parvulescu, B. Tesche, H. Bönnemann, J.F. Roux, S. Kaliaguine, P.A. Jacobs, J. Mol. Catal. A 146 (1999) 247.

[127] S. Coman, M. Florea, F. Cocu, V.I. Parvulescu, P.A. Jacobs, C. Danumah, S. Kaliaguine, J. Chem. Soc., Chem. Commun. (1999) 2175.

[128] M. Florea, M. Sevinci, V.I. Parvulescu, G. Lemay, S. Kaliaguine, Micropor. Mesopor. Mater. 44–45 (2001) 483.
[129] C. Bischof, M. Hartman, in: Proceedings 12th International Zeolite Conference, Materials Research Society, Warrandale, 1999, p. 795.
[130] M. Hartman, C. Bischof, Z. Luan, L. Kevan, Micropor. Mesopor. Mater. Mater. 44–45 (2001) 385.
[131] D.S. Shephard, T. Maschmeyer, G. Sankar, J.M. Thomas, D. Ozkaya, B.F. Johnson, R. Raja, R.D. Oldroyd, R.G. Bell, Chem. Eur. J. 4 (1998) 1214.
[132] D.S. Shephard, T. Maschmeyer, B.F. Johnson, J.M. Thomas, G. Sankar, D. Ozkaya, W. Zhou, R.D. Oldroyd, Angew. Chem. 109 (1997) 2337.
[133] D.S. Shephard, T. Maschmeyer, B.F. Johnson, J.M. Thomas, G. Sankar, D. Ozkaya, W. Zhou, R.D. Oldroyd, Angew. Chem. Int. Ed. 36 (1997) 2242.
[134] S. Valange, J. Barrault, A. Derouault, Z. Gabelica, Micropor. Mesopor. Mater. 44–45 (2001) 211.
[135] S. Valange, Z. Gabelica, Stud. Surf. Sci. Catal. 117 (1998) 95.
[136] X. Gao, S.R. Bare, J.L.G. Fierro, M.A. Banares, I.E. Wachs, J. Phys. Chem. 102 (1998) 5653.
[137] T. Maschmeyer, F. Rey, G. Sankar, J.M. Thomas, Nature 378 (1995) 159.
[138] J.V. Walker, M. Morey, H. Carlsson, A. Davidson, G.D. Stucky, A. Butler, J. Am. Chem. Soc. 119 (1997) 6921.
[139] R.D. Oldroyd, G. Sankar, J.M. Thomas, D. Özkaya, J. Phys. Chem. B102 (1998) 1849.
[140] L. Marchese, E. Gianotti, V. Dellarocca, T. Maschmeyer, F. Rey, S. Coluccia, J.M. Thomas, Phys. Chem. Chem. Phys. 1 (1999) 585.
[141] B.J. Aronson, C.F. Blanford, A. Stein, Chem. Mater. 9 (1997) 2842.
[142] A. Hagen, D. Wei, G.L. Haller, Stud. Surf. Sci. Catal. 117 (1998) 191.
[143] Z. Luan, E.M. Maes, P.A.W. van der Heide, D. Zhao, R.S. Czernuszewicz, L. Kevan, Chem. Mater. 11 (1999) 3680.
[144] M. Widenmeyer, S. Grasser, K. Köhler, R. Anwander, Micropor. Mesopor. Mater. 44–45 (2001) 327.
[145] K. Schrinemakers, E.F. Vansant, in: Proceedings of the 2nd International Symposium on Mesoporous Molecular Sieves, Quebec, 30 August–2 September 2000, Poster 49.
[146] Y. Xu, C.H. Langford, J. Phys. Chem. B 101 (1997) 3115.
[147] M. Morey, A. Davidson, H. Eckert, G. Stucky, Chem. Mater. 8 (1996) 486.
[148] P. Van DerVoort, M. Morey, G.D. Stucky, M. Mathieu, E.F. Vansant, J. Phys. Chem. B 102 (1998) 585.
[149] P. Van Der Voort, M. Morey, G.D. Stucky, M. Mathieu, E.F. Vansant, Stud. Surf. Sci. Catal. 117 (1998) 333.
[150] Z. Luan, L. Kevan, J. Phys. Chem. B101 (1997) 2020.
[151] Z. Luan, P.A. Meloni, R.S. Czernuszewicz, L. Kevan, J. Phys. Chem. B101 (1997) 9046.
[152] P. Van Der Voort, E.F. Vansant, Micropor. Mesopor. Mater. 38 (2000) 385.
[153] P. Van der Voort, E.F. Vansant, J. Phys. Chem. B103 (1999) 10102.
[154] P. Van Der Voort, E.F. Vansant, Stud. Surf. Sci. Catal. 129 (2000) 317.
[155] K.A. Vercruysse, D.M. Klingeleers, T. Colling, P.A. Jacobs, Stud. Surf. Sci. Catal. 117 (1998) 469.
[156] S. Mark, M.S. Morey, G.D. Stucky, S. Schwarz, M. Fröba, J. Phys. Chem. B 103 (1999) 2037.
[157] F. Schueth, A. Wingen, J. Sauer, Micropor. Mesopor. Mater. Mater. 44–45 (2001) 465.
[158] C.H.F. Peden, personal communications.
[159] T. Abe, Y. Tachibana, T. Uematsu, M. Iwamoto, J. Chem. Soc., Chem. Commun. (1995) 1617.
[160] Z.Y. Luan, S.Q. Liu, T.H. Chen, J.Z. Wang, H.X. Li, J. Chem. Soc. Chem. Commun. (1995) 973.
[161] J. Cao, N. He, C. Li, J. Dong, Q. Xu, Stud. Surf. Sci. Catal. 117 (1998) 461.
[162] S.K. Badamali, S.E. Dapukar, S.K. Mohapatra, P. Selvam, in: Proceedings of the 2nd International Symposium on Mesoporous Molecular Sieves, Quebec, 30 August–2 September, 2000, Poster 146.
[163] M. Fröba, R. Köhn, G. Bouffaud, Chem. Mater. 11 (1999) 2858.
[164] M. Cheng, F. Kumata, T. Saito, T. Komatsu, T. Yashima, Stud. Surf. Sci. Catal. 117 (1998) 485.
[165] M.S. Morey, J.D. Bryan, S. Schwarz, G.D. Stucky, Chem. Mater. 12 (2000) 3435.
[166] J.M. Brégeault, J.Y. Piquemal, E. Briot, E. Duprey, F. Launay, L. Salles, M. Vennat, A.P. Legrand, Micropor. Mesopor. Mater. 44–45 (2001) 409.
[167] M. Hartmann, A. Pöppl, L. Kevan, J. Phys. Chem. 99 (1995) 17494.
[168] M. Hartmann, A. Pöppl, L. Kevan, J. Phys. Chem. 100 (1996) 9906.
[169] M. Hartmann, A. Pöppl, L. Kevan, Stud. Surf. Sci. Catal. 101 (1996) 801.
[170] D.J. Lensveld, J.G. Mesu, A.J. van Dillen, K.P. de Jong, Micropor. Mesopor. Mater. 44–45 (2001) 401.
[171] R. Rao, B.M. Weckhuysen, R.A. Schoonheydt, J. Chem. Soc., Chem. Commun. (1999) 445.
[172] Z. Zhu, M. Hartmann, E.M. Maes, R.S. Czernuszewicz, L. Kevan, J. Phys. Chem. B 104 (2000) 4690.
[173] W.H. Zhang, J.L. Shi, L.Z. Wang, D.S. Yan, Chem. Mater. 12 (2000) 1408.
[174] S. Kowalak, K. Stawinski, A. Mackowiak, Micropor. Mesopor. Mater. 44–45 (2001) 283.
[175] R. Burch, N. Cruise, D. Gleeson, S.C. Tsang, Chem. Commun. (1996) 951.
[176] R. Burch, N.A. Cruise, D. Gleeson, S.C. Tsang, J. Mater. Chem. 8 (1998) 227.
[177] D. Gleeson, R. Burch, N.A. Cruise, S.C. Tsang, Nanostruct. Mater. 12 (1999) 1007.
[178] A. Zecchina, D. Scarano, G. Spoto, S. Bordiga, C. Lamberti, G. Bellussi, Stud. Surf. Sci. Catal. 117 (1998) 343.
[179] K.R. Kloetstra, J. Van den Broek, H. van Bekkum, Catal. Lett. 47 (1997) 235.
[180] K.R. Kloetstra, M. van Laren, H. van Bekkum, J. Chem. Soc., Faraday Trans. 93 (1997) 1211.
[181] K.R. Kloetstra, H. van Bekkum, J. Chem. Soc., Chem. Commun. (1995) 1005.
[182] K.R. Kloetstra, H. van Bekkum, Stud. Surf. Sci. Catal. 105 (1997) 431.

[183] A. Tuel, Micropor. Mesopor. Mater. 27 (1999) 151.

[184] D. Trong On, P.N. Joshi, S. Kaliaguine, J. Phys. Chem. 100 (1996) 6743.

[185] D. Trong On, P.N. Joshi, G. Lemay, S. Kaliaguine, Stud. Surf. Sci. Catal. 97 (1995) 543.

[186] E. Dumitru, D. Trong On, S. Kaliaguine, J. Catal. 170 (1997) 150.

[187] R. Fricke, H. Kosslick, G. Lischke, M. Richter, Chem. Rev. 100 (2000) 2303.

[188] H. Kosslick, H. Landmesser, R. Fricke, J. Chem. Soc., Faraday Trans. 93 (1997) 1849.

[189] H. Kosslick, G. Lischke, G. Wather, W. Storek, A. Martin, R. Fricke, Micropor. Mater. 9 (1997) 13.

[190] H. Kosslick, G. Lischke, H. Landmesser, B. Parlitz, W. Storek, R. Fricke, J. Catal. 176 (1998) 102.

[191] H. Landmesser, H. Kosslick, U. Kurshner, R. Fricke, J. Chem. Soc., Faraday Trans. 94 (1998) 971.

[192] S. Lim, G.L. Haller, Stud. Surf. Sci. Catal. 130C (2000) 3053.

[193] L. Pasqua, F. Testa, R. Aiello, Stud. Surf. Sci. Catal. 117 (1998) 317.

[194] N.-Y. He, S.-L. Bao, Q.-H. Xu, Stud. Surf. Sci. Catal. 105 (1997) 85.

[195] R. Mokaya, W. Jones, J. Catal. 172 (1997) 211.

[196] A. Corma, V. Fornes, M.T. Navarro, J. Perez-Pariente, J. Catal. 148 (1994) 569.

[197] M. Busio, J. Janchen, J.H.C.V. Hoof, Micropor. Mater. 5 (1995) 211.

[198] X.S. Zhao, G.Q. Lu, G.J. Millar, Catal. Lett. 38 (1996) 33.

[199] A. Jentys, N.H. Pham, H. Vinek, J. Chem. Soc., Faraday Trans. 92 (1996) 3287.

[200] J-H. Kim, M. Tanabe, M. Niwa, Micropor. Mater. 10 (1997) 85.

[201] X. Chen, L. Huang, G. Ding, Q. Li, Catal. Lett. 44 (1997) 123.

[202] A. Liepold, K. Roos, W. Reschetilowski, R. Schmidt, M. Stocker, A. Philippou, M.W. Anderson, A.P. Esculcas, J. Rocha, Stud. Surf. Sci. Catal. 105A (1997) 423.

[203] B. Chakraborty, B. Viswanathan, Catal. Today 49 (1999) 253.

[204] R. Schmidt, D. Akporiaye, M. Stocker, O.H. Ellestad, J. Chem. Soc., Chem. Commun. (1994) 1493.

[205] R. Mokaya, J. Phys. Chem. B 104 (2000) 8279.

[206] C.-Y. Chen, H.-X. Li, M. Davis, Micropor. Mesopor. Mater. 2 (1993) 27.

[207] K.M. Reddy, C. Song, Catal. Lett. 36 (1996) 103.

[208] K.M. Reddy, C. Song, Mater. Res. Soc. Symp. Proc. 454 (1997) 125.

[209] K.M. Reddy, C. Song, Stud. Surf. Sci. Catal. 117 (1998) 291.

[210] M.L. Occelli, S. Biz, A. Auroux, G.L. Ray, Micropor. Mesopor. Mater. 26 (1998) 193.

[211] S. Biz, M.G. White, J. Phys. Chem. B 103 (1999) 8432.

[212] S.K. Badamali, A. Sakthivel, P. Selvam, Catal. Today 63 (2000) 291.

[213] Y. Cesteros, G.L. Haller, Micropor. Mesopor. Mater. 43 (2001) 171.

[214] D. Trong On, S.M.J. Zaidi, S. kaliaguine, Micropor. Mesopor. Mater. 22 (1998) 211.

[215] S. Cabrera, J.E. Haskouri, S. Mendioroz, C. Guillem, J. Latorre, A. Beltran-Porter, D. Beltran-Ponter, M.D. Marcos, P. Amoros, Chem. Commun. (1997) 1679.

[216] M. Chatterjee, T. Iwasaki, H. Hayashi, Y. Onodera, T. Ebina, T. Nagase, Catal. Lett. 52 (1998) 21.

[217] M.T. Janicke, C.C. Landry, S.C. Christiansen, S. Birtalan, G.D. Stucky, B.F. Chmelka, Chem. Mater. 11 (1999) 1342.

[218] H.H.P. Yiu, D.R. Brown, Catal. Lett. 56 (1998) 57.

[219] X.S. Zhao, G.Q. Lu, G.J. Millar, A.J. Whittaker, H.Y. Zhu, J. Phys. Chem. B 101 (1997) 6525.

[220] X.S. Zhao, G.Q. Lu, J. Phys. Chem. B 102 (1998) 1556.

[221] X.S. Zhao, F. Audsley, G.Q. Lu, J. Phys. Chem. B 102 (1998) 4143.

[222] A. Jentys, K. Kleestorfer, H. Vinek, Micropor. Mesopor. Mater. 27 (1999) 321.

[223] X.S. Zhao, G.Q. Lu, X. Hu, Micropor. Mesopor. Mater. 41 (2000) 37.

[224] R. Ryoo, S. Jun, J. Phys. Chem. B 101 (1997) 317.

[225] D. Das, C-M. Tsai, S. Cheng, Chem. Commun. (1999) 473.

[226] J.M. Kim, S. Jun, R. Ryoo, J. Phys. Chem. 103 (1999) 6200.

[227] L. Chen, T. Horiuchi, T. Mori, K. Maeda, J. Phys. Chem. B 103 (1999) 1216.

[228] S. Jun, R. Ryoo, J. Catal. 195 (2000) 237.

[229] R. Ryoo, J.M. Kim, Chem. Commun. (1995) 711.

[230] S. Hitz, A. Kogelbauer, B. Lindlar, R. Prins, Stud. Surf. Sci. Catal. 117 (1998) 519.

[231] B. Lindlar, A. Kogelbauer, R. Prins, Micropor. Mesopor. Mater. 38 (2000) 167.

[232] A. Matsumoto, H. Chen, K. Tsutumi, M. Grun, K. Unger, Micropor. Mesopor. Mater. 32 (1999) 55.

[233] S. Hitz, R. Prins, J. Catal. 168 (1997) 194.

[234] Q. Kan, V. Fornes, F. Rey, A. Corma, J. Mater. Chem. 10 (2000) 993.

[235] Y. Yue, A. Gedeon, J.-L. Bonardet, J. d'Espinose, N. Melosh, J. Fraissard, Chem. Commun. (1999) 1967.

[236] Y.-H. Yue, A. Gedeon, J.-L. Bonardet, J.B. d'Espinose, N. Melosh, J. Fraissard, Stud. Surf. Sci. Catal. 129 (2000) 209.

[237] A. Gedeon, A. Lassoued, J.L. Bonardet, J. Fraissard, Micropor. Mesopor. Mater. 44–45 (2001) 801.

[238] A. Corma, A. Martinez, V. Martinez-Soria, J.B. Monton, J. Catal. 153 (1995) 25.

[239] A. Galarneau, A. Barodawalla, T.J. Pinnavaia, Nature 374 (1995) 529.

[240] A. Galarneau, A. Barodawalla, T.J. Pinnavaia, Chem. Commun. (1997) 1661.

[241] A. Galarneau, A. Barodawalla, T.J. Pinnavaia, in: Proceedings of the 11th International Clay Conference, Ottawa, Canada, 1997, p. 21.

[242] M. Polverejan, T.R. Pauly, T.J. Pinnavaia, Chem. Mater. 12 (2000) 2698.

[243] R. Ryoo, S. Jun, J.M. Kim, M.J. Kim, Chem. Commun. (1997) 2225.

[244] R. Mokaya, W. Jones, Chem. Commun. (1997) 2185.

[245] R. Mokaya, Chem. Commun. (1998) 1839.

[246] R. Mokaya, Angew. Chem. Int. Ed. 38 (1999) 2930.

[247] R. Mokaya, W. Jones, Phys. Chem. Chem. Phys. 1 (1999) 207.

[248] R. Mokaya, Chem. Commun. (2000) 1891.

[249] R. Mokaya, J. Catal. 193 (2000) 103.

[250] S. Kawi, S.C. Shen, Stud. Surf, Sci. Catal. 129 (2000) 219.

[251] S. Kawi, S.C. Shen, Stud. Surf. Sci. Catal. 129 (2000) 227.

[252] S. Sumiya, Y. Oumi, T. Uozumi, T. Sano, J. Mater. Chem. 11 (2001) 1111.

[253] K. Hamaguchi, H. Hattori, React. Kinet. Catal. Lett. 61 (1997) 13.

[254] Z. Luan, M. Hartmann, D. Zhao, W. Zhou, L. Kevan, Chem. Mater. 11 (1999) 1621.

[255] R. Mokaya, Chem. Commun. (2001) 633.

[256] R. Anwander, C. Palm, O. Groeger, G. Engelhard, Organometlics 17 (1998) 2027.

[257] M. Misono, N. Mizuno, K. Katamura, A. Kasai, Y. Konishi, T. Okuhara, Y. Yoneda, Bull. Chem. Soc. Jpn. 55 (1982) 400.

[258] I.V. Kozhevnikov, A. Sinnema, R.J.J. Jansen, K. Pamin, H. van Bekkum, Catal. Lett. 30 (1995) 241.

[259] I.V. Kozhevnikov, K.R. Kloestra, A. Sinnema, H.W. Zandbergen, H. van Bekkum, J. Mol. Catal. A: Chem. 114 (1996) 287.

[260] F. Marne, G. Coudurier, J.C. Vedrine, Micropor. Mesopor. Mater. 22 (1998) 151.

[261] A. Ghanbari-Siahkali, A. Philippou, J. Dwyer, M.W. Anderson, Appl. Catal. A: Gen. 192 (2000) 57.

[262] T. Blasco, A. Corma, A. Martinez, P. Martinez-Escolano, J. Catal. 177 (1998) 306.

[263] P.A. Jalil, M.A. Al-Daous, A.-R.A. Al-Arfaj, A.M. Al-Amer, J. Beltramini, S.A.I. Barri, Appl. Catal. A: Gen. 207 (2001) 159.

[264] Y. Wang, C.H.F. Peden, S. Choi, 2000 WO2000029107, p. 30.

[265] Y. Wang, A.Y. Kim, S. Li, L-Q. Wang, C.H.F. Peden, B.C. Bunker, ACS. Symp. Ser. 738 (2000) 353.

[266] S. Choi, Y. Wang, Z. Nie, D. Khambapati, J. Liu, C.H.F. Peden, Stud. Surf. Sci. Catal. 130 (2000) 965.

[267] S. Choi, Y. Wang, Z. Nie, J. Liu, C.H.F. Peden, Catal. Today 55 (2000) 117.

[268] S. Soled, S. Miseo, G. Mc Vicker, W.E. Gates, A. Gutierrez, J. Paes, Catal. Today 36 (1997) 441.

[269] L. Mercier, C. Detellier, Environ. Sci. Technol. 29 (1995) 1318.

[270] G.M. Whitesides, Sci. Am. 273 (1995) 146.

[271] A. Ulman, Chem. Rev. 96 (1996) 1533.

[272] J.-C. Lin, W.-H. Chuang, J. Biomed. Mater. Res. 51 (2000) 413.

[273] V. Boiadjiev, A. Blumenfeld, J. Gutow, W.T. Tysoe, Chem. Mater. 12 (2000) 2604.

[274] N. Sandhyarani, M.R. Resmi, R. Unnikrishnan, K. Vidyasagar, S. Ma, M.P. Antony, G. Panneer Selvam, V. Visalakshi, N. Chandrakumar, K. Pandian, Y.-T. Tao, T. Pradeep, Chem. Mater. 12 (2000) 104.

[275] L. Mercier, T.J. Pinnavaia, Environ. Sci. Technol. 32 (1998) 2749.

[276] J. Liu, X. Feng, G.E. Fryxell, L.-Q. Wang, A.Y. Kim, M. Gong, Adv. Mater. 10 (1998) 161.

[277] L. Mercier, T. Pinnavaia, Chem. Mater. 12 (2000) 188.

[278] A.M. Liu, K. Hidajat, S. Kawi, D.Y Zhao, Chem. Commun. (2000) 1145.

[279] J. Brown, R. Richer, L. Mercier, Micropor. Mesopor. Mater. 37 (2000) 41.

[280] M.H. Lim, C.F. Blanford, A. Stein, Chem. Mater. 10 (1998) 467.

[281] W.M. Van Rhijn, D.E. De Vos, B.F. Sels, W.D. Bossaert, P.A. Jacobs, Chem. Commun. (1998) 317.

[282] W.M. Van Rhijn, D.E. Vos, W.D. Bossaert, J. Bullen, B. Vouters, P. Grobert, P.A. Jacobs, Stud. Surf. Sci. Catal. 117 (1998) 183.

[283] W.D. Bossaert, D.E. De Vos, W.M. Van Rhijn, J. Bullen, P.J. Grobert, P.A. Jacobs, J. Catal. 182 (1999) 156.

[284] I. Diaz, C. Marquez-Alvarez, F. Mohino, J. Perez-Pariente, E. Sastre, Micropor. Mesopor. Mater. 44–45 (2001) 295.

[285] I. Diaz, C. Marquez-Alvarez, F. Mohino, J. Perez-Pariente, E. Sastre, J. Catal. 193 (2000) 283.

[286] I. Diaz, C. Marquez-Alvarez, F. Mohino, J. Perez-Pariente, E. Sastre, J. Catal. 193 (2000) 295.

[287] I. Diaz, F. Mohino, J. Perez-Pariente, E. Sastre, Appl. Catal. A: Gen. 205 (2001) 19.

[288] D. Margolese, J.A. Melero, S.C. Christiansen, B.F. Chmelka, G.D. Stucky, Chem. Mater. 12 (2000) 2448.

[289] X. Feng, G.E. Fryxell, L.-Q. Wang, A.Y. Kim, J. Liu, K.M. Kemmer, Science 276 (1997) 923.

[290] V. Antochshuck, M. Jaroniec, Chem. Commun. (1999) 2373.

[291] V. Antochshuk, M. Jaroniec, Chem. Mater. 12 (2000) 2496.

[292] H.-P. Lin, L.-Y. Yang, C.-Y. Mou, S.-B. Liu, H.-K. Lee, New J. Chem. 24 (2000) 253.

[293] S.L. Burkett, S.D. Sims, S. Mann, Chem. Commun. (1996) 1367.

[294] Y. Mori, T.J. Pinnavaia, Chem. Mater. 13 (2001) 2173.

[295] C.W. Jones, K. Tsuji, M.E. Davis, Nature 393 (1998) 52.

[296] C.W. Jones, K. Tsuli, M.E. Davis, Micropor. Mesopor. Mater. 33 (1999) 223.

[297] C.W. Jones, M. Tsapatsis, T. Okudo, M.E. Davis, Micropor. Mesopor. Mater. 42 (2001) 21.

[298] C.M. Bambrough, R.C.T. Slade, R.T. Williams, J. Mater. Chem. 8 (1998) 569.

[299] F. Babonneau, L. Leite, S. Fontlupt, J. Mater. Chem. 9 (1999) 175.

[300] K.R. Kloetstra, H.W. Zandbergen, J.C. Jansen, H. van Bekkum, Micropor. Mater. 6 (1996) 287.

[301] A. Karlsson, M. Stocker, R. Schmidt, Micropor. Mesopor. Mater. 27 (1999) 181.

[302] A. Karlsson, M. Stöcker, K. Schäfer, Stud. Surf. Sci. Catal. 129 (2000) 99.

[303] L. Huang, W. Guo, P. Deng, Z. Xue, Q. Li, J. Phys. Chem. B 104 (2000) 2817.

[304] A. Corma, V. Fornes, S.B. Pergher, Th.L.M. Maesen, J.G. Buglass, Nature 396 (1998) 353.

[305] A. Corma, U. Diaz, M.E. Domine, V. Fornes, J. Am. Chem. Soc. 122 (2000) 2804.

[306] K.R. Kloetstra, H. van Bekkum, J.C. Jansen, Chem. Commun. (1997) 2281.

[307] Y. Liu, W. Zhang, T.J. Pinnavaia, J. Am. Chem. Soc. 122 (2000) 8791.

[308] Y. Liu, W. Zhang, T.J. Pinnavaia, Angew. Chem. Int. Ed. 40 (2001) 1255.

[309] Z. Zhang, Y. Han, L. Zhu, R. Wang, Y. Yu, S. Qiu, D. Zhao, F-S. Xiao, Angew. Chem. Int. Ed. 40 (2001) 1258.

[310] D. Trong On, S. Kaliaguine, US Patent pending (2000).

[311] D. Trong On, S. Kaliaguine, Angew. Chem. Int. Ed. Mater. 40 (2001) 3248; Angew. Chem. 113 (2001) 3348.

[312] D. Trong On, D. Lutic, S. Kaliaguine, Micropor. Mesopor. Mater. 44–45 (2001) 435.

[313] D. Trong On, P. Reinert, L. Bonneviot, S. Kaliaguine, Stud. Surf. Sci. Catal. 135 (2001) 135.

[314] A. Corma, S. Iborra, S. Miquel, J. Primo, J. Catal. 173 (1998) 315.

[315] C. Noda Perez, E. Moreno, C.A. Henriques, S. Valange, Z. Gabelica, J.L.F. Monteiro, Micropor. Mesopor. Mater. 41 (2000) 137.

[316] S. Jaenicke, G.K. Chuah, X.H. Lin, X.C. Hu, Micropor. Mesopor. Mater. 35/36 (2000) 143.

[317] D. Brunel, A. Cauvel, F. Fajula, F. Di Renzo, Stud. Surf. Sci. Catal. 97 (1995) 173.

[318] P. Sutra, D. Brunel, Chem. Commun. (1996) 2485.

[319] A. Cauvel, G. Renard, D. Brunel, J. Org. Chem. 62 (1997) 749.

[320] M. Lasperas, T. Llorett, L. Chaves, I. Rodriguez, A. Cauvel, D. Brunel, Stud. Surf. Sci. Catal. 108 (1997) 75.

[321] A. Derrien, G. Renard, D. Brunel, Stud. Surf. Sci. Catal. 117 (1998) 445.

[322] D. Brunel, Micropor. Mesopor. Mater. 27 (1999) 329.

[323] D. Brunel, L. Lentz, P. Sutra, B. Deroide, F. Fajula, J.B. Nagy, Stud. Surf. Sci. Catal. 125 (1999) 237.

[324] P. Sutra, F. Fajula, D. Brunel, P. Lentz, G. Daelen, J.B. Nagy, Colloids Surf. A: Eng. Aspects 158 (1999) 21.

[325] D. Brunel, A. Cauvel, F. Di Renzo, F. Fajula, B. Fubini, B. Onida, E. Garrone, New J. Chem. 24 (2000) 807.

[326] A.C. Blanc, D.J. Macquarrie, S. Valle, G. Renard, C.R. Quinn, D. Brunel, Green Chem. 2 (2000) 283.

[327] X. Lin, G.K. Chuah, S. Jaenicke, J. Mol. Catal. A: Chem. 150 (1999) 287.

[328] B.M. Choudary, M. Lakshmi Kantam, P. Sreekanth, T. Bandopadhyay, F. Figueras, A. Tuel, J. Mol. Catal. A: Chem. 142 (1999) 361.

[329] D.J. Macquarrie, Chem. Commun. (1996) 1961.

[330] D.J. Macquarrie, D.B. Jackson, Chem. Commun. (1997) 1781.

[331] J.E.G. Mdoe, J.H. Clark, D.J. Macquarrie, Synlett 6 (1998) 625.

[332] D.J. Macquarrie, Green Chem. 1 (1999) 195.

[333] D.J. Macquarrie, D.B. Jackson, S. Tailland, K. Wilson, J.H. Clark, Stud. Surf. Sci. Catal. 129 (2000) 275.

[334] D. Barthomeuf, J. Phys. Chem. 88 (1984) 42.

[335] M. Huang, S. Kaliaguine, J. Chem. Soc., Faraday Trans. 88 (1992) 751.

[336] M. Huang, A. Adnot, S. Kaliaguine, J. Catal. 137 (1992) 322.

[337] M. Huang, A. Adnot, S. Kaliaguine, J. Am. Chem. Soc. 114 (1992) 10005.

[338] Y.V. Subba Rao, D.E. De Vos, P.A. Jacobs, Angew. Chem. Int. Ed. 36 (1997) 2661.

[339] B.A. Morrow, A.J. McFarlan, Langmuir 7 (1991) 1695.

[340] S. Haukka, A. Root, J. Phys. Chem. 98 (1994) 1695.

[341] S.A. Miller, E. Kim, D.H. Gray, D.L. Gin, Angew. Chem. Int. Ed. 38 (1999) 3021.

[342] D.L. Gin, S.A. Miller, E. Kim, D.H. Gray, Polymer 41 (2000) 925 (Preprints).

[343] M.P. Attfield, G. Sankar, J.M. Thomas, Catal. Lett. 70 (2000) 155.

[344] A. Neumann, M. Khenkin, J. Chem. Soc., Chem. Commun. (1996) 2643.

[345] C. Liu, X. Ye, Y. Wu, Catal. Lett. 36 (1996) 263.

[346] H.G. Ang, K.S. Chan, G.K. Chuah, S. Jaenicke, S.K. Neo, J. Chem. Soc., Dalton Trans. (1995) 3753.

[347] R. Anwander, R. J. Roesky, J. Chem. Soc., Dalton Trans. (1997) 137.

[348] P. Ferreira, I. S. Gonçalve, F. Mosselmans, M. Pillinger, J. Rocha, A. Thursfield, Eur. J. Inorg. Chem. (2000) 97.

[349] T. Maschmeyer, R.D. Oldroyd, G. Sankar, J.M. Thomas, I.J. Shannon, J.A. Klepetko, A.F. Masters, J.K. Beattie, C.R.A. Catlow, Angew. Chem. Int. Ed. 36 (1997) 1639.

[350] S. O'Brien, J. Tudor, S. Barlow, M.J. Drewitt, S.J. Heyes, D. O'Hare, J. Chem. Soc., Chem. Commun. (1997) 641.

[351] C. Huber, K. Moller, T. Bein, Chem. Commun. (1994) 2619.

[352] R. Anwander, I. Nagl, M. Widenmeyer, G. Engelhardt, O. Groeger, C. Palm, T. Röser, J. Phys. Chem. B 104 (2000) 3532.

[353] J.H. Clark, D.J. Macquarrie, Chem. Commun. (1998) 853.

[354] D. Brunel, N. Bellocq, P. Sutra, A. Cauvel, M. Lasperas, P. Moreau, F. Di Renzo, A. Galarneau, F. Fajula, Coord. Chem. Rev. 178–180 (Pt. 2) (1998) 1085.

[355] D. Brunel, P. Sutra, in: Proceedings of the 3rd International Symposium Supported Reagents and Catalysis in Chemistry, Limerik, Ireland, July 1997, Royal Soc. Chem. (1998) 54.

[356] B.M. Choudary, M.L. Kantam, B. Bharathi, P. Sreekanth, F. Figueras, J. Mol. Catal. A: Chem. 159 (2000) 417.

[357] Z. Luan, J. Xu, L. Kevan, Chem. Mater. 10 (1998) 3699.

[358] S. Zheng, L. Gao, Jinkun Guo, J. Solid State Chem. 152 (2000) 447.

[359] K. Melis, D. De Vos, P.A. Jacobs, F. Verpoort, J. Mol. Catal. A: Chem. 169 (2001) 47.

[360] L. Zhang, T. Sun, J.Y. Ying, Chem. Commun. (1999) 1103.

[361] L. Zhang, J.Y. Ying, AIChE J. 43 (1997) 1427.

[362] G.-J. Kim, D.-W. Park, Catal. Today 63 (2000) 537.

[363] J. Evans, A.B. Zaki, M.Y. El-Sheikh, S.A. El-Safty, J. Phys. Chem. 104 (2000) 10274.

[364] R. Anwander, O. Runte, J. Eppinger, G. Gerstberger, E. Herdtweck, M. Spiegler, J. Chem. Soc., Dalton Trans. (1998) 847.

[365] J.M. Thomas, T. Maschmeyer, B.F.G. Johnson, D.S. Shephard, J. Mol. Catal. A: Chem. 141 (1999) 139.

[366] D.S. Shephard, W. Zhou, T. Maschmeyer, J.M. Matters, C.L. Roper, S. Parsons, B.F. Johnson, M.J. Duer, Angew. Chem. Int. Ed. Engl. 37 (1998) 2719.

[367] A. Togni, T. Hayashi (Eds.), Ferrocenes, Weinheim, Germany, 1995, Chapter 2 and references therein.

[368] A. Corma, M. Iglesias, C. del Pino, F. Sanchez, J. Organomet. Chem. 431 (1992) 233.

[369] B.F.G. Johnson, S.A. Raynor, D.S. Shephard, T. Mashmeyer, J.M. Thomas, G. Sankar, S. Bromley, R. Oldroyd, L. Gladden, M.D. Mantle, Chem. Commun. (1999) 1167.
[370] S.A. Raynor, J.M. Thomas, R. Raja, B.F.G. Johnson, R.G. Bell, M.D. Mantle, Chem. Commun. (2000) 1925.
[371] D.S. Shephard, T. Maschmeyer, B.F.G. Johnson, J.M. Thomas, G. Sankar, D. Ozkaya, W. Zhou, R.D. Oldroyd, Angew. Chem. Int. Ed. 36 (1997) 2242.
[372] T. Hayashi, T. Hagihara, Y. Katsuro, M. Kumada, Bull. Chem. Soc. Jpn. 56 (1983) 363.
[373] Y. Ito, M. Sawamura, T. Hayashi, J. Am. Chem. Soc. 108 (1986) 6405.
[374] T. Hayashi, N. Kawamura, Y. Ito, Tetrahedron Lett. 46 (1988) 5969.
[375] G. Consiglio, P. Pino, Top. Curr. Chem. 105 (1982) 77.
[376] Mahe, Y. Sasaki, C. Bruneau, P.H. Dixneuf, J. Org. Chem. 54 (1982) 1989.
[377] A.R. Badiei, L. Bonneviot, Inorg. Chem. 37 (1998) 4142.
[378] F. Béland, A.R. Badiei, M. Rönning, D. Nicholson, L. Bonneviot, Phys. Chem. Chem. Phys. 1 (1999) 605.
[379] S. Dai, Y. Shin, Y. Ju, M.C. Burleigh, J.S. Lin, C.E. Barnes, Z. Xue, Adv. Mater. 11 (1999) 1226.
[380] H.P. Lin, L.Y. Yang, C.Y. Mou, S.B. Liu, H.K. Lee, New J. Chem. 24 (2000) 263.
[381] S.S. Kim, W. Zhang, T.J. Pinnavaia, Catal. Lett. 43 (1997) 149.
[382] J. Kim, S.H. Kim, Catal. Lett. 57 (1999) 139.
[383] H. Chen, A. Matsumoto, N. Nishimiya, K. Tsutsumi, Chem. Lett. 57 (1999) 139.
[384] J.M. Thomas, Nature 368 (1994) 289.
[385] J.F. Diaz, K.J. Balkus Jr., J. Mol. Catal. B: Enzym. 2 (1996) 115.
[386] M.E. Gimon-Kinsed, V.I. Jimenez, L. Washmon, K.J. Balkus Jr., Stud. Surf. Sci. Catal. 117 (1998) 373.
[387] Y.J. Han, G.D. Stucky, A. Butlet, J. Am. Chem. Soc. 121 (1999) 9897.
[388] H. Takahashi, B. Li, T. Sasaki, C. Miyazaki, T. Kajino, S. Inagaki, Chem. Mater. 12 (2000) 3301.
[389] H. Takahashi, B. Li, T. Sasaki, C. Miyazaki, T. Kajino, S. Inagaki, Micropor. Mesopor. Mater. 44–45 (2001) 755.
[390] L. Washmon, V.I. Jimenez, K.J. Balkus Jr., J. Mol. Catal. B: Enzym. 10 (2000) 453.
[391] H.H.P. Yiu, P.A. Wright, N.P. Botting, Micropor. Mesopor. Mater. 44–45 (2001) 763.
[392] B. Li, H. Takahashi, Biotechnol. Lett. 22 (2000) 1953.
[393] J.P. Brunelle, Pure Appl. Chem. 50 (1978) 1211.
[394] Y. Wei, J. Xu, Q. Feng, H. Dong, M. Lin, Mater. Lett. 44 (2000) 6.
[395] J. Deere, E. Magner, J.G. Wall, B.K. Hodnett, Chem. Commun. (2001) 465.
[396] C. Phelps, L. Forlani, E. Antonini, Biochem. J. 124 (1971) 605.
[397] D.M. Antonelli, A. Nakahira, J. Ying, Inorg. Chem. 35 (1996) 3126.
[398] J. Xu, H. Dong, Q. Feng, Y. Wei, Polym. Prepr. (Am. Chem. Soc., Div. Polym. Chem.) 41 (1) (2000) 1042.
[399] J. Liu, Y. Shin, Z. Nie, J.H. Chang, L.Q. Wang, G.E. Fryxell, W.D. Samuels, G. Exarhos, J. Phys. Chem. A 104 (36) (2000) 8328.
[400] J. Xu, H. Dong, Q. Feng, Y. Wei, Polym. Prepr. (Am. Chem. Soc., Div. Polym. Chem.) 41 (2) (2000) 1673.
[401] J. Xu, H. Dong, Q. Feng, Y. Wei, Polym. Prepr. (Am. Chem. Soc., Div. Polym. Chem.) 41 (1) (2000) 1044.
[402] G.-W. Xing, X.-W. Li, G.-L. Tian, Y.-H. Ye, Tetrahedron 56 (22) (2000) 3517.
[403] Q. Feng, J. Xu, M. Lin, H. Dong, Y. Wei, Polym. Mater. Sci. Eng. 83 (2000) 502.
[404] J. Xu, Q. Feng, H. Dong, Y. Wei, Polym. Prepr. (Am. Chem. Soc., Div. Polym. Chem.) 41 (1) (2000) 1046.
[405] S. Cosnier, A. Senillou, M. Gratzel, P. Comte, N. Vlachopoulos, N. Jaffrezic Renault, C. Martelet, J. Electroanal. Chem. 469 (2) (1999) 176.
[406] Y. Ma, W. Tong, H. Zhou, S.L. Suib, Micropor. Mesopor. Mater. 37 (2000) 243.
[407] Q. Huo, D.I. Margolese, U. Ciesla, D.G. Demuth, P. Feng, T.E. Gier, P. Sieger, A. Firouzi, B.F. Chmelka, F. Shüth, G.D. Stucky, Chem. Mater. 6 (1994) 2317.
[408] D.M. Antonelli, J.Y. Ying, Angew. Chem. Int. Ed. Engl. 34 (1995) 2014.
[409] H. Fujii, Ohtaki, K. Eguchi, J. Am. Chem. Soc. 120 (1998) 6832.
[410] R.L. Putnam, N. Nakagawa, K.M. McGrath, N. Yao, I.A. Aksay, S.M. Gruner, A. Navrotsky, Chem. Mater. 9 (1997) 2690.
[411] V.F. Stone Jr., R.J. Davis, Chem. Mater. 10 (1998) 1469.
[412] D. Trong On, Langmuir 15 (1999) 8561.
[413] D.M. Antonelli, J.Y. Ying, Angew. Chem. Int. Ed. Engl. 35 (1996) 426.
[414] D.M. Antonelli, J.Y. Ying, Chem. Mater. 8 (1996) 874.
[415] Y. Takahara, J.N. Kondo, T. Takata, D. Lu, K. Domen, Chem. Mater. 13 (2001) 1199.
[416] J.N. Kondo, Y. Takahara, D. Lu, K. Domen, Chem. Mater. 13 (2001) 1200.
[417] F. Vaudry, S. Khodabandeh, M.E. Davis, Chem. Mater. 8 (1996) 1451.
[418] M. Yada, H. Hiyoshi, K. Ohe, M. Machida, T. Kijima, Inorg. Chem. 36 (1997) 5565.
[419] W. Zhang, T.J. Pinnavaia, Chem. Commun. (1998) 1185.
[420] A. Stein, B. Holland, J. Porous Mater. 3 (1996) 83.
[421] S. Valange, J.-L. Guth, F. Kolenda, S. Lacombe, Z. Gabelica, Micropor. Mesopor. Mater. 35/36 (2000) 597.
[422] F. Kolenda, J.-L. Guth, S. Valange, Z. Gabelica, S. Lacombe, French Patent Application 97/15450 (1997).
[423] F. Kolenda, J.-L. Guth, S. Valange, Z. Gabelica, S. Lacombe, French Patent Application 97/15451 (1997).
[424] M. Yada, M. Machida, T. Kijima, Chem. Commun. (1996) 769.
[425] K.G. Severin, T.M. Abdel-Fattah, T.J. Pinnavaia, Chem. Commun. (1998) 1471.
[426] Z-R. Tian, W. Tong, J.-Y. Wang, N.-G. Duan, V.V. Krishnan, S.L. Suib, Science 276 (1997) 926.
[427] J. Luo, S.L. Suib, Chem. Commun. (1997) 1031.
[428] D. Terribile, A. Trovarelli, C. de Leitenburg, G. Dolcetti, J. Llorca, Chem. Mater. 9 (1997) 2676.

[429] M.J. Hudson, J.A. Knowles, J. Mater. Chem. 6 (1996) 89.
[430] J.S. Reddy, A. Sayari, Catal. Lett. 38 (1996) 219.
[431] U. Ciesla, S. Schacht, G.D. Stucky, K.K. Unger, F. Schüth, Angew. Chem. Int. Ed. Engl. 35 (1996) 541.
[432] U. Ciesla, M. Fröba, G.D. Stucky, F. Schüth, Chem. Mater. 11 (1999) 227.
[433] Y.-Y. Huang, T.J. McCarthy, W.M.H. Sachtler, Appl. Catal. 148 (1996) 135.
[434] M.S. Wong, D.M. Antonelli, J.Y. Ying, Nanostr. Mater. 9 (1997) 165.
[435] M.S. Wong, J.Y. Ying, Chem. Mater. 10 (1998) 2067.
[436] R.A. Boyse, E.I. Ko, Catal. Lett. 38 (1996) 225.
[437] A. Kim, P. Bruinsma, Y. Chen, L.-Q. Wang, J. Liu, Chem. Commun. (1997) 161.
[438] G. Pacheco, E. Zhao, A. Garcia, A. Sklyarov, J.J. Fripiat, Chem. Commun. (1997) 491.
[439] E. Zhao, S.E. Hardcastle, G. Pacheco, A. Garcia, A.L. Blumenfeld, J.J. Fripiat, Micropor. Mesopor. Mater. (1999) 9.
[440] G. Pacheco, J.J. Fripiat, J. Phys. Chem. B (2000) 11906.
[441] M.E. Spahr, P. Bitterli, R. Nesper, M. Müller, F. Krumeich, H.U. Nissen, Angew. Chem. Int. Ed. 37 (1998) 1263.
[442] V. Luca, J.M. Hook, Chem. Mater. 9 (1997) 2731.
[443] S. Oliver, A. Kuperman, N. Coombs, A. Lough, G.A. Ozin, Nature 378 (1995) 47.
[444] A. Sayari, I. Moudrakovski, J.S. Reddy, C.I. Ratcliffe, J.A. Ripmeester, K.F. Preston, Chem. Mater. 8 (1996) 2080.
[445] A. Chenite, I. Le Page, V.R. Karra, A. Sayari, Chem. Commun. (1996) 413.
[446] P. Feng, Y. Xia, J. Feng, X. Bu, G.D. Stucky, Chem. Commun. (1997) 949.
[447] D. Zhao, Z. Luan, L. Kevan, Chem. Commun. (1997) 1009.
[448] B. Chakraborty, A.C. Pulikottil, S. Das, B. Viswanathan, Chem. Commun. (1997) 991.
[449] B. Chakraborty, A.C. Pulikottil, S. Das, B. Viswanathan, Appl. Catal. A: Gen. 167 (1998) 173.
[450] S. Cabrera, J.E. Haskouri, C. Guillem, A. Beltran-Porter, D. Beltran-Porter, S. Mendioroz, M.D. Marcos, P. Amoros, Chem. Commun. (1999) 333.
[451] T. Kimura, Y. Sugahara, K. Kuroda, Micropor. Mesopor. Mater. 22 (1998) 115.
[452] T. Kimura, Y. Sugahara, K. Kuroda, Chem. Lett. (1997) 983.
[453] T. Kimura, Y. Sugahara, K. Kuroda, Chem. Commun. (1998) 559.
[454] T. Kimura, Y. Sugahara, K. Kuroda, Chem. Mater. 11 (1999) 508.
[455] M.P. Kapoor, A. Raj, Appl. Catal. A: Gen. 203 (2000) 311.
[456] M. Tiemann, M. Fröba, G. Rapp, S.S. Funari, Chem. Mater. 12 (2000) 1342.
[457] B.T. Holland, P.K. Isbester, C.F. Blanford, E.J. Munson, A. Stein, J. Am. Chem. Soc. 119 (1997) 6796.
[458] D.A. Kron, B.T. Holland, R. Wipson, C. Maleke, A. Stein, Langmuir 15 (1999) 8300.
[459] M. Eswaramoorthy, S. Neeraj, C.N.R. Rao, Micropor. Mesopor. Mater. 28 (1999) 205.
[460] T. Abe, A. Taguchi, M. Iwamoto, Chem. Mater. 7 (1995) 1429.
[461] T. Doi, T. Miyake, Chem. Commun. (1996) 1635.
[462] J.E. Haskouri, M. Moca, S. Cabreca, J. Alamo, A. Beltran-Porter, D. Beltran-Porter, M.D. Marcos, Chem. Mater. 11 (1999) 1446.
[463] N. Mizuno, H. Hatayama, S. Uchida, A. Taguchi, Chem. Mater. 13 (2001) 179.
[464] H. Hatayama, M. Misono, A. Taguchi, N. Mizuno, Chem. Lett. 13 (2000) 884.
[465] M. Mamak, N. Coombs, G.A. Ozin, Adv. Mater. 12 (2000) 198.
[466] M. Mamak, N. Coombs, G.A. Ozin, J. Am. Chem. Soc. 122 (2000) 8932.
[467] M. Yada, H. Kitomura, A. Ichinose, M. Machida, T. Kijima, Angew. Chem. Int. Ed. 38 (1999) 3506.
[468] Y. Wang, L. Yin, O. Palchik, Y.R. Hacohen, Y. Koltypin, A. Gedanken, Chem. Mater. 13 (2001) 1248.
[469] H.-R. Chen, J.-L. Shi, J. Yu, L.-Z. Wang, D.-S. Yan, Micropor. Mesopor. Mater. 39 (2000) 171.
[470] S.H. Elder, Y. Gao, X. Li, J. Liu, D.E. McCready, C.F. Windish Jr., Chem. Mater. 10 (1998) 3140.
[471] G.S. Attard, S.A.A. Leclerc, S. Maniguet, A.E. Russell, I. Nandha Kumar, P.N. Bartlett, Chem. Mater. 13 (2001) 1444.
[472] S. Valange, Z. Gabelica, A. Derouault, J. Barrault, Stud. Surf. Sci. Catal. 130 (2000) 3477.
[473] P. Yang, D. Zhao, D.I. Margolese, B.F. Chmelka, G.D. Stucky, Nature (1998) 153.
[474] P. Yang, D. Zhao, D.I. Margolese, B.F. Chmelka, G.D. Stucky, Chem. Mater. (1999) 2813.
[475] Y. Yue, Z. Gao, Chem. Commun. (2000) 1755.
[476] M.A. Camblor, A. Corma, A. Martinez, A. Pérez-Pariente, J. Primo, Stud. Surf. Sci. Catal. 78 (1994) 393.
[477] S. Kawi, M. Te, Catal. Today 44 (1998) 101.
[478] A. Sayari, Chem. Mater. 8 (1996) 1840.
[479] M. Mathieu, P. Van Der Voort, B.M. Weckhuysen, R.R. Rao, G. Catana, R.A. Schoonheydt, E.F. Vansant, J. Phys. Chem. B 105 (2001) 3393.
[480] C.N. Wu, T.S. Tsai, C.N. Liao, K.J. Chao, Micropor. Mater. 7 (1996) 173.
[481] A. Tuel, S. Gontier, R. Teissier, Chem. Commun. (1996) 651.
[482] S.A. Bagshaw, F. Di Renzo, F. Fajula, Chem. Commun. (1996) 2209.
[483] S.A. Bagshaw, T. Kemmitt, N.B. Milestone, Micropor. Mesopor. Mater. 22 (1998) 419.
[484] K.M. Reddy, I. Moudrakovski, A. Sayari, J. Chem. Soc. Chem. Commun. (1994) 1059.
[485] D.H. Park, C.-F. Cheng, J. Klinowski, Bull. Korean Chem. Soc. 18 (1997) 70.
[486] F. Béland, B. Echchahed, A.-R. Badiei, L. Bonneviot, Stud. Surf. Sci. Catal. 117 (1998) 567.
[487] A. Corma, M.T. Navarro, J.P. Pariente J. Chem. Soc. Chem. Commun. (1994) 147.
[488] J. El Haskouri, S. Cabrera, M. Guytierrez, A. Beltran-Porter, D. Beltran-Porter, M. Dolores Marcos, P. Amoros, Chem. Commun. (2001) 309.
[489] W. Zhang, T.J. Pinnavaia, Catal. Lett. 38 (1996) 261.
[490] M. Morey, A. Davidson, G. Stucky, Micropor. Mater. 6 (1996) 99.

[491] M.S. Morey, S. O'Brien, S. Schwarz, G.D. Stucky, Chem. Mater. 12 (2000) 898.

[492] K.A. Koyano, T. Tatsumi, Chem. Commun. (1996) 145.

[493] D. Trong On, M.P. Kapoor, P.N. Joshi, L. Bonneviot, S. Kaliaguine, Catal. Lett. 44 (1997) 171.

[494] S. Gontier, A. Tuel, Zeolites 15 (1995) 601.

[495] J.S. Reddy, A. Dicko, A. Sayari, in: M. Occelli, H. Kessler (Eds.), Synthesis of Porous Materials: Zeolites, Clays and Nanostructures, Marcel Dekker, New York, 1997, pp. 405–415.

[496] S. Gontier, A. Tuel, J. Catal. 157 (1995) 124.

[497] G.S. Attard, J.C. Glyde, G.C. Göltner, Nature 378 (1995) 366.

[498] S.A. Bagshaw, Chem. Commun. (1999) 271.

[499] S.G. Zhang, Y. Fujii, H. Yamashita, K. Koyano, T. Tatsumi, M. Anpo, Chem. Lett. (1997) 659.

[500] K. Kosuge, P.S. Singh, Chem. Lett. (1999) 9.

[501] K. Kageyama, S.M. Ng, H. Ichikawa, T. Aida, Macromol. Symp. 157 (2000) 137.

[502] L.-X. Dai, K. Tabata, E. Suzuki, T. Tatsumi, Chem. Mater. 13 (2001) 208.

[503] G. Grubert, J. Rathousky, G. Schulz-Ekloff, M. Wark, A. Zukal, Micropor. Mesopor. Mater. 22 (1998) 225.

[504] J.S. Reddy, P. Liu, A. Sayari, Appl. Catal. A148 (1996) 7.

[505] J.S. Reddy, A. Sayari, J. Chem. Soc. Chem. Commun. (1995) 2231.

[506] D. Wei, W.-T. Chueh, G.L. Haller, Catal. Today 51 (1999) 501.

[507] V. Luca, D.J. MacLachlan, K. Morgan, Chem. Mater. 9 (1997) 2720.

[508] M.E. Raimondi, E. Gianotti, L. Marchese, G. Martra, T. Maschmeyer, J.M. Seddon, S. Collucia, J. Phys. Chem. B104 (2000) 7102.

[509] S. Gontier, A. Tuel, Appl. Catal. A143 (1996) 125.

[510] D.J. Jones, J. Jimenez-Jimenez, A. Jimenez-Lopez, P. Maireles-Torres, P. Olivera-Pastore, E. Rodriguez-Castellon, J. Roziere, Chem. Commun. (1997) 431.

[511] X.X. Wang, F. Lefebvre, J. Patarin, J.M. Basset, Micropor. Mesopor. Mater. 42 (2001) 269.

[512] M.L. Occelli, S.Biz, US Patent pending, 1997.

[513] J. Janas, R. Janik, T. Machej, E.M. Serwicka, E. Bielanska, E. Bastardo-Gonzales, W. Jones, Catal. Today 59 (2000) 241.

[514] B. Echchahed, A.-R. Badiei, F. Béland, L. Bonneviot, Stud. Surf. Sci. Catal. 117 (1998) 559.

[515] B. Echchahed, A. Moen, D. Nicholson, L. Bonneviot, Chem. Mater. 9 (1997) 1716.

[516] J.B. Kim, T. Inui, Catal. Lett. 36 (1996) 255.

[517] S. Gontier, A. Tuel, Stud. Surf. Sci. Catal. 105 (1997) 29.

[518] N. He, J. Cao, B. Bao, Q. Xu, Mater. Lett. 33 (1997) 133.

[519] A. Tuel, Stud. Surf. Sci. Catal. 117 (1998) 159.

[520] N. Ulagapan, C.N.R. Rao, J. Chem. Soc. Chem. Commun. (1996) 1047.

[521] T.Kr. Das, K. Chaudhari, A.J. Chandwadkar, S. Sivasanker, Chem. Commun. (1995) 2495.

[522] T.M. Abdel-Fattah, T.J. Pinnavaia, J. Chem. Soc. Chem. Commun. (1996) 665.

[523] D. Zhao, D. Goldfarb, J. Chem. Soc. Chem. Commun. (1995) 875.

[524] C. Pak, G.L. Haller, Micropor. Mesopor. Mater. 44–45 (2001) 321.

[525] M. Ziolek, I. Sobczak, I. Nowak, P. Decyk, A. Lewandowska, J. Kujawa, Micropor. Mesopor. Mater. 35 (2000) 195.

[526] C.L. Tsai, B. Chou, S. Cheng, J.F. Lee, Appl. Catal. A: Gen. 128 (2001) 279.

[527] A.S. Araujo, M. Jaroniec, J. Colloid Interf. Sci. 218 (1999) 462.

[528] L.-X. Dai, K. Tabata, E. Suzuki, S.-A. Che, T. Tatsumi, Micropor. Mesopor. Mater. 44–45 (2001) 573.

[529] W.A. Carvalho, P.B. Varaldo, M. Wallau, U. Schuchardt, Zeolite 18 (1997) 408.

[530] J.E. Gallot, S. Kaliaguine, Can. J. Chem. Eng. 76 (5) (1998) 833.

[531] J. Bu, H.-K. Rhee, Stud. Surf. Sci. Catal. 129 (2000) 179.

[532] A.Corma, M. Domine, J.A. Gaona, J.L. Jorda, M.T. Navarro, F. Rey, J. Perez-Pariente, J. Tsuji, B. McCulloch, L.T. Nemeth, Chem. Commun. (1998) 2211.

[533] B.C. Gates, J.R. Katzer, G.C.A. Schuit, Chemistry of Catalytic Processes, McGraw-Hill, New York, 1979.

[534] K.H. Algelt, M.M. Boduszynski, Composition and Analysis of Heavy Petroleum Fractions, Marcel Dekker, New York, 1994.

[535] E.J. Swain, Oil Gas J. (1991) 59.

[536] Recent EPA regulations will impose a 15 ppm S content for highway diesel fuels by 2006–2007, Diesel Fuel News 4 (2000) 1.

[537] T.F. Degnan, K.M. Keville, M.E. Landis, D.O. Marler, D.N. Mazzone, US Patent 5,183,557 (1993).

[538] M.R. Apelian, T.F. Degnan, D.O. Marler, D.N. Mazzone, US Patent 5,227,353 (1993).

[539] T.F. Degnan, K.M. Keville, M.E. Landis, D.O. Marler, D.N. Mazzone, US Patent 5,290,744 (1993).

[540] S.S. Shih, US Patent 5,344,553 (1994).

[541] N.A. Bhore, I.D. Johnson, K.M. Keville, Q.N. Le, G.H. Yokomizo, US Patent 5,260,501 (1993).

[542] J.S. Beck, C.T-W. Chu, I.D. Johnson, C.T. Kresge, M.E. Leonowicz, W.J. Roth, J.C. Vartuli WO 91/11390.

[543] B. Kraushaar-Czarnetzki, J. Wijnbelt, WO 97/20016.

[544] C. Song, K.M. Reddy, Am. Chem. Soc., Div. Petro. Chem. Prep. 41 (3) (1996) 567.

[545] C. Song, K.M. Reddy, Appl. Catal. A: Gen. 176 (1999) 1.

[546] K.M. Reddy, B. Wei, C. Song, Catal. Today 43 (1998) 261.

[547] A. Klemt, A. Taouli, H. Koch, W. Reschetilowski, Stud. Surf. Sci. Catal. 127 (1999) 405.

[548] T. Klimova, J. Ramirez, M. Calderon, J.M. Dominguez, Stud. Surf. Sci. Catal. 117 (1998) 493.

[549] J. Ramirez, R. Contreras, P. Castillo, T. Klimova, R. Zarate, R. Luna, Appl. Catal. A: Gen. 197 (2000) 69.

[550] A. Wang, Y. Wang, T. Kabe, Y. Chen, A. Ishihara, W. Qian, J. Catal. 199 (2001) 19.

[551] Y.H. Yue, Y. Sun, Z. Gao, Catal. Lett. 47 (1997) 167.

[552] J. Cui, Y.N. Yue, Y. Sun, W.Y. Dong, Z. Gao, Stud. Surf. Sci. Catal. 105A (1997) 687.

[553] T. Halachev, J.A. de Los Reyes, C. Araujo, L. Dimitrov, G. Cordoba, Stud. Surf. Sci. Catal. 127 (1999) 401.

[554] T. Halachev, R. Nava, L. Dimitrov, Appl. Catal. A: Gen. 169 (1998) 111.
[555] T. Chiranjeevi, P. Kumar, S.K. Maity, M.S. Rana, G. Murali Dhar, T.S.R. Prasada Rao, Micropor. Mesopor. Mater. 44–45 (2001) 547.
[556] A. Corma, M.S. Grande, V. Gonzalez-Alfaro, A.V. Orchilles, J. Catal. 159 (1996) 375.
[557] E. Armengol, M. L. Cano, A. Corma, H. Garcia, M. T. Navarro, Chem. Commun. (1995) 519.
[558] E. Armengol, A. Corma, H. Garcia, J. Primo, Appl. Catal. A: Gen. 149 (1997) 411.
[559] J. Medina-Valtierra, O. Zaldivar, M.A. Sanchez, J.A. Montoya, J. Navarrete, J.A. Reyes, Appl. Catal. A: Gen. 166 (1998) 387.
[560] T.R. Pauly, Y. Liu, T.J. Pinnavaia, S.J.L. Billinge, T.P. Rieker, J. Am. Chem. Soc. 121 (1999) 8835.
[561] S.-S. Kim, Y. Liu, T. Pinnavaia, Micropor. Mesopor. Mater. 44–45 (2001) 489.
[562] M. Polverejan, Y. Liu, T.J. Pinnavaia, Stud. Surf. Sci. Catal. 129 (2000) 401.
[563] N. He, S. Bao, Q. Xu, Appl. Catal. A: Gen. 169 (1998) 29.
[564] V.R. Choudhary, S.K. Jana, B.P. Kiran, Catal. Lett. 64 (2000) 223.
[565] G.D. Yahav, M.S. Krishnan, N.S. Doshi, A.A. Purjari, M.S.M. Mujeebur Rahuman, 1999 Patent GB2332155, pp 34.
[566] P. Beltrame, G. Zuretti, F. Demartin, Ind. Eng. Res. 39 (2000) 1209.
[567] K. Okumura, K. Nishigaki, M. Niwa, Micropor. Mesopor. Mater. 44–45 (2001) 509.
[568] V.R. Choudhary, S.K. Jana, B.P. Kiran, J. Catal. 192 (2000) 257.
[569] G. Bellussi, C. Perego, A. Carati, S. Peratello, E. Previde Massara, G. Perego, Stud. Surf. Sci. Catal. 84 (1994) 85.
[570] P.M. Price, J.H. Clark, K. Martin, D.J. Macquarrie, T.W. Bastock, Org. Proc. Res. Dev. 2 (1998) 221.
[571] P.M. Price, J.H. Clark, K. Martin, D.J. Macquarrie, T.W. Bastock, Spec. Publ.-R. Soc. Chem. 216 (1998) 229.
[572] C. Perego, S. Amarilli, A. Caracti, C. Flego, G. Pazzuconi, C. Rizzo, G. Bellussi, Micropor. Mesopor. Mater. 27 (1999) 345.
[573] X. Hu, W.L. Foo, G.K. Chuah, S. Janicke, J. Catal. 195 (2000) 412.
[574] J.H. Clark, G.L. Monks, D.J. Nightingale, P.M. Price, J. Catal. 193 (2000) 348.
[575] E.G. Kodenev, A.N. Shmakov, A.Y. Derevyankin, O.B. Lapina, V.N. Romannikov, J. Mol. Catal. A: Chem. 158 (2000) 349.
[576] D.J. McIntosh, R.A. Kydd, Micropor. Mesopor. Mater. 37 (2000) 281.
[577] J. Cejka, A. Krejci, N. Zilkova, J. Dedecek, J. Hanika, Micropor. Mesopor. Mater. 44–45 (2001) 499.
[578] A. Sakthivel, S.K. Badamali, P. Selvam, Micropor. Mesopor. Mater. 39 (2000) 457.
[579] S.K. Badamali, A. Sakthivel, P. Selvam, Catal. Lett. 65 (2000) 153.
[580] T.Y. Stoylkova, C.D. Chanev, H.T. Lechert, C.P. Bezouhanova, Catal. Lett. 69 (2000) 109.
[581] B.M. Choudary, M.L. Kantam, M. Sateesh, K.K. Rao, P.L. Santhi, Appl. Catal. A: Gen. 149 (1997) 257.
[582] O.W. Webster, Science 251 (1991) 887.
[583] T. Aida, Progr. Polym. Sci. 19 (1994) 469.
[584] D.S. Breslow, N.R. Newburg, J. Am. Chem. Soc. 79 (1957) 5072.
[585] Z.J. Jedlinski, in: H.A. Krichedorf (Ed.), Handbook of Polymer Synthesis, Part A, Marcel Dekker: New York, 1992, Chapter 11, p. 645.
[586] H. Yasuga, Prog. Polym. Sci. 25 (2000) 573.
[587] L.K. Van Looveren, D.F. Geysen, K.A. Vercruysse, B.H. Wouters, P.J. Grobet, P.A. Jacobs, Angew. Chem., Int. Ed. 37 (1998) 517.
[588] H.H. Brintzinger, D. Fischer, R. Mülhaupt, B. Rieger, W. Waymouth, Angew. Chem. Int. Ed. Eng. 107 (1995) 1255.
[589] A.E. Hamielec, J.B.P. Soares, Progr. Polym. Sci. 21 (1996) 651.
[590] W. Kaminsky, Macromol. Chem. Phys. 197 (1996) 3907.
[591] W. Kaminsky, C. Strübel, H. Lechert, D. Genske, S.I. Woo, Macromol. Rapid Commun. 21 (2000) 909.
[592] T. Sano, K. Doi, H. Hagimoto, Z.B. Wang, T. Uozumi, K. Soga, J. Chem. Soc., Chem. Commun. (1999) 733.
[593] I. Kiricsi, G. Pal-Borbely, J.B. Nagy, H.G. Karge (Eds.), Porous Materials in Environmentally Friendly Process, Stud. Surf. Sci. Catal. 125 (1999) 777.
[594] T. Sano, H. Hagimoto, S. Sumiya, Y. Naito, Y. Oumi, T. Uozumi, K. Soga, Micropor. Mesopor. Mater. 44–45 (2001) 557.
[595] E.H. Licht, H.G. Alt, J. Mol. Catal. A: Chem. 154 (2000) 65.
[596] G.G. Hlatky, Chem. Rev. 100 (2000) 1347.
[597] G.W. Coates, Chem. Rev. 100 (2000) 1223.
[598] H. Schneider, G.T. Puchta, F.A.R. Kaul, G. Raudaschl-Sieber, F. Lefebvre, G. Saggio, D. Mihalios, W.A. Herrmann, J.M. Basset, J. Mol. Catal. A: Chem. 170 (2001) 127.
[599] A. Köppl, H.G. Alt, R. Schmidt, J. Organometal. Chem. 577 (1999) 351.
[600] H.C. Welborn, US Patent 4,808,561 (1989).
[601] T. Takahashi, US Patent 5,026,797 (1991).
[602] K. Moller, T. Bein, R.X. Fischer, Chem. Mater. 11 (1999) 665.
[603] K. Kageyama, S.-I. Ogino, T. Aida, Macromol. 31 (1998) 4069.
[604] Y.S. Ko, T.K. Han, J.W. Park, S.I. Woo, Macromol. Rapid Commun. 17 (1996) 749.
[605] J. Tudor, D. O’Hare, Chem. Commun. (1997) 603.
[606] S. O’Brien, J. Tudor, T. Maschmeyer, D. O’Hare, Chem. Commun. (1997) 1905.
[607] B.M. Weckhuysen, R. Ramachandra Rao, J. Pelgrims, R.A. Schoonheydt, P. Bodart, G. Debras, O. Collart, P. Van Der Voort, E.F. Vansant, Chem. Eur. J. 6 (2000) 2960.
[608] M.P. Coles, R.F. Jordan, J. Am. Chem. Soc. 119 (1997) 8125.
[609] K. Kageyama, T. Tatsumi, T. Aida, Polym. J. 31 (1999) 1005.

[610] O. Moriya, A. Matsui, T. Sugisaki, M. Oikawa, T. Kageyama, Y. Nakamura, T. Endo, Polym. J. 32 (2000) 82.

[611] S.M. Ng, S.-I. Ogino, T. Aida, K.A. Koyano, T. Tatsumi, Macromol. Rapid Commun. 18 (1997) 991.

[612] K. Kageyama, J.I. Tamazawa, T. Aida, Science 285 (1999) 2113.

[613] D. Curran, J. Grimshaw, S.D. Perera, Chem. Soc. Rev. 20 (1992) 391.

[614] S. Spange, A. Graeser, P. Rehak, C. Jager, M. Schulz, Macromol. Rapid Commun. 21 (2000) 146.

[615] R. Noyori, M. Kitamura, Angew. Chem, Int. Ed. Engl. 30 (1991) 49.

[616] K. Soai, S. Niwa, Chem. Rev. 92 (1992) 833.

[617] K. Soai, A. Ookawa, T. Kaba, K. Ogawa, J. Am. Chem. Soc. 109 (1987) 7111.

[618] M. Laspéras, N. Bellocq, D. Brunel, P. Moreau, Tetrahedron: Asym. 9 (1998) 3053.

[619] N. Bellocq, S. Abramson, M. Laspéras, D. Bruel, P. Moreau, Tetrahedron: Asym. 10 (1999) 3229.

[620] S.J. Bae, S. W. Kim, T. Hyeon, B. Moon Kim, Chem. Commun. (2000) 31.

[621] S. Abramson, M. Laspéras, A. Galarneau, D. Desplantier-Giscard, D. Brunel, Chem. Commun. (2000) 1773.

[622] S. Abramson, N. Bellocq, M. Laspéras, Top. Catal. 13 (2000) 339.

[623] J. M. Thomas, R. Raja, Chem. Commun. (2001) 675.

[624] T. Yamamoto, T. Shido, S. Inagaki, Y. Fukushima, M. Ichikawa, J. Am. Chem. Soc. 118 (1996) 5810.

[625] M. Ichikawa, T. Yamamoto, W. Pan, T. Shido, Stud. Surf. Sci. Catal. 105 (1997) 679.

[626] T. Shido, T. Yamamoto, M. Harada, M. Ichikawa, J. Phys. IV 7 (1997) 855.

[627] D.S. Shephard, T. Maschmeyer, G. Sankar, J.M. Thomas, D. Ozkaya, B.F.G. Johnson, R. Raja, R.D. Oldroyd, R.G. Bell, Angew. Chem. Int. Ed. 4 (1997) 1214.

[628] S. Hermans, R. Raja, J.M. Thomas, B.F.G. Johson, G. Sankar, D. Gleeson, Angew. Chem. Int. Ed. 40 (2001) 1211.

[629] P. Piaggio, P. McMorn, C. Langham, D. Bethell, P. C. Bulman-Page, F. E. Hancock, G. J. Hutching, New J. Chem. (1998) 1167.

[630] X.G. Zhou, X.Q. Yu, J.S. Huang, S.G. Li, L.S. Li, C.M. Che, Chem. Commun. (1999) 1789.

[631] T. Maschmeyer, Curr. Opin. Solid State Mater. Sci. 3 (1998) 71.

[632] D. Brunel, P. Sutra, F. Fajula, Stud. Surf. Sci. Catal. 129 (2000) 773.

[633] D. Brunel, Supported Reagents and Catalysis in Chemistry, Chem. R. Soc. London (2000).

[634] E. Knoevenagel, Chem. Ber. 27 (1894) 2345.

[635] G. Jones, Org. React. 15 (1967) 204.

[636] J. March, Advanced in Organic Chemistry, 4th edition, 1992.

[637] E. Angeletti, C. Canepa, G. Martinetti, P. Venturello, Tetrahedron. Lett. 29 (1988) 2261.

[638] A. Reyes, R.M. Scott, J. Phys. Chem. 84 (1980) 3600.

[639] P. Laszlo, Acc. Chem. Res. 19 (1986) 121.

[640] P.W. Lednor, R. de Ruiter, Chem. Commun. (1991) 1625.

[641] S.R. Hall, C.E.Fowler, B. Lebeau, S. Mann, Chem. Commun. (1999) 201.

[642] Y. Kubota, Y. Nishizaki, Y. Sugi, Chem. Lett. 9 (2000) 998.

[643] B.T. Holland, C.F. Blanford, T. Do, A. Stein, Chem. Mater. 11 (1999) 795.

[644] B. Lebeau, C.E. Fowler, S. Mann, C. Farcet, B. Charleux, C. Sanchez, J. Mater. Chem. 10 (2000) 2105.

[645] C. Danumah, S. Vaudreuil, L. Bonneviot, M. Bousmina, S. Giasson, S. Kaliaguine, Micropor. Mesopor. Mater. 44–45 (2001) 241.

[646] P. Yang, T. Deng, D. Zhao, P. Feng, D. Pine, B.F. Chmelka, G.M. Whitesides, G.D. Stucky, Science 292 (1998) 2244.

[647] S.A. Davis, S.L. Burkett, N.H. Mendelson, S. Mann, Nature 385 (1997) 420.

[648] V. Pedroni, P.C. Schulz, M.E. Gschaider de Ferreira, M.A. Morini, Colloid Polym. Sci. 278 (2000) 964.

[649] D. Trong On, S. Kaliaguine, Angew. Chem., Int. Ed. 41 (2002) 1036.

[650] D. Trong On, S. Kaliaguine, US Pat. Pending (2001).